

FINAL REPORT

RESEARCH PROJECT 2001-04

**A Mechanistic Approach to Evaluate Contribution of Prime and Tack Coat
In Composite Asphalt Pavements**

by

Akhtarhusein A. Tayebali, Ph.D., P.E.

M. S. Rahman, Ph.D.

Moreshwar B. Kulkarni

Qingxia Xu

June 25, 2004

**Department of Civil Engineering
North Carolina State University**

Technical Report Documentation Page

1. Report No. FHWA/NC/2004-05	2. Government Accession No.	3. Recipient's Catalog No.	
4. Title and Subtitle A Mechanistic Approach to Evaluate Contribution of Prime and Tack Coat In Composite Asphalt Pavements.		5. Report Date June 25, 2004	
		6. Performing Organization Code	
7. Author(s) A. A. Tayebali, M. S. Rahman, M. B. Kulkarni, Q. Xu		8. Performing Organization Report No.	
9. Performing Organization Name and Address Department of Civil Engineering North Carolina State University Raleigh, NC 27695-7908		10. Work Unit No. (TRAIS)	
		11. Contract or Grant No.	
12. Sponsoring Agency Name and Address North Carolina Department of Transportation Research and Analysis Group 1 South Wilmington Street Raleigh, North Carolina 27601		13. Type of Report and Period Covered Final Report 7/01/2000-12/31/2003	
		14. Sponsoring Agency Code 2001-04	
15. Supplementary Notes: Project Monitor: Mustansir Kadibhai, P.E.			
16. Abstract <p style="text-align: justify;">This investigation was undertaken to develop a mechanistic design procedure for selection of tack and prime coat type in relation to traffic loading, pavement temperature and the AC overlay required thickness. The methodology used in this study to compare the performance of different tack and prime coats required the development of a 3-D computer program that takes into account the horizontal shear stresses induced on the pavement surface due to vehicle braking effects (acceleration and deceleration). Taking into account the induced shear loading, the shear stresses at the interface layers were computed. Next, these shear stresses were compared to the bond strength of the tack or prime coat under consideration. This research study provides a methodology and design guide based on mechanistic analysis to select appropriate tack or prime coat for given field conditions. Based on the AC layer thickness a suitable tack or prime coat can be chosen (or vice versa in some cases) to minimize the delamination distress.</p>			
17. Key Words Mechanistic design, interfacial shear stress, delamination, debonding, bond strength, shear testing, axial testing, slippage, tack coat, prime coat, PCC, CTB, AC		18. Distribution Statement	
19. Security Classif. (of this report) Unclassified	20. Security Classif. (of this page) Unclassified	21. No. of Pages 278	22. Price

Disclaimer

The contents of this report reflect the views and opinions of the author(s) and not necessarily the views of the University. The authors are responsible for the facts and the accuracy of the data presented herein. The contents do not necessarily reflect the official views or policies of either the North Carolina Department of Transportation or the Federal Highway Administration at the time of publication. This report does not constitute a standard, specification, or regulation.

Acknowledgements

The authors extend sincere appreciation to the authorities of the North Carolina Department of Transportation (NCDOT) for funding this project as well as performing laboratory tests. Thanks to Mr. Chris Bacchi, who was instrumental in coordinating the testing at NCDOT Materials and Tests Unit, answering our queries and helping us with material procurement.

Thanks are due to Prasad Kollipara, Kevin Fischer, Yuanxiong Huang, and Priya Nimbole for their assistance in fabricating rolling wheel samples. Steven Wade, departmental mechanic, has been helpful in fabrication of molds for slab construction, and maintaining the rolling wheel compactor.

Many subroutines used in the Finite Layer Computer program developed in this study were provided by Professor John Small of the University of Sydney, Australia. We sincerely appreciate his help.

Executive Summary

This investigation was undertaken to develop a mechanistic design procedure for selection of tack and prime coat type in relation to traffic loading, pavement temperature and the required AC overlay thickness.

The need for this research was based on the occurrence of excessive delamination problems in Division 13 of NCDOT. Pavements in Buncombe County where emulsions were used as tack coat, experienced higher incidence of delamination distress compared to the pavement sections in Rutherford County where PG64-22 asphalt cement was used as tack coat.

The question that arose was, is PG64-22 a better tack coat compared to the emulsions used? The first task undertaken to answer this question was a survey of practices followed by other departments of transportation. The survey included both the use of tack and prime coats.

In all, 26 states responded to the survey questionnaire. With regards to the use of prime coats, of the 26 states, 10 states responded that there is no requirement for the use of prime coats for new construction. Two states, Georgia and New Jersey, require use of prime coat if the AC thickness is less than 5 inches, and Missouri requires it if the AC thickness is less than 4 inches. With regards to the use of tack coats, a host of materials is used that includes emulsions as well as asphalt cements of various grades.

In North Carolina, CMS-2 emulsion is popularly used as tacking material. So in this study, its performance was compared to the asphalt cement with Superpave™ grade PG64-22.

The methodology used in this study to compare the performance of different tack and prime coats required first, the development of a 3-D computer program that takes into account the horizontal shear stresses induced on the pavement surface due to vehicle braking effects (acceleration and deceleration). Taking into account the induced shear loading, the shear stresses at the interface layers were computed. These shear stresses were then compared to the bond strength of the tack or prime coat under consideration. It should be

noted here that: 1) the induced shear stress at the interface depends on the AC overlay material properties as well as the temperature that the pavement is subjected to; and 2) the thickness of the overlay. If the induced shear stress is more than the bond strength, delamination will be imminent.

The tack coat performance was evaluated for both AC over AC and AC over PCC (PCC-AC) pavements. The results of this study indicate that PG64-22 used as a tack coat for AC-AC shows superior performance compared to the CMS-2 emulsion. There are two possible reasons for this: 1) the residual asphalt in CMS-2 emulsion had a Superpave™ grading of PG52 as compared to asphalt cement that was PG64 (higher viscosity); and 2) the rate of application was same for both tack coat, and therefore the amount of residual asphalt in CMS-2 is less.

On the other hand, for PCC-AC composite pavement, the CMS-2 emulsion performs better relative to the PG64-22. The reason for this behavior is attributed to the imperviousness of the PCC layer. It appears that a higher amount of PG64-22 actually enables the slippage between layers to occur more readily giving poor bond strength. It is, therefore, apparent that the application rate of tack coat plays a very important role. Too much will not only lead to delamination but may also result in bleeding of asphalt on the surface.

With respect to prime coats, three were evaluated in this study – CSS-1h, EPR-1, and EA-P. All three are on the NCDOT approved list. It should be noted here that prime coats are usually used on subgrades, subbases and aggregate bases. However, in this study CTB was used as it was not possible to determine the bond strength with subgrade or subbase due to their low stiffness. Results of the analysis conducted in this study shows that CSS-1h performs better than the other two emulsions. Mechanistic analysis indicates that, in general, a prime coat must be used to counteract induced shear stresses and hence prevent delamination when the AC overlay thickness is less than 3.5 to 4 inches. These results support current construction practices followed by Georgia, New Jersey, and Missouri.

Finally, this research study provides a methodology and design guide based on mechanistic analysis to select appropriate tack or prime coat for given field conditions. Based

on the AC layer thickness a suitable tack or prime coat can be chosen (or vice versa in some cases) to minimize the delamination distress.

Key Words: Mechanistic design, interfacial shear stress, delamination, debonding, bond strength, shear testing, axial testing, slippage, tack coat, prime coat, PCC, CTB, AC

Table of Contents

DISCLAIMER	ii
ACKNOWLEDGEMENTS	iii
EXECUTIVE SUMMARY	iv
TABLE OF CONTENTS	vii
LIST OF TABLES	xi
LIST OF FIGURES	xiii
LIST OF ABBREVIATIONS AND SYMBOLS	xvii
1 BACKGROUND	1
1.1 INTRODUCTION	1
1.2 LITERATURE SURVEY	3
1.2.1 Study by Mohammad et al [31]	3
1.2.2 Study by Shahin et al [35]	4
1.2.3 Study by Uzan et al [47, 48]	5
1.2.4 Study by Tschegg et al [45]	7
1.2.5 Study by Ameri-Gaznon et al [7]	8
1.2.6 Study by Ishai et al [25]	10
1.2.7 Study by Hachiya et al [21]	11
1.2.8 Study by Mukhtar et al [32]	13
1.2.9 Study by Sholar et al [38]	13
1.2.10 Prime Coats	14
1.2.11 Tack Coats	15
1.3 RESEARCH NEED	16
1.3.1 Prior Work	16
2 RESEARCH APPROACH AND METHODOLOGY	19
2.1 OBJECTIVE	19
2.2 RESEARCH METHODOLOGY	19
2.2.1 Literature Review and Survey	19
2.2.2 Asphalt and Mastics Testing	20
2.2.3 SST Testing of SGC Specimens, TSR and APA Tests	20
2.2.4 Material Characterization	21
2.2.5 Fabrication of Slabs and Test Specimens	21
2.2.6 Bond Strength Determination using Shear Testing	22
2.2.7 Mechanistic Analysis	22
3 SURVEY RESULTS	24
3.1 DEVELOPMENT OF QUESTIONNAIRE	24
3.2 SURVEY RESPONSES	24
4 RHEOLOGICAL EVALUATION	28
4.1 INTRODUCTION	28
4.2 SELECTION OF FINES	28
4.3 GRADATION ANALYSIS OF FINES USING FHWA PARTICLE ANALYZER	29
4.3.1 Method Description	29
4.3.2 Results and Discussion	29

4.4	<u>ANALYSIS OF ASPHALT -FINES MASTICS USING DSR</u>	30
4.4.1	<u>Specimen Preparation</u>	31
4.4.2	<u>Test Parameters</u>	31
4.4.3	<u>Test Results and Discussion</u>	32
4.5	<u>DSR TESTING OF EMULSIONS</u>	33
4.5.1	<u>Test Results and Discussion</u>	34
4.6	<u>BROOKFIELD VISCOSITY</u>	35
4.7	<u>CONCLUSIONS</u>	35
5	<u>PERFORMANCE TESTING OF SGC SPECIMENS</u>	45
5.1	<u>INTRODUCTION</u>	45
5.2	<u>TEST PARAMETERS</u>	45
5.3	<u>TEST TEMPERATURE</u>	46
5.3.1	<u>Selection of Testing Temperature</u>	46
5.3.2	<u>Temperature Zones</u>	46
5.3.3	<u>Selection of Depth for Computation of Testing Temperature</u>	47
5.3.4	<u>Reliability Factors</u>	47
5.3.5	<u>Temperature Selection Method</u>	47
5.4	<u>PERFORMANCE TEST RESULTS OF LAB MIXES WITH BAGHOUSE FINES</u>	48
5.4.1	<u>Specimen Fabrication</u>	48
5.4.2	<u>FSCH Test</u>	49
5.4.3	<u>RSCH Test</u>	50
5.5	<u>ASPHALT PAVEMENT ANALYZER TESTS</u>	51
5.5.1	<u>APA Test Results</u>	52
5.6	<u>EFFECT OF BAGHOUSE FINES ON MOISTURE SENSITIVITY</u>	52
5.7	<u>SUMMARY AND CONCLUSION</u>	53
6	<u>SPECIMEN FABRICATION USING ROLLING WHEEL COMPACTOR</u>	64
6.1	<u>INTRODUCTION</u>	64
6.2	<u>FABRICATION OF STEEL MOLDS</u>	64
6.3	<u>SPECIMEN FABRICATION</u>	65
6.3.1	<u>Asphalt Concrete Slabs</u>	65
6.3.2	<u>Portland Cement Concrete Slabs</u>	66
6.3.3	<u>Cement Treated Base Slab</u>	66
6.4	<u>TACK / PRIME COAT APPLICATION</u>	67
6.5	<u>CORING AND CUTTING SAMPLES</u>	68
7	<u>MATERIAL CHARACTERIZATION</u>	76
7.1	<u>INTRODUCTION</u>	76
7.2	<u>ASPHALT MIX CHARACTERIZATION</u>	76
7.2.1	<u>Frequency Sweep Test at Constant Height (FSCH)</u>	77
7.2.2	<u>Repeated Shear Test at Constant Height (RSCH)</u>	78
7.2.3	<u>Axial Frequency Sweep Test (AFST)</u>	78
7.2.4	<u>Repeated Axial Test</u>	79
7.3	<u>PORTLAND CEMENT CONCRETE (PCC) CHARACTERIZATION</u>	80
7.3.1	<u>Mixing, Casting and Curing of Specimens</u>	80
7.3.2	<u>Compressive Strength of Cylindrical Concrete Specimens</u>	82
7.3.3	<u>Modulus of Rupture for Concrete Specimens</u>	83
7.3.4	<u>Splitting Tension Test for Concrete Specimens</u>	83
7.3.5	<u>Elastic Modulus Test for Concrete Specimens</u>	83
7.4	<u>CEMENT TREATED BASE (CTB) CHARACTERIZATION</u>	84
7.4.1	<u>CTB Composition</u>	84
7.4.2	<u>Atterberg Limits for CTB Aggregates</u>	85
7.4.3	<u>Modified Proctor Density Test</u>	85
8	<u>BOND STRENGTH DETERMINATION</u>	107

8.1	<u>INTRODUCTION</u>	107
8.1.1	<u>Shear Test Description</u>	107
8.2	<u>BOND STRENGTH USING METAL PLATENS</u>	108
8.3	<u>BOND STRENGTH OF AC-AC SPECIMENS</u>	109
8.3.1	<u>Axial and Shear Ramp Test</u>	109
8.3.2	<u>Axial Test Results</u>	110
8.3.3	<u>Shear Test Results</u>	110
8.4	<u>BOND STRENGTH OF PCC-AC SPECIMENS</u>	111
8.5	<u>BOND STRENGTH OF CTB-AC SPECIMENS</u>	113
8.6	<u>SUMMARY AND CONCLUSIONS</u>	115
9	<u>DEVELOPMENT OF DESIGN GUIDELINES FOR USE OF TACK AND PRIME COATS</u>	135
9.1	<u>3-D LAYERED ELASTIC PROGRAM DESCRIPTION</u>	135
9.2	<u>LOAD CONDITIONS</u>	136
9.3	<u>TEMPERATURE EFFECTS</u>	137
9.4	<u>ANALYSIS OF AC-AC BONDING</u>	138
9.5	<u>ANALYSIS OF PCC-AC BONDING</u>	139
9.6	<u>ANALYSIS OF CTB-AC BONDING</u>	140
9.7	<u>OUTLINE OF GUIDELINE DEVELOPMENT FOR USE OF TACK OR PRIME COAT</u>	141
9.8	<u>SUMMARY AND CONCLUSIONS</u>	141
10	<u>SUMMARY, CONCLUSIONS AND RECOMMENDATIONS</u>	150
11	<u>ANALYSIS OF STRESSES IN PAVEMENTS: LITERATURE REVIEW</u>	156
11.1	<u>INTRODUCTION</u>	156
11.2	<u>PAVEMENT MODELING</u>	156
11.2.1	<u>Analytic Methods</u>	156
11.2.2	<u>Numerical Methods</u>	157
11.2.3	<u>Semi-Analytic Finite Element Method</u>	158
11.3	<u>APPROACH TO BE USED</u>	158
12	<u>3-D ANALYSIS OF LAYERED LINEAR ELASTIC PAVEMENT SYSTEM UNDER VERTICAL AND HORIZONTAL LOADING</u>	160
12.1	<u>GENERAL APPROACH AND FORMULATION</u>	160
12.1.1	<u>Vertical Load over a Circular Area on Layered System</u>	160
12.1.2	<u>Horizontal Load over a Circular Area on Layered System</u>	166
12.2	<u>TEST PROBLEMS</u>	177
12.2.1	<u>Stresses under a Uniform Vertical Load: Half Space</u>	177
12.2.2	<u>Stresses under Uniform Vertical Load: 3-Layered System</u>	178
12.2.3	<u>Stresses under Uniform Horizontal Load: Half Space</u>	178
12.2.4	<u>Stresses under Uniform Horizontal Load: 2-Layered System</u>	178
12.3	<u>PAVEMENT DELAMINATION ANALYSIS</u>	179
12.3.1	<u>Effect of Various Magnitude of Horizontal Load and Constant Vertical Load on Interlayer Shear Stress</u>	181
12.3.2	<u>Effect of Overlay Thickness on Interlayer Shear Stress: Only Horizontal load Applied</u>	182
12.3.3	<u>Effect of Overlay Thickness on Interlayer Shear Stress: Both Vertical and Horizontal Loadings Applied</u>	182
12.3.4	<u>Effect of Anisotropic Properties of Layer Material on Shear Stress at the Interface</u>	183
12.3.5	<u>Effect of Layer Modulus on Maximum Interlayer Shear Stress</u>	185
12.4	<u>SUMMARY</u>	185
13	<u>REFERENCES</u>	201
	APPENDIX A	207
	APPENDIX B	209
	APPENDIX C	215

APPENDIX D	219
APPENDIX E	224
APPENDIX F	234
APPENDIX G	241

List of Tables

TABLE 4-1 PROPERTIES OF FINES FROM PARTICLE SIZE ANALYSIS (SET 2) [23]	36
TABLE 4-2 TEMPERATURES FOR RESIDUAL BINDERS WHEN $G^* /\sin\delta \geq 1.0$ KPA	36
TABLE 5-1 AIR VOIDS AND G_{MM} OF 150-MM DIAMETER LABORATORY MIX SPECIMENS	54
TABLE 5-2 NATIONWIDE PAVEMENT TEMPERATURES, [37]	54
TABLE 5-3 AVERAGE DEPTHS AND TEST TEMPERATURES	54
TABLE 5-4 G^* (PA) VERSUS FREQUENCY (HZ) FOR LAB MIXES, 50.2 °C, BUNCOMBE COUNTY	55
TABLE 5-5 δ(DEGREES) VERSUS FREQUENCY (HZ) FOR LAB MIXES, 50.2 °C, BUNCOMBE COUNTY	55
TABLE 5-6 AVERAGE G^*, δ, AND $G^* /\sin \delta$ VALUES, 50.2 °C, LAB MIXES BUNCOMBE COUNTY	55
TABLE 5-7 G^* (PA) VERSUS FREQUENCY (HZ) FOR LAB MIXES, 50.2 °C, RUTHERFORD COUNTY	56
TABLE 5-8 δ(DEGREES) VERSUS FREQUENCY (HZ) FOR LAB MIXES, 50.2 °C, RUTHERFORD COUNTY	56
TABLE 5-9 AVERAGE G^*, δ, AND $G^* /\sin \delta$ VALUES, 50.2 °C, LAB MIXES RUTHERFORD COUNTY	56
TABLE 5-10 STRAIN AT THE END OF RSCH TEST, 50.2 °C, LAB MIXES	57
TABLE 5-11 AIR VOIDS AND HEIGHTS OF 6-INCH DIAMETER LABORATORY SPECIMENS FOR APA TEST	57
TABLE 5-12 BUNCOMBE COUNTY (WITH BAGHOUSE FINES) TSR RESULTS (4-INCH SPECIMENS)	57
TABLE 5-13 BUNCOMBE COUNTY (W/OUT BAGHOUSE FINES) TSR RESULTS (4-INCH SPECIMENS)	57
TABLE 5-14 RUTHERFORD COUNTY (WITH BAGHOUSE FINES) TSR RESULTS (4-INCH SPECIMENS)	58
TABLE 5-15 RUTHERFORD COUNTY (W/OUT BAGHOUSE FINES) TSR RESULTS (4-INCH SPECIMENS)	58
TABLE 5-16 SUMMARY OF TSR RESULTS	58
TABLE 7-1 AIR VOIDS OF AC MIX SAMPLES	86
TABLE 7-2 G^* VS. FREQUENCY FOR AC MIX, 20 °C, IN PA	86
TABLE 7-3 SHEAR PHASE ANGLE (DEGREES) VS. FREQUENCY FOR AC MIX, 20 °C	87
TABLE 7-4 G^* VS. FREQUENCY FOR AC MIX, 30 °C, IN PA	87
TABLE 7-5 SHEAR PHASE ANGLE (DEGREES) VS. FREQUENCY FOR AC MIX, 30 °C	87
TABLE 7-6 G^* VS. FREQUENCY FOR AC MIX, 40 °C, IN PA	88
TABLE 7-7 SHEAR PHASE ANGLE (DEGREES) VS. FREQUENCY FOR AC MIX, 40 °C	88
TABLE 7-8 G^* VS. FREQUENCY FOR AC MIX, 60 °C, IN PA	88
TABLE 7-9 SHEAR PHASE ANGLE (DEGREES) VS. FREQUENCY FOR AC MIX, 60 °C	89
TABLE 7-10 RSCH CYCLES, AT 40 AND 60 °C	89
TABLE 7-11 AIR VOIDS OF AXIAL TEST SAMPLES	89
TABLE 7-12 E^* VS. FREQUENCY FOR AC MIX, 20 AND 30 °C, IN PA	89
TABLE 7-13 AXIAL PHASE ANGLE (DEGREES) VS. FREQUENCY FOR AC MIX, 20 AND 30 °C	90
TABLE 7-14 E^* VS. FREQUENCY FOR AC MIX, 40 AND 60 °C, IN PA	90
TABLE 7-15 AXIAL PHASE ANGLE (DEGREES) VS. FREQUENCY FOR AC MIX, 40 AND 60 °C	90
TABLE 7-16 REPEATED AXIAL TEST CYCLES, AT 40 AND 60 °C	90
TABLE 7-17 AGGREGATE MOISTURE CONTENTS AND SPECIFIC GRAVITIES	91
TABLE 7-18 BATCH WEIGHTS FOR PCC	91
TABLE 7-19 PROPERTIES OF CONCRETE	91
TABLE 7-20 ELASTIC MODULUS FOR PCC	91
TABLE 7-21 GRADATION (% PASSING) FOR AGGREGATE PILES USED FOR CTB	92
TABLE 7-22 GRADATION CRITERIA FOR MATERIAL PASSING #10 SIEVE (SOIL MORTAR)	92
TABLE 7-23 MOISTURE DENSITY DETERMINATION FOR CTB	92
TABLE 7-24 LIQUID LIMIT PROPERTY FOR CTB USING DOT MODIFIED METHOD	92
TABLE 8-1 RESULTS FOR AC-AC AXIAL RAMP TESTS (TENSILE), 40 °C	116
TABLE 8-2 RESULTS FOR AC-AC AXIAL RAMP TESTS (TENSILE), 60 °C	116
TABLE 8-3 RESULTS FOR AC-AC SHEAR RAMP TESTS, 20 °C	117
TABLE 8-4 RESULTS FOR AC-AC SHEAR RAMP TESTS, 40 °C	117
TABLE 8-5 RESULTS FOR AC-AC SHEAR RAMP TESTS, 60 °C	117
TABLE 8-6 RESULTS FOR PCC-AC SHEAR RAMP TESTS, 20 °C	118

TABLE 8-7 RESULTS FOR PCC-AC SHEAR RAMP TESTS, 40 °C	118
TABLE 8-8 RESULTS FOR PCC-AC SHEAR RAMP TESTS, 60 °C	118
TABLE 8-9 RESULTS FOR CTB-AC SHEAR RAMP TESTS, 40 °C	119
TABLE 8-10 RESULTS FOR CTB-AC SHEAR RAMP TESTS, 60 °C	119
TABLE 9-1 RECOMMENDED MINIMUM SKID NUMBERS FOR RURAL HIGHWAYS [28]	143
TABLE 9-2 INTERFACIAL SHEAR BOND STRENGTH SUMMARY FOR PG64-22 AND CMS-2	143
TABLE 9-3 AC-CTB SHEAR BOND STRENGTH SUMMARY FOR CSS-1H, EA-P, AND EPR-1	143
TABLE 12-1 BRAKING EFFECT AND FORCE TRANSFERRED TO THE PAVEMENT DUE TO SKID RESISTANCE [1]	186
TABLE 12-2 MAXIMUM SHEAR STRESS PRODUCED BY VARIOUS MODULI OF THE FIRST AND SECOND LAYERS	187

List of Figures

FIGURE 1-1 DELAMINATION OF SURFACE COURSE (SOURCE: HTTP://WWW.KOCHPAVEMENTSOLUTIONS.COM/DISTRESSES/PUSHING.HTM)	2
FIGURE 1-2 DELAMINATION, EXPOSURE OF UNDERLYING LAYER (SRC: HTTP://WWW.DEFENCE.GOV.AU/DEMG/7TECHNICAL_GUIDANCE/AIRCRAFT_PAVEMENT_MANUAL/PART_A/A4.HTM)	2
FIGURE 1-3 DISTORTION AND SHOWING, DEFORMATION OF SURFACE LAYER UNDER LOAD (SRC: HTTP://WWW.DEFENCE.GOV.AU/DEMG/7TECHNICAL_GUIDANCE/AIRCRAFT_PAVEMENT_MANUAL/PART_A/A4.HTM)	2
FIGURE 1-4 TYPICAL SLIPPAGE FAILURE [17, 32]	3
FIGURE 1-5 COLLARS DESIGNED FOR TESTING SAMPLES IN SHEAR, [31]	4
FIGURE 1-6 SCHEMATIC OF SPECIMEN DEFORMATION DURING SHEAR TESTING, [48]	7
FIGURE 1-7 SPECIMEN SHAPES FOR WEDGE SPLITTING TESTS, [45]	9
FIGURE 1-8 SETUP OF WEDGE SPLITTING TEST, [45]	9
FIGURE 1-9 SPECIMEN SHAPES AND TESTING METHOD, [21]	12
FIGURE 1-10 SHEAR TEST ON EMULSIONS, [21]	12
FIGURE 1-11 SPECIMENS WITH TACK COAT AT INTERFACE, [32]	13
FIGURE 1-12 SHEARING DEVICE DEVELOPED BY SHOLAR ET AL [38]	14
FIGURE 2-1 SUMMARY OF RESEARCH OUTLINE AND METHODOLOGY	23
FIGURE 4-1 GRADATION ANALYSIS OF FINES USING FHWA PARTICLE ANALYZER, SET 2	37
FIGURE 4-2 GRADATION ANALYSIS OF FINES USING FHWA PARTICLE ANALYZER, SET 1	37
FIGURE 4-3 MASTER CURVES (G^*) FOR BUNCOMBE COUNTY, 64°C	38
FIGURE 4-4 MASTER CURVES (G^*) FOR RUTHERFORD COUNTY, 64°C	38
FIGURE 4-5 MASTER CURVES ($G^* /\sin \delta$) FOR BUNCOMBE COUNTY, UNAGED, 64°C	39
FIGURE 4-6 MASTER CURVES ($G^* /\sin \delta$) FOR BUNCOMBE COUNTY, AGED, 64°C	39
FIGURE 4-7 MASTER CURVES ($G^* /\sin \delta$) FOR RUTHERFORD COUNTY, UNAGED, 64°C	40
FIGURE 4-8 MASTER CURVES ($G^* /\sin \delta$) FOR RUTHERFORD COUNTY, AGED, 64°C	40
FIGURE 4-9 COMPARISON OF $G^* /\sin(\delta)$ AT VARIOUS TEMPERATURES FOR RESIDUAL BINDERS	41
FIGURE 4-10 COMPARISON OF G^* AT VARIOUS TEMPERATURES FOR RESIDUAL BINDERS	41
FIGURE 4-11 COMPARISON OF δ AT VARIOUS TEMPERATURES FOR RESIDUAL BINDERS	42
FIGURE 4-12 VISCOSITY VS. RPM, 150 °C	42
FIGURE 4-13 PERCENT TORQUE VS. RPM, 150 °C	43
FIGURE 4-14 VISCOSITY VS. RPM, 135 °C	43
FIGURE 4-15 PERCENT TORQUE VS. RPM, 135°C	44
FIGURE 5-1 NINE CLIMATIC REGIONS IN US	59
FIGURE 5-2 DYNAMIC SHEAR MODULUS (G^*) VS. FREQ., 50.2°C, BUNCOMBE, LAB MIXES	59
FIGURE 5-3 PHASE ANGLE (δ) VERSUS FREQUENCY, 50.2°C, BUNCOMBE, LAB MIXES	60
FIGURE 5-4 AVERAGE G^* AND δ VALUES VS. FREQ., 50.2°C, BUNCOMBE, LAB MIXES	60
FIGURE 5-5 DYNAMIC SHEAR MODULUS (G^*) VS. FREQ., 50.2°C, RUTHERFORD, LAB MIXES	61
FIGURE 5-6 PHASE ANGLE (δ) VS. FREQUENCY, 50.2°C, RUTHERFORD, LAB MIXES	61
FIGURE 5-7 AVERAGE G^* AND δ VALUES VS. FREQ., 50.2°C, RUTHERFORD, LAB MIXES	62
FIGURE 5-8 PLASTIC SHEAR STRAIN VS. RSCH CYCLES, 50.2°C, BUNCOMBE COUNTY, LAB MIXES	62
FIGURE 5-9 PLASTIC SHEAR STRAIN VS. RSCH CYCLES, 50.2°C, RUTHERFORD COUNTY, LAB MIXES	63
FIGURE 6-1 VIEW OF MOLD WITH ADJUSTABLE RAMPS (ON LEFT)	69
FIGURE 6-2 MOLD WITH ROLLER	69
FIGURE 6-3 FRESHLY CAST PCC SLAB	70
FIGURE 6-4 SIDE VIEW WITH ROLLER ON THE MOLD	70
FIGURE 6-5 PHOTO OF A 1-INCH THICK CTB ‘DISK’	71
FIGURE 6-6 CTB ‘DISKS’ COATED WITH EMULSION	71
FIGURE 6-7 MOLD TOP – PART J	72

FIGURE 6-8 MOLD BOTTOM – PART I	73
FIGURE 6-9 MOLD TOP – PART II	74
FIGURE 6-10 MOLD BOTTOM – PART II	75
FIGURE 7-1 DYNAMIC SHEAR MODULUS (G^*) VS. FREQUENCY FOR AC MIX, 20 °C	93
FIGURE 7-2 SHEAR PHASE ANGLE (δ) VS. FREQUENCY FOR AC MIX, 20 °C	93
FIGURE 7-3 DYNAMIC SHEAR MODULUS (G^*) VS. FREQUENCY FOR AC MIX, 30 °C	94
FIGURE 7-4 SHEAR PHASE ANGLE (δ) VS. FREQUENCY FOR AC MIX, 30 °C	94
FIGURE 7-5 DYNAMIC SHEAR MODULUS (G^*) VS. FREQUENCY FOR AC MIX, 40 °C	95
FIGURE 7-6 SHEAR PHASE ANGLE (δ) VS. FREQUENCY FOR AC MIX, 40 °C	95
FIGURE 7-7 DYNAMIC SHEAR MODULUS (G^*) VS. FREQUENCY FOR AC MIX, 60 °C	96
FIGURE 7-8 SHEAR PHASE ANGLE (δ) VS. FREQUENCY FOR AC MIX, 60 °C	96
FIGURE 7-9 AVERAGE DYNAMIC SHEAR MODULUS (G^*) VS. FREQUENCY FOR AC MIX	97
FIGURE 7-10 AVERAGE SHEAR PHASE ANGLE (δ) VS. FREQUENCY FOR AC MIX	97
FIGURE 7-11 G^* MASTER CURVE FOR AC MIX, 30 °C	98
FIGURE 7-12 SHEAR PHASE ANGLE (δ) MASTER CURVE FOR AC MIX, 30 °C	98
FIGURE 7-13 G^* MASTER CURVE FOR AC MIX, 40 °C	99
FIGURE 7-14 SHEAR PHASE ANGLE (δ) MASTER CURVE FOR AC MIX, 40 °C	99
FIGURE 7-15 G^* MASTER CURVE FOR AC MIX, 30 AND 40 °C	100
FIGURE 7-16 SHEAR PHASE ANGLE (δ) MASTER CURVE FOR AC MIX, 30 AND 40 °C	100
FIGURE 7-17 PLASTIC SHEAR STRAIN VS. RSCH CYCLES, 40 AND 60 °C FOR AC MIXES	101
FIGURE 7-18 DYNAMIC AXIAL MODULUS (E^*) VS. FREQUENCY FOR AC MIX	101
FIGURE 7-19 AVERAGE DYNAMIC AXIAL MODULUS (E^*) VS. FREQUENCY FOR AC MIX	102
FIGURE 7-20 AVERAGE AXIAL PHASE ANGLE (δ) VS. FREQUENCY FOR AC MIX	102
FIGURE 7-21 PLASTIC AXIAL STRAIN VS. CYCLES, 40 AND 60 °C FOR AC MIXES	103
FIGURE 7-22 RELATIONSHIP BETWEEN G^* AND E^* FOR AC MIXES	103
FIGURE 7-23 RELATIONSHIP BETWEEN SHEAR AND AXIAL PHASE ANGLE FOR AC MIXES	104
FIGURE 7-24 SET UP FOR ELASTIC MODULUS OF CONCRETE USING A 6×12 CYLINDER	104
FIGURE 7-25 AXIAL STRESS VS. STRAIN AT 7 DAYS FOR PCC	105
FIGURE 7-26 GRADATION OF MATERIALS USED FOR CTB	105
FIGURE 7-27 MOISTURE DENSITY CURVE FOR CTB	106
FIGURE 7-28 RESILIENT MODULUS OF CEMENT TREATED BASES (CTB), [1, 24]	106
FIGURE 8-1 DEBONDED COMPOSITE AC-AC SLAB WITHOUT TACK COAT	120
FIGURE 8-2 AXIAL FAILURE OF CMS-2 SPECIMEN (C4 6-3-2) AT 2.5 MM/MIN, 40 °C	120
FIGURE 8-3 AXIAL FAILURE OF CMS-2 SPECIMEN (C4 6-3-2) AT 2.5 MM/MIN, 40 °C	121
FIGURE 8-4 AXIAL FAILURE OF PG64-22 SPECIMEN (M1 5-16-2) AT 2.5 MM/MIN, 40 °C	121
FIGURE 8-5 AXIAL FAILURE OF PG64-22 SPECIMEN (M1 5-16-2) AT 2.5 MM/MIN, 40 °C	122
FIGURE 8-6 AVERAGE SHEAR STRESS VS. TIME FOR AC-AC INTERFACE TACKED WITH CMS-2	122
FIGURE 8-7 AVERAGE SHEAR STRESS VS. TIME FOR AC-AC INTERFACE TACKED WITH PG64-22	123
FIGURE 8-8 SUMMARY OF BOND STRENGTHS FOR AC-AC INTERFACE	123
FIGURE 8-9 SHEAR FAILURE OF CMS-2 SPECIMEN (M1 6-16-2) AT 1.0MM/MIN, 40 C	124
FIGURE 8-10 SHEAR FAILURE OF CMS-2 SPECIMEN (M3 6-3-2) AT 1.0MM/MIN, 40 C	124
FIGURE 8-11 SHEAR FAILURE OF CMS-2 SPECIMEN (C1 6-3-2) AT 2.5MM/MIN, 40 C	125
FIGURE 8-12 SHEAR FAILURE OF PG64-22 SPECIMEN (M1 5-7-2) AT 2.5 MM/MIN, 40 C	125
FIGURE 8-13 SHEAR FAILURE OF PG64-22 SPECIMEN (1MMC2 1) AT 1.0 MM/MIN, 20 C	126
FIGURE 8-14 SHEAR FAILURE OF PG64-22 SPECIMEN (25MMM3) AT 2.5 MM/MIN, 20 C	126
FIGURE 8-15 DEBONDING OF COMPOSITE PCC-AC SPECIMEN WITHOUT TACK COAT	127
FIGURE 8-16 DEBONDED COMPOSITE PCC-AC SLABS WITHOUT TACK COAT	127
FIGURE 8-17 AVERAGE SHEAR STRESS VS. TIME FOR PCC-AC INTERFACE TACKED WITH CMS-2	128
FIGURE 8-18 AVERAGE SHEAR STRESS VS. TIME FOR PCC-AC INTERFACE TACKED WITH PG64-22	128
FIGURE 8-19 SUMMARY OF BOND STRENGTHS FOR PCC-AC INTERFACE	129
FIGURE 8-20 PCC-AC SPECIMEN TACKED WITH PG64-22 (CRACKS HIGHLIGHTED IN WHITE)	129
FIGURE 8-21 PCC-AC SPECIMEN TACKED WITH CMS-2	130
FIGURE 8-22 COMPOSITE CTB-AC SPECIMEN	130
FIGURE 8-23 AVERAGE SHEAR STRESS VS. TIME FOR CTB-AC INTERFACE PRIMED WITH CSS-1H	131

FIGURE 8-24 AVERAGE SHEAR STRESS VS. TIME FOR CTB-AC INTERFACE PRIMED WITH EAP	131
FIGURE 8-25 AVERAGE SHEAR STRESS VS. TIME FOR CTB-AC INTERFACE PRIMED WITH EPR-1	132
FIGURE 8-26 SUMMARY OF BOND STRENGTHS FOR CTB-AC INTERFACE	132
FIGURE 8-27 CTB-AC SPECIMEN PRIMED WITH CSS-1H, SHEARED AT 1MM/MIN (40 °C)	133
FIGURE 8-28 CTB-AC SPECIMEN PRIMED WITH EPR-1, SHEARED AT 1MM/MIN (60 °C)	133
FIGURE 8-29 DEBONDED CTB-AC SPECIMEN PRIMED WITH EA-P, 60 °C	134
FIGURE 9-1 TIRE LAYOUT, TRAVEL DIRECTION, AND AXES ORIENTATION	144
FIGURE 9-2 AC AVERAGE 7-DAY MAXIMUM HIGH PAVEMENT TEMP. VS. DEPTH	144
FIGURE 9-3 DYNAMIC AXIAL MODULUS FOR ASPHALT MIXES VS. TEMPERATURE	145
FIGURE 9-4 PAVEMENT STRUCTURE AND LAYER PROPERTIES, AC OVER AC	145
FIGURE 9-5 MOBILIZED INTERFACIAL SHEAR VS. OVERLAY THICKNESS, AC-AC, 20 °C	146
FIGURE 9-6 MOBILIZED INTERFACIAL SHEAR VS. OVERLAY THICKNESS, AC-AC, 7-D MAX TEMP	146
FIGURE 9-7 PAVEMENT STRUCTURE AND LAYER PROPERTIES, AC OVER PCC	147
FIGURE 9-8 MOBILIZED INTERFACIAL SHEAR VS. OVERLAY THICKNESS, PCC-AC, 20 °C	147
FIGURE 9-9 MOBILIZED INTERFACIAL SHEAR VS. OVERLAY THICKNESS, PCC-AC, 7-D MAX TEMP	148
FIGURE 9-10 PAVEMENT STRUCTURE AND LAYER PROPERTIES, AC OVER CTB	148
FIGURE 9-11 MOBILIZED INTERFACIAL SHEAR VS. OVERLAY THICKNESS, CTB-AC, 40 °C	149
FIGURE 9-12 MOBILIZED INTERFACIAL SHEAR VS. OVERLAY THICKNESS, CTB-AC, 7-D MAX TEMP	149
FIGURE 12-1 MODEL OF LAYERED PAVEMENT SYSTEM	188
FIGURE 12-2 ILLUSTRATION OF NORMAL STRESS AND SHEAR STRESS AT THE INTERFACE	188
FIGURE 12-3 CONTINUITY CONDITION AT THE INTERFACE	189
FIGURE 12-4 INTEGRATION SCHEME	189
FIGURE 12-5 FLOW CHART FOR SOLUTION PROCEDURE	190
FIGURE 12-6 AXIS TRANSFORMATION	190
FIGURE 12-7 NORMAL STRESS DISTRIBUTIONS ALONG THE CENTERLINE FOR SINGLE LAYER	191
FIGURE 12-8 NORMAL STRESS DISTRIBUTIONS ALONG THE CENTERLINE FOR A THREE-LAYERED SYSTEM	191
FIGURE 12-9 DISTRIBUTION OF STRESSES AT SURFACE $Z/A = 1$ FOR A HALF SPACE	192
FIGURE 12-10 INTERFACE SHEAR STRESS FOR A TWO-LAYERED SYSTEM SUBJECTED TO CIRCULAR SHEAR LOAD AT SURFACE	192
FIGURE 12-11 TYPICAL SLIPPAGE FAILURE [17, 32]	193
FIGURE 12-12 PAVEMENT MODEL USED IN THE ANALYSIS	193
FIGURE 12-13 DISTRIBUTION OF SHEAR STRESS t_{xz} AT THE INTERFACE ($z=1.5''$) ALONG Y-AXIS (VP: VERTICAL PRESSURE, HP: HORIZONTAL PRESSURE)	194
FIGURE 12-14 DISTRIBUTION OF SHEAR STRESS t_{yz} AT THE INTERFACE ($z=1.5''$) ALONG X-AXIS (VP: VERTICAL PRESSURE, HP: HORIZONTAL PRESSURE)	194
FIGURE 12-15 3-D PRESENTATION OF SHEAR STRESS RESULTANT AT THE INTERFACE ($z=1.5''$)	195
FIGURE 12-16 DISTRIBUTION OF SHEAR STRESS RESULTANT AT THE INTERFACE ($z = 1.5''$) FOR VARIOUS THICKNESS OF THE OVERLAY AND ONLY 68PSI HORIZONTAL LOAD BEING APPLIED	195
FIGURE 12-17 DISTRIBUTION OF SHEAR STRESS AT THE INTERFACE ($z = 1.5''$) FOR VARIOUS THICKNESS OF THE FIRST LAYER WITH 100PSI VERTICAL PRESSURE AND 68PSI HORIZONTAL PRESSURE BEING APPLIED	196
FIGURE 12-18 COMPARISON OF SHEAR STRESS AT THE FIRST INTERFACE BETWEEN ISOTROPIC AND ANISOTROPIC CASES OF FIRST LAYER UNDER 100PSI VERTICAL PRESSURE OF BOTH TIRES	196
FIGURE 12-19 COMPARISON OF SHEAR STRESS AT THE FIRST INTERFACE BETWEEN ISOTROPIC AND ANISOTROPIC CASES OF FIRST LAYER UNDER 50PSI HORIZONTAL PRESSURE OF BOTH TIRES	197
FIGURE 12-20 COMPARISON OF SHEAR STRESS AT THE FIRST INTERFACE BETWEEN ISOTROPIC AND ANISOTROPIC CASES OF FIRST LAYER UNDER 100PSI VERTICAL PRESSURE AND 50PSI HORIZONTAL PRESSURE OF BOTH TIRES	197
FIGURE 12-21 COMPARISON OF SHEAR STRESS AT THE FIRST INTERFACE BETWEEN ISOTROPIC AND ANISOTROPIC CASES OF SECOND LAYER UNDER 100PSI VERTICAL PRESSURE OF BOTH TIRES	198
FIGURE 12-22 COMPARISON OF SHEAR STRESS AT THE FIRST INTERFACE BETWEEN ISOTROPIC AND ANISOTROPIC CASES OF SECOND LAYER UNDER 50PSI HORIZONTAL PRESSURE OF BOTH TIRES	198
FIGURE 12-23 COMPARISON OF SHEAR STRESS AT THE FIRST INTERFACE BETWEEN ISOTROPIC AND ANISOTROPIC CASES OF SECOND LAYER UNDER 100PSI VERTICAL PRESSURE AND 50PSI HORIZONTAL PRESSURE OF BOTH TIRES	199

[FIGURE 12-24 COMPARISON OF SHEAR STRESS AT THE FIRST INTERFACE AMONG 4 CASES UNDER 100PSI VERTICAL PRESSURE AND 50PSI HORIZONTAL PRESSURE OF BOTH TIRES](#) 199

[FIGURE 12-25 RELATIONSHIP BETWEEN MAXIMUM SHEAR STRESS AND MODULUS WHEN UPPER TWO LAYERS ARE OF SAME MODULUS](#)200

[FIGURE 12-26 VARIATION OF MAXIMUM SHEAR STRESS WITH MODULUS OF FIRST LAYER HIGHER THAN SECOND LAYER](#).....200

List of Abbreviations and Symbols

$ G^* $	magnitude of complex shear modulus
δ	phase angle
d/a	Distance Ratio, distance from the center of wheel divided by contact radius
AC	Asphalt Concrete
AEA	Air Entraining Admixture
AFST	Axial Frequency Sweep Test
APA	Asphalt Pavement Analyzer
ASTM	American Society of Testing and Materials
BISAR	Bitumen Structures Analysis in Roads
CMS	Cationic Medium Setting emulsion
CRS	Cationic Rapid Setting emulsion
CSS	Cationic Slow Setting emulsion
CTB	Cement Treated Base
DSR	Dynamic Shear Rheometer
FSCH	Frequency Sweep test at Constant Height
G_{mm}	Theoretical Maximum Specific Gravity (ASTM D2041)
HDS	High Density Surface course
HF-	High Float
MC	Medium Curing cutback
MTS	Material Test System
MS	Anionic Medium Setting emulsion

NCDOT	North Carolina Department of Transportation
PCC	Portland Cement Concrete
PG	Performance Graded
RC	Rapid Curing cutback
RS	anionic Rapid Setting emulsion
RSCH	Repeated Shear test at Constant Height
RV	Rotational Viscometer
SGC	Superpave Gyrotory Compactor
SN	Skid Number
SS	anionic Slow Setting emulsion
SST	Simple Shear Testing machine
SUPERPAVE™	SUperior PERforming PAVEMENTs
UTM	Universal Testing Machine

1 Background

1.1 Introduction

Asphalt pavements constitute 96 percent of the hard surfaced roads in the US. In terms of distance, approximately 2.2 million miles of roads have asphalt surfaces and approximately 91 percent of the 2 trillion annual vehicular miles of travel occur on these pavements. With an ever increasing number of vehicles on the roads, the need for proper maintenance of the existing infrastructure cannot be overemphasized.

Typically for thicker asphalt pavements, construction is done in layers. This is due to ease of construction and economic reasons. Before paving a rehabilitation asphalt layer, the top surface of the existing layer is cleaned and a tack coat is applied to bond the new surface to the underlying layer. The tack coat consists of a light application of asphalt binder, usually in the form of asphalt emulsion or liquid asphalt. For optimal performance, it is important that the tack coat be thin and uniform, and ‘breaks’ just before the new asphalt concrete layer is paved [33]. The process of breaking of an emulsion is characterized by the separation of liquid asphalt and water into two separate phases; after evaporation of water the residual asphalt forms a bond with the underlying surface. Similarly, prime coat is used between the aggregate base and the overlying layer. Functionally, it is same as the tack coat. For the pavement to be structurally and functionally sound there should be proper bonding between the structural layers. Lack of interface bonding may lead to several premature distresses of which slippage cracking, delamination and distortion are most prominent. Slippage cracks (Figure 1-4), formed in the surface course, are crescent shaped and are generally formed in the opposite direction of horizontal force on the pavement. Delamination (Figure 1-1 and Figure 1-2) involves loss of bond between various lifts of asphalt concrete and distortion (Figure 1-3) is the deformation occurring predominantly in the surface course. The loss of bond leads to increased subgrade deformation due to higher vertical compressive stresses and has a negative impact on ride quality. In the literature available so far, assumptions of either full friction or no friction between interlayer surfaces have been made when designing pavements. Although a lot of progress has been made in the field of polymer composites in modeling the interlayer bond behavior, similar research is lacking in the field of pavements.



Figure 1-1 Delamination of surface course

(Source: <http://www.kochpavementsolutions.com/Distresses/pushing.htm>)



Figure 1-2 Delamination, exposure of underlying layer

(Src: http://www.defence.gov.au/demg/7technical_guidance/aircraft_pavement_manual/part_a/a4.htm)



Figure 1-3 Distortion and shoving, deformation of surface layer under load

(Src: http://www.defence.gov.au/demg/7technical_guidance/aircraft_pavement_manual/part_a/a4.htm)

1.2 Literature Survey

Currently, the design and evaluation of flexible pavements is based on an elastic multi-layered analysis. For the design of pavements, the interfaces are assumed rough with no slippage occurring between the two layers. This, however, is not the case in practice. The state of adhesion at the interfaces between various layers affects the performance of flexible pavements by influencing the stressing level of materials. The stress distribution is more influenced by the interfacial condition of the upper layers than the lower ones. Hence, the knowledge of the interfacial conditions in the upper layers is important. Pertinent research conducted in the area of delamination and shoving is briefly described in the following section.

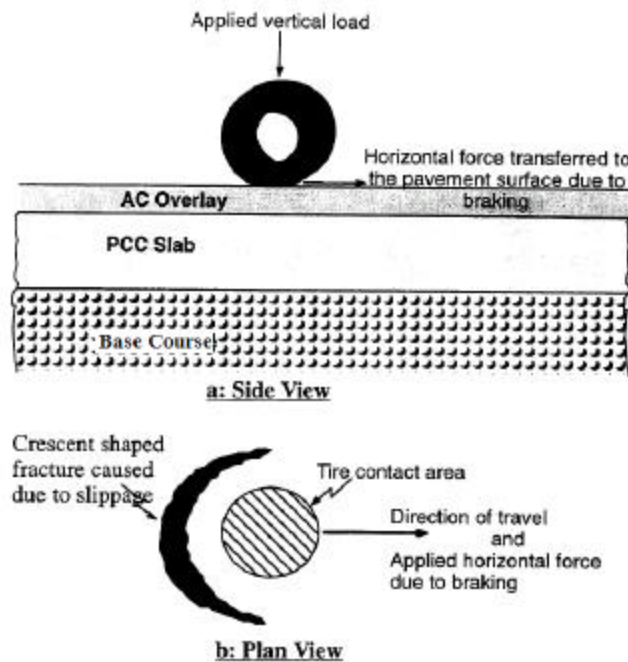


Figure 1-4 Typical slippage failure [17, 32]

1.2.1 Study by Mohammad et al [31]

Mohammad, et al [31] has measured the influence of different tack coats on interface shear strength. They conducted a load-controlled, simple shear test by shearing the specimens

at interface. Lateral confinement was provided by a collar (Figure 1-5) that ensured the failure was at interface and nowhere else. The specimens were manufactured in three steps:

- Compact the 'bottom' part of the specimen in a Superpave gyratory compactor
- After cooling, apply the tack coat at the specified rate
- Insert the 'bottom' specimen in the gyratory mold, pour loose asphalt mix over the tack coat, and compact.

The target air void content for each of the bottom and top specimens was 6%. Each of those specimens was tested in a SST machine at a loading rate of 50 lb/min until failure. The testing was conducted at temperatures of 25 and 55 °C. It was observed that CRS-2P emulsion performed better than PG64-22, PG76-22M, SS-1, SS-1H, and CSS-1h. In addition, for each of the tack coats, an optimum rate of application that gave the highest shear strength was determined. The study demonstrated that even under the most optimal performance of tack coat, the maximum strength attained is only 83% of monolithic mixture strength, implying that interfaces potentially cause slip planes.

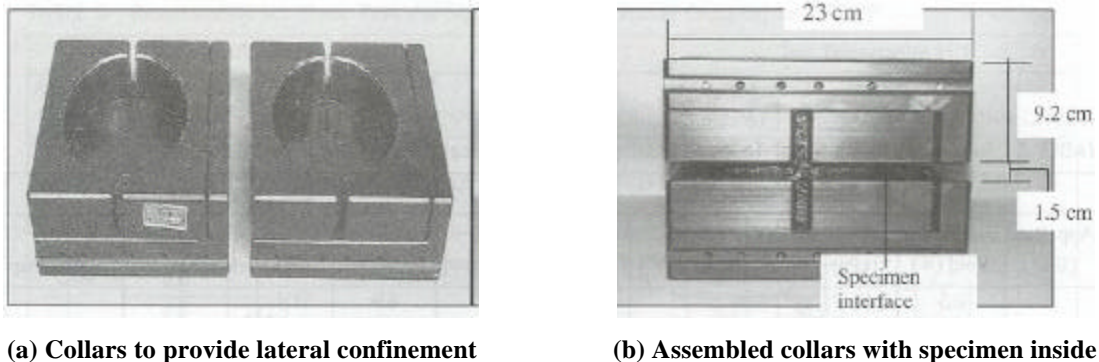


Figure 1-5 Collars designed for testing samples in shear, [31]

1.2.2 Study by Shahin et al [35]

Shahin et al [35] have discussed the effect of layer slippage on the performance of asphalt pavements. Using an example of an airfield pavement and with BISAR (Bitumen Structure Analysis in Roads) and the French Shell model [12] for analysis, various scenarios were evaluated about the fatigue life of the pavement. The pavement section considered had a 2-inch thick overlay over a 4-inch thick asphalt cement (AC) surface course. The base course

was 25-inches thick with elastic modulus of 75000 psi and a CBR value of 80. The subgrade was very weak with California Bearing Ratio (CBR) of 5 and stiffness of 7500 psi. The tensile stress at the bottom of the asphalt layers (overlay and the original surface course) and the vertical compressive strain on the subgrade were the criteria for failure. It was found that for full friction between the interfaces, the maximum tensile strain in the section is located at the bottom surface of the original asphalt layer. If the slippage was allowed below the uppermost layer, the tensile strain also existed at the bottom of the overlay. In addition, the following observations were made:

- Only a small amount of slippage is sufficient to produce strains in the pavement that approach those of the free slippage case.
- The tensile stress at the bottom of the overlay causes a compressive stress to develop on the upper surface of the asphalt surface layer. This causes a relative movement of points on the either side of the interface. This distortion further weakens the bond between the asphalt layers, allowing more slippage leading to higher strains.
- The subgrade strains increase with increasing slippage. Because two thinner layers are not as stiff as one layer of the same overall thickness, the compressive vertical strain on the subgrade increases.
- Further, under the action of horizontal loads, the study found that for no friction, the horizontal strains are much higher than those with full friction.

The principal normal tensile strains, developed by the horizontal loads along the back edge of the contact area, are of the same magnitude and cause progressive failure along the rear edge. This tensile failure would cause slippage cracks in the overlay. If the overlay is not properly bonded to the underlying layers, the overlay moves resulting in opening of the cracks. These cracks are crescent shaped. In order to fix these cracks, either the existing layer needs to be removed and re-paved or a thicker well-bonded overlay be placed on the existing overlay. In addition to strong interlayer bonding, the authors suggested an overlay stiffness of at least 500,000 psi and a minimum overlay thickness of 2 inch.

1.2.3 Study by Uzan et al [47, 48]

A research to evaluate the adhesion between asphalt mixes was conducted by Uzan, et al. [47, 48] using the Goodman's constitutive law:

$$\tau = K \cdot \Delta u$$

Equation 1-1

where:

τ is the shear stress at interface,

Δu the relative horizontal displacement of the two faces at the interface, and

K is the horizontal interface reaction modulus.

The interface behavior was described, which formerly was restricted only to perfectly rough or perfectly smooth conditions. The analysis was carried out using the BISAR program for a test section at different levels of adhesion. It was observed that for a perfectly smooth interface ($K=0$) the tensile radial strain at the bottom of the uppermost layer was higher than for the perfectly rough interface. The top of the second layer also changed to compressive strain when K approached zero. Further, it has been shown that even an adherence of 90% was very close to a smooth condition as described in Shahin et al [35]. Direct shear tests were performed on the layered asphalt concrete specimens with shearing along the tack coat and the variables were temperature, vertical pressure and rate of application of tack coat (Figure 1-6). It was concluded that the components of the interface shear strength were:

- Adhesion, represented by the tensile properties of the slip plane.
- Interlocking, from the penetration of aggregates into the voids of the other layer. The interlocking component depends on the texture of the surfaces in contact and properties of the asphalt mix.
- Friction, from rugosity of the two faces. Further, the friction component was included in the other two components. It was suggested that measurement of the adhesion component, which is indicated by rupture of the bond between layers in the bitumen or mastic phase, could be done by a tensile test. (The interlocking effect would be absent for pure tension.)

The following factors largely influenced the interface shear strength:

- Temperature: It is known that temperature affects the asphalt properties. The stiffness decreases with increase in the temperature and vice versa. The effect of higher temperatures is more dominant while testing in tension than in compression. In order to offset the effect of increased temperature, higher vertical pressures are applied. With

increasing vertical pressures, the interlocking component gets more dominant than the adhesion component.

- Tack Coat Rate: The tack coat bonding the two layers usually functions in two ways:
 - (a) Fill voids on the surface.
 - (b) Increase the interface film thickness or get absorbed in the adjacent layers.The filling of voids on the surface of the mixes increases the contact area and consequently the adhesion. However, excessive film thickness decreases the adhesion and aggregate interlock. Very low tack coat rate could mean loss of adhesion component. Hence, it is required that the tack coat be applied at optimum rate.
- Rate of Deformation: The rate of shear deformation is an important factor in controlling the strength and deformation ability of the interface. Generally, with increasing rate of deformation, the magnitude of stress developed increases.

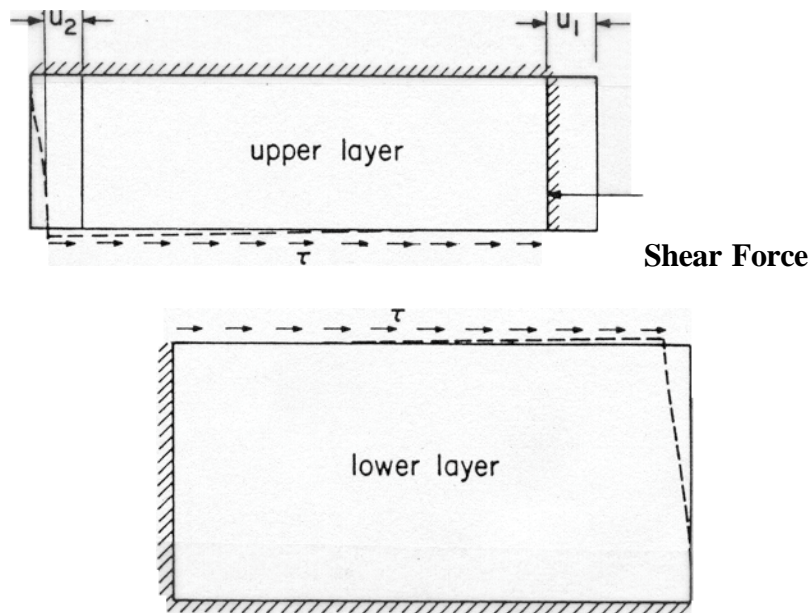


Figure 1-6 Schematic of specimen deformation during shear testing, [48]

1.2.4 Study by Tschegg et al [45]

A common method for measuring the bond strength of asphalt cores is the pull-off test [45]. For this test, cores with a diameter of 100 mm were drilled from the top surface

down through the overlay, through the interface, and about 50 mm into the base layer. Steel plates were glued to the top surface of the cores. Then the drill core was pulled off with a tension machine in axial direction of the base layer. The maximum load is registered during the pull-off test. This is a simple test method but gave only the adhesive tensile strength and showed extensive scattering of results. The reasons for wide scattering of results were: eccentricity of load, small core diameter and large aggregate size, notches at the surface of the cores by drilling or burst out aggregates, stress concentrations, uncontrolled temperature, and indentation effects owing to rough surfaces. In addition, the test was useless if the tensile strength of the mix was lower than the interface bond strength.

For avoiding such drawbacks, a 'Wedge Splitting Test' was developed. In this test, a block of asphalt concrete was made to crack along a predetermined joint at steady rate. The splitting was done by a wedge that was located in a groove between the two blocks of asphalt. The force and the displacements were recorded during stable crack propagation until complete separation of the specimen took place. Based on the shape of the force-displacement curve, a differentiation between brittle and ductile behavior is possible. Figure 1-7 and Figure 1-8 show the test setup and the specimens used for testing purposes. It was found that with increasing temperature, the plastic behavior of the asphalt increased. There was a decrease in the peak load values with an increase in the temperature. At low temperatures, it was found that the relationship between the force and the crack opening displacement was linear. However, this test could not distinguish between the two different types of tack coats used for that study.

1.2.5 Study by Ameri-Gaznon et al [7]

Ameri-Gaznon et al [7] evaluated the octahedral shear stress (OSS) and the octahedral shear stress ratio (OSR) for different pavement sections. In particular, the OSR and the rut resistance in an asphalt concrete pavement (ACP) overlay is evaluated based on the overlay thickness, interlayer bonding, effect of stiffness, and horizontal surface shear. The material properties of the bituminous materials were evaluated using the tri-axial test and cohesion, c , and angle of internal friction, f , values were determined at 104 °F at a loading rate of 4-inch per minute. The modified ILLIPAVE finite element computer program was used to calculate the OSRs within ACP layers.

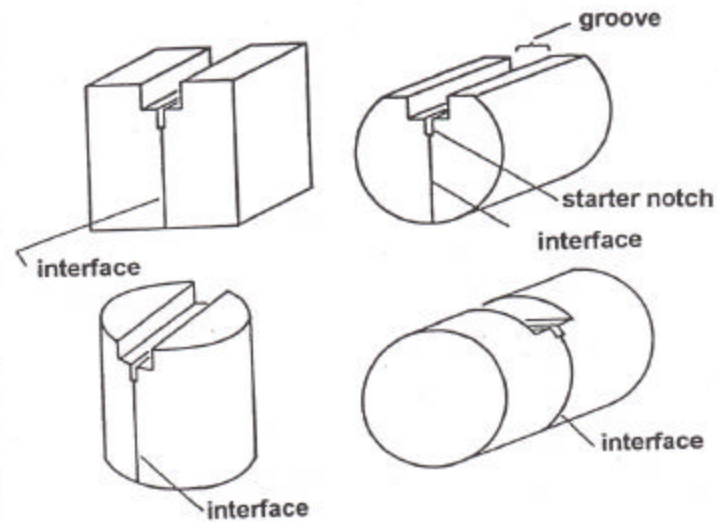


Figure 1-7 Specimen shapes for wedge splitting tests, [45]

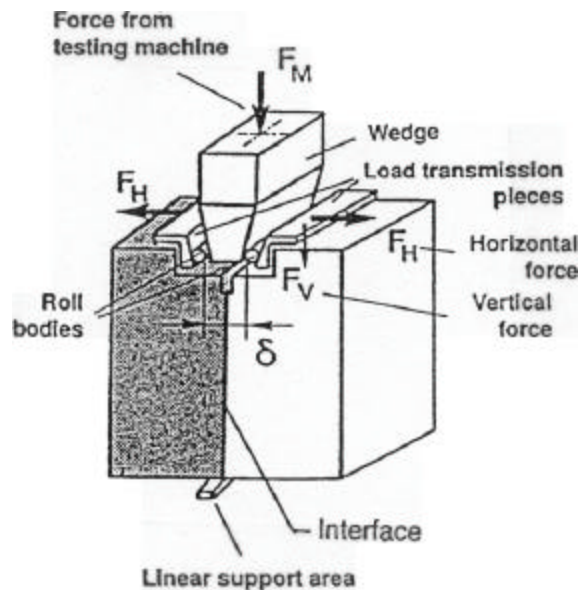


Figure 1-8 Setup of wedge splitting test, [45]

The effect of interfacial bonding has been discussed in great detail. In absence of interlayer bond, the overlay acts independently of the rest of the pavement system allowing greater relative movement between two asphalt layers. This reduces the confining stress

causing larger OSS in the overlay. Pavements of various thicknesses have been analyzed and the 4 inch thick overlay is the most critical one when there is free slippage.

With increase in the bonding, the critical thickness increases to 6 inches for ACP overlays. For a complete bond, the stress levels are critical at the mid height of the ACP overlay. With loss of bond, the critical stress shifts to the bottom of the surface layer. Also, the stress levels are far more critical than when a complete bond exists. Typically, with increasing stiffness, it is expected that the shear stresses would decrease but it works otherwise if there is a poor interlayer bond. The authors have also considered the effect of horizontal surface shear on pavements. It has been shown that presence of horizontal surface shear force doubles the OSS induced in the ACP overlay for full bond and no-bond conditions.

1.2.6 Study by Ishai et al [25]

The authors carried out an investigation on the functional and structural role of prime coat in flexible pavements. The areas of investigation were the contribution of prime coat to pavement performance and evaluation of emulsions as an alternative source of prime coats. The experimental program consisted of following:

- Evaluation of the rate of increase of viscosity and evaporation characteristics of the prime coat material.
- Measurement of absorption of prime coat material into the base course.
- Quantification of change in the hardness of the base layer with time.
- And adhesion between the base course and the asphalt layer.

The conclusions drawn from the tests were:

1. Cutbacks had higher viscosity than the emulsions. Hence, it was necessary to heat the cutbacks whereas there was no such problem with emulsions.
2. Rate of loss of liquid for emulsions is much higher than for cutbacks. This translates into faster construction of the overlying pavement structure. Also retention of organic vapors from cutbacks in the base layers could be detrimental to the overlying ACP, if paved immediately. In addition to this, cutback residues have lower viscosity than the emulsion residue, which translates to poorer interlayer bond for cutbacks.

3. The penetration of cutback was higher than that of the emulsions for granular material but for sandy material the values were comparable.
4. The surface hardness of the base layer was measured using a pocket penetrometer. It was found that for cutbacks there was not a significant gain of strength in the first ten days of curing, however, for emulsions, the strength gain was much faster. The accelerated rate of strength gain can be attributed to harder asphalt in the emulsions and faster curing.
5. The interfacial adhesion was measured using the direct shear test performed on composite samples of base and asphalt concrete layers. For unprimed surfaces, the failure was observed along the geometric interface between two layers. For a cutback prime coat, a little bonding was observed due to the interlocking effect created by absorption of the asphalt. The highest interface adhesion was observed when priming was done with emulsions. This could be because of deep penetration and strong adhesive bonds. Also, the failure shear stress was observed to be dependent on the vertical load due to more efficient interlocking and greater adhesion.

It can, therefore, be concluded that emulsion based prime coats enhance the shear strength of the interface at base and asphalt concrete layers.

1.2.7 Study by Hachiya et al [21]

The study consisted of mainly three steps. The first step consisted of analyzing an airport runway and taxiway using BISAR to calculate the interface shear stresses and strains. The results showed that shear stresses at interfaces depended on surface layer thickness (lower thickness producing higher shear stresses) and horizontal force on the surface. An increase in the horizontal force, in the form of acceleration and braking, caused an increase in the interfacial shear stresses. The pavement failure was caused by interlayer separation due to increased shear and tensile cracking at the bottom of the top layer. Construction of thicker lifts can help reduce the interlayer shear stresses. In the second step, laboratory tests were conducted on asphalt concrete specimens (Figure 1-9) and emulsions (Figure 1-10) in the laboratory. Asphalt specimens were tested in shear and tension at various temperatures in a strain-controlled mode. The interfaces (Figure 1-9) were hot jointed, cold jointed, tack coated (0.088 gal/yd²) and monolithic. Tack coated joints performed better than cold joints but not

as well as hot joints or monolithic construction. The interlayer shear strength was dependent on type of tack coat used (modified emulsions worked best), rate of application, curing time, and temperature. In the third part, three sections were constructed and subjected to loading by an assembly similar to aircraft landing gear. The top layer in each of the sections was of the same thickness but constructed differently: for the first section it was constructed in three lifts, for the second it was in two lifts, and for the third it was a single lift. The section constructed in a single lift rutted more than the other two, probably due to inadequate compaction at the bottom of the layer when placed in one deep lift. The section least likely to rut was the one with three lifts. Overall, it was suggested that adequate compaction combined with the use of modified emulsions could reduce the interlayer slippage on airport pavements.

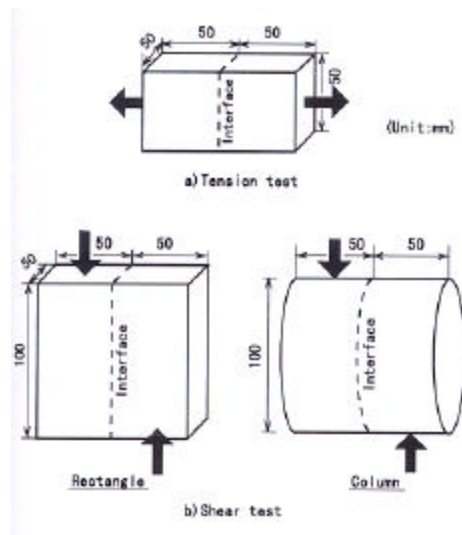


Figure 1-9 Specimen shapes and testing method, [21]

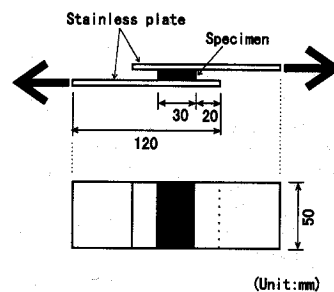


Figure 1-10 Shear test on emulsions, [21]

1.2.8 Study by Mukhtar et al [32]

Tests similar to the current study were conducted by Mukhtar et al [32] to evaluate the shear strength of AC-PCC interface. PCC specimens of dimensions shown in Figure 1-11 were cast and cured for a period of 28 days. Subsequently, a tack coat was applied at one of the surfaces and the PCC specimen was inserted in a mold having 2-inch internal diameter. Loose asphalt mix was compacted to a density of 147 pcf in three lifts each with 1-inch thickness. A vertical confining load of 79 psi was applied to simulate the field condition of having a 2.5 inch thick AC overlay over PCC. The specimens were then sheared at interface in a strain-controlled mode at rates of 1.0, 30 and 300 inch per min. The testing was carried out at temperatures of 0, 20, 40, 60, 80 and 100 °F. It was observed that, regardless of the testing temperature and shearing rate, monolithic AC specimens had higher shear strength than specimens jointed at the interface. The shear strength of the interface increased with higher rate of shear and lowering of temperature. Analysis performed by the authors indicated maximum shear stresses below the wheel.

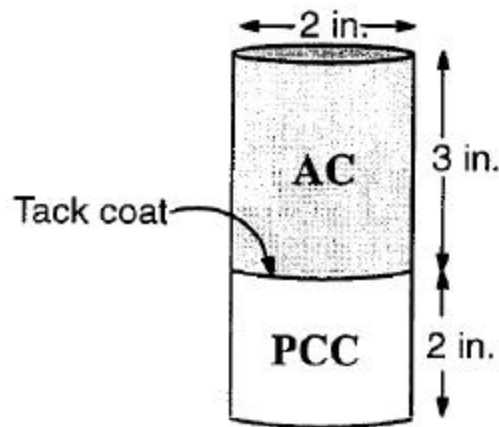


Figure 1-11 Specimens with tack coat at interface, [32]

1.2.9 Study by Sholar et al [38]

The authors have investigated the effect of different tack coat application rates, curing time, types of aggregates, rates of shear and moisture on the interfacial bond strength of composite asphalt specimens. A device, shown in Figure 1-12, was developed to measure the

test the specimens in shear. The device was mounted in a temperature controlled MTS test chamber. The shear strengths of composite samples were measured at constant strain rates. The shear strength of the interface was directly related to the rate of shear and inversely to the test temperature. It was observed that exposure of tack coat to moisture, prior to paving a new overlay, caused reduction in the interfacial shear strength. This emphasizes the need to have proper curing of tack coats before paving a new layer. Further, coarser gradations (19.0mm) performed significantly better than finer (12.5mm) gradations in terms of shear strengths. Increasing the rate of application of tack coat caused a marginal increase in the shear strength of the interface.

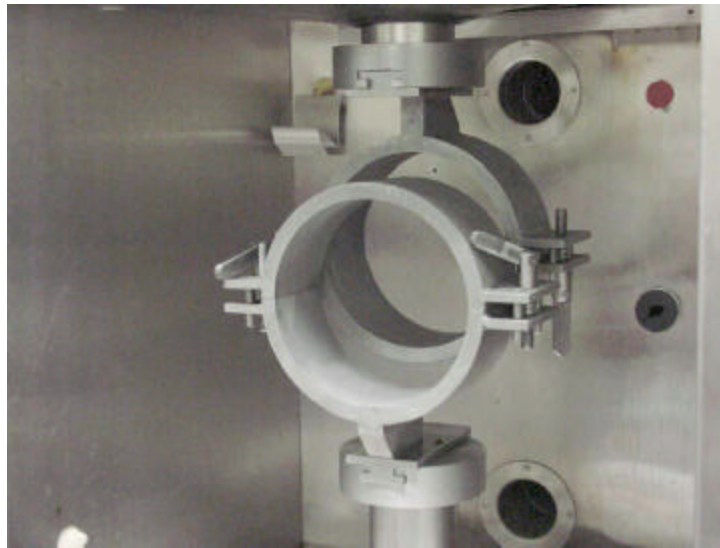


Figure 1-12 Shearing device developed by Sholar et al [38]

1.2.10 Prime Coats

Prime coating is the spray application of asphalt on the surface of a non-asphalt base course. Usually untreated materials are primed with cutback asphalt that helps waterproof the surface of the base, plug capillary voids, coat and bind loose mineral particles, and provide adhesion between the base and asphalt concrete. Although, emulsion based primes have been used as an alternative to cutback, HMA industry experience suggests that emulsions are not

as effective as cutbacks. Due to this reason, for many asphalt pavement constructions, priming is completely eliminated.

Asphalt Institute suggests that prime coats be used for asphalt layers less than 3-4 inches thick. This issue is particularly important for thick pavements placed directly on sub-base or base materials, especially in case of low-volume roads. During construction of pavement sections, asphalt concrete mats are usually placed in 1.5-2 inch lifts. Construction equipment such as rollers and heavy truck traffic can induce slippage distress in the first AC layer placed over the base even before the pavement is open to traffic. It is, therefore, critical to understand the contribution of prime coat in dissipating the induced shear stresses. Prior studies on the subject of prime coats have investigated the effectiveness of emulsions versus cutbacks, effectiveness of different emulsions, and construction techniques to improve prime coat performance. The current study measures the interlayer bond strength for various prime coats and attempts to correlate them to the mobilized interlayer shear stresses in typical pavement sections.

1.2.11 Tack Coats

In composite asphalt concrete pavements, tack coat provides the interface bond between two AC layers, or AC over PCC layers so that they form a monolithic structure to withstand traffic and environment. A strong tack coat is essential for the distribution of shear stresses within the pavement structure. Factors such as traffic level, interface bond strength and surface-layer thickness directly affect the performance and life of the pavement. The study outlined in the next section compares the bond strength of field cores tacked with PG64-22 and CRS-2.5. Certain types of tack coat (e.g. PG 64-22) have been found to perform better than others (e.g. CRS-2.5 emulsion). In North Carolina, efficient use of tack coat is critical for asphalt overlay construction, especially for overlay of the rigid concrete pavement surfaces that need to be opened to traffic within 12 to 24 hours. In many cases contractors preferably use PG64-22 asphalt cement as a tack coat over CRS-2.5 emulsion because the former does not require a curing period before opening to traffic.

For overlay as well as new construction of AC pavements, asphalt concrete mats are usually placed in 1.5-2 inch lifts. As discussed earlier for prime coats, construction

equipment and heavy truck traffic can induce slippage distresses during construction that can propagate to the surface. It is, therefore, necessary, to understand the relationship between tack coat bond strength and pavement layer thickness for dissipation of traffic induced shear stresses.

1.3 Research Need

The extensive network of highways and interstates add up to very high maintenance costs. The delamination distresses are due to traffic acceleration and deceleration. Poor tack coat undermines the pavement condition at these locations by increasing the shear stresses significantly. A study, that evaluates the material properties as well as their suitability, would enhance the quality of ride and extend the life of pavements thereby reducing the associated direct and indirect costs.

1.3.1 Prior Work

The motivation for this study was from an investigation launched in Division 13 of the North Carolina Department of Transportation (NCDOT), by Tayebali et al [43] to examine the severe distresses manifested in the form of asphalt concrete layer delamination and distortion. The goal was to evaluate and identify the causes of delamination and distortion of asphalt concrete mat. The methodology adopted for investigation consisted of evaluating the field cores and testing of laboratory prepared specimens. In the first stage a survey was conducted across plants in Division 13 of NCDOT to acquire information about the use of different tack coats and type of material used in the field. Based on the questionnaire responses, two sections were chosen, each with a different type of tack coat. Enka, Buncombe County and Rutherfordton, Rutherford County had used CRS-2.5 emulsion and PG64-22 binder, respectively, as a tack coat.

After the selection, cores of 4-inch and 6-inch diameters were drilled from distressed and non-distressed areas from two counties. The 4-inch specimens were used to determine whether the mixes conformed to the NCDOT job mix formula specifications based on air voids and Marshall mix design criteria. It was found that the mixes indeed conformed to the NCDOT specifications and the only possible cause of distress could be improper interlayer

bonding or construction technique. An on-site inspection and initial survey indicated no such construction abnormalities and the focus was to evaluate the interlayer bonding. The 6 inch diameter cores were tested on the Simple Shear Test (SST) machine.

A frequency sweep test at constant height (FSCH) was conducted on the cores from distressed and non-distressed sections. The test measures the shear viscoelastic properties (dynamic shear modulus, $|G^*|$, and the phase shift, δ) over a range of testing frequencies and at different temperatures. It should be noted that the measured dynamic response of the core is a composite response of the two asphalt layers separated by a thin film of tack coat. It was concluded from the FSCH test that cores from non-distressed sections had higher $|G^*|$ and $G^*/\sin \delta$ values over the cores from distressed sections. This implied that the non-distressed mixes had a higher stiffness and a lower propensity to rut justifying their better performance.

The repeated shear test at constant height (RSCH) was used to measure the rutting potential of the mix over a range of temperatures. This test is performed in a controlled stress mode in accordance with AASHTO TP-7, Procedure F [6]. The RSCH gave results similar to FSCH. It was found that non-distressed cores withstood higher number of cycles than the distressed cores. Also, for cores from Buncombe County (CRS-2.5) there was a distinct difference between the 'good' and 'bad' (i.e., non-distressed and distressed) cores. Examination of the failed core samples showed a distinct pattern of cracking with diagonal cracks in both upper and lower asphalt concrete layers with a horizontal crack joining the diagonal cracks at interface. It should be noted that CRS-2.5 was used as a bonding (tacking) agent. For Rutherford County (where PG64-22 binder was used as tack coat) the difference in the number of cycles to failure was relatively smaller and the failure pattern was consistent with that observed in a monolithic single layer specimen. In addition to this, no interlayer separation or horizontal crack was evident at the interface. It should be noted that Rutherford County cores used PG64-22 as a tack coat. Thus, it was shown that the type of emulsion contributes significantly to the performance and the interface failure pattern.

An axial frequency sweep test (AFST), similar to the FSCH, was performed on the 6-inch diameter specimens. A dynamic axial load is applied and the dynamic axial stiffness modulus ($|E^*|$) along with the phase shift, δ , of an asphalt mix are measured. Ideally, taller specimens would have been preferable but the test was conducted on samples of 50-mm height. The trend in $|E^*|$ values was very much similar to that of $|G^*|$ for both the counties

and $|E^*|$ was found to be higher for non-distressed specimens. Thus, the results were found in agreement with the FSCH and it also proved that this test was robust to detect the difference between 'good' and 'bad' cores. In the ramp test, the specimens were pulled apart at a rate of 2.5mm/minute after gluing them to metal platens. This test is used to measure the tensile strength of asphalt mixtures and, in particular, for layered specimens it represents the (tensile) strength of the interfacial joint. It was found that bond strength of the CRS-2.5 emulsion was 46% lower compared to cores from Rutherford County. The failure for Rutherford County cores was in the mix whereas for the Buncombe County cores, the failure was at the interface. Based on the field core test results, it was concluded that sections tacked using PG64-22 performed better when compared to sections tacked with CRS-2.5 emulsion. However, it may be noted that based on field core test results it is not possible to conclude whether PG64-22 is a better tacking material than CRS-2.5. This is because the rate of tack coat application could have been different and/or a construction problem such as uniform application, emulsion curing time before construction, and environmental issues. Therefore, it became imperative to investigate in a controlled laboratory test program to determine whether PG64-22 was indeed superior to the use of emulsions as a tacking material.

2 Research Approach and Methodology

2.1 Objective

The goal of this investigation is to mechanistically evaluate the contribution of prime and tack coat in composite asphalt concrete pavements. The current work undertaken for this study was based on the work conducted earlier [43]. In order to comprehend the contribution of prime and tack coats, it is necessary to understand and quantify the distribution of interlayer shear stresses, and their effect on the interface bonding. The project has two main components: experimental and analytical. The experimental part involves determination of material properties; and the analytical portion involves mechanistic analysis and development of software that will enable the selection of appropriate pavement thickness and/or the choice of tack coat given an input of material properties, structural thicknesses and loading conditions. The result of this study will also enable designers to choose appropriate tacking materials for a specific application. At the same time, with regard to prime coats, the use of emulsions has not been very popular in comparison to cutbacks. Specifically, many highway agencies (AZ, KS, NE, NH, NY and RI) do not use prime coats (emulsion based) any more.

2.2 Research Methodology

In order to achieve the objectives stated above, this investigation was conducted using the following tasks described below and as shown in Figure 2-1.

2.2.1 Literature Review and Survey

In this task, a review (§1.2) on the contribution of prime and tack coats to pavement performance was conducted. A survey questionnaire (Appendix A) was designed and sent to all state highway agencies to gather data on their experience for pavement construction with and without the use of prime and tack coats. At the same time, a review of the methods of stress analysis for layered systems was conducted. The most promising

method, 3-D semi-analytic approach, was chosen and a program developed for use in this investigation.

2.2.2 Asphalt and Mastics Testing

The Asphalt Institute Manual Series MS-16 [9] recognizes the detrimental effect of rounded particles and its contribution to mixture instability. Although the present mix in NCDOT Division 13 may not contain high sand content, it was hypothesized that the variable amount of baghouse fines purged intermittently into the asphalt mixture may account for the mix instability and significant changes in volumetric properties.

Therefore, the objective of this (§2.2.2) and the next task (§2.2.3) was to evaluate contribution of baghouse fines. The objective of this task was to evaluate the rheological properties of the binder in presence of baghouse fines using a dynamic shear Rheometer (DSR). This task consists of three subtasks:

- evaluate the properties of aged and virgin binders,
- rheological properties of mastics (aged and unaged), and
- viscosity of virgin asphalts and emulsion residues using rotational viscometer.

2.2.3 SST Testing of SGC Specimens, TSR and APA Tests

The objective of this subtask was to evaluate the effect of baghouse fines on mix characteristics using controlled mixes, and investigate their sensitivity to moisture exposure. Raw materials including baghouse fines and job-mix were obtained from NCDOT Division 13. Two mixes were prepared in the laboratory based on the job mix formula with materials passing #200 sieve (mineral filler) containing:

- zero percent baghouse fines; and
- 100 percent baghouse fines.

All other mix parameters such as asphalt content, and aggregate gradation were kept constant. These two mixes were subjected to the following laboratory testing:

- Laboratory FSCH and RSCH test on 6-inch diameter specimens compacted using SGC;

- Georgia wheel rutting test at NCDOT M&T Unit on 6-inch diameter specimens prepared using SGC; and
- Moisture sensitivity testing using the modified AASHTO T283 procedure.

2.2.4 Material Characterization

The objective of this task was to obtain material characteristics that would be needed for mechanistic analysis of the pavement sections elaborated in Chapter 9. The compressive strength and the elastic modulus of the CTB and the PCC specimens were evaluated at 28 days using cylindrical specimens. For the asphalt concrete mix, the axial and shear stiffness were characterized at different temperatures and frequencies. Stiffness versus frequency master curves was prepared from the data obtained. These results will enable the selection of the appropriate stiffness and moduli values required for the mechanistic evaluation.

2.2.5 Fabrication of Slabs and Test Specimens

In this task, composite slabs – AC over PCC and AC over CTB – were fabricated using rolling wheel compaction. Approximate size of the slab was 24-inches by 24-inches. To cast the slabs, steel molds were fabricated. The lower layer of the slab was either 2-inch thick CTB layer or PCC layer for the evaluation of prime and tack coats, respectively. The CTB and PCC layers were allowed to cure for 7-days. Appropriate prime and tack coat was applied (to CTB and PCC, respectively) and allowed to cure according to manufacturer's recommendation.

For prime coat evaluation, slabs were prepared without any prime coating, and using three prime coats that are on NCDOT's approved product list. These are EPR-1, CSS-1h and EA-P. Similarly for tack coat evaluation, slabs will be prepared without any tack coating, and using CMS-2 emulsions and PG64-22 asphalt cement. A dense mix asphalt concrete layer was then rolled using a rolling wheel compactor. After the mix cooled down, the slabs were cored to produce 6-inch diameter specimens, which were tested in shear for bond strength properties.

2.2.6 Bond Strength Determination using Shear Testing

The objective of this task was to evaluate the CTB or PCC-AC layer interface bond strength of various prime and tack coats used. In this study, the bond strength was proposed to be evaluated using the simple shear test at constant height. Testing was conducted at 40 and 60 °C. For AC-AC interface the testing was conducted at 20 °C as well. Two different shear strain rates were applied. Two replicates were tested at each strain level. For a given shear strain rate, the shear and axial stresses were monitored and the cohesion value determined for each prime and tack coat being evaluated. In addition to the testing of composite core specimens, an attempt was also made to test prime and tack coat using two metal platens.

2.2.7 Mechanistic Analysis

Three dimensional stress analysis software based on a semi-analytic method was developed as part of the overall project. The pavement is modeled primarily as a layered system of linear elastic materials with surface asphalt layer as an elastic material. Using the software, a detailed parametric study was conducted to investigate the effect of system parameters including layer thickness and stiffness on the stress-strain-displacement fields induced in the pavement. The effect of vehicle load characteristics on the response was also examined.

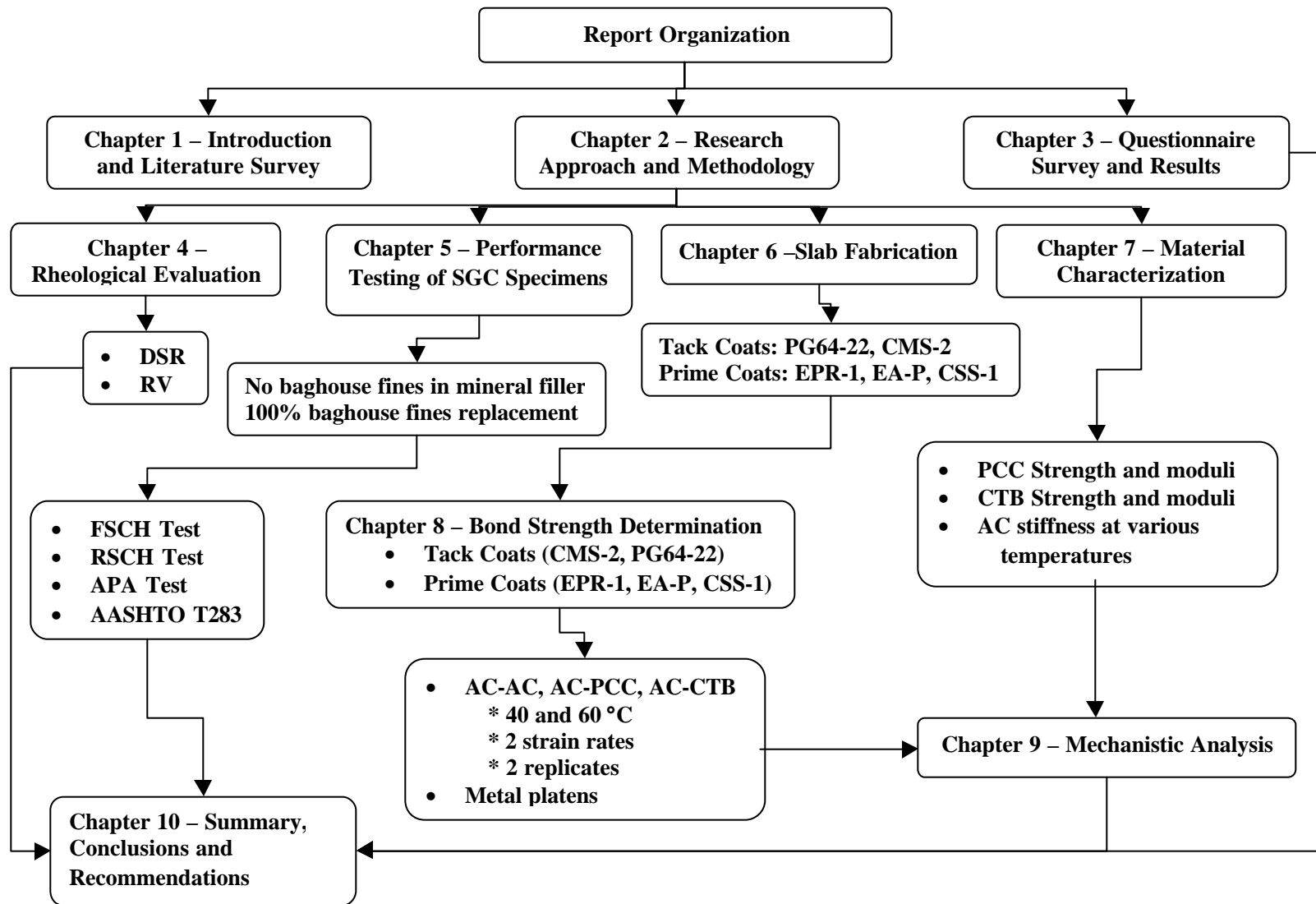


Figure 2-1 Summary of research outline and methodology

3 Survey Results

3.1 Development of Questionnaire

The goal of the current investigation was to examine the effect of various tack and prime coats on interface strength. In order to acquire the information as to the use of different tack coats and prime coats in the field, it was necessary to conduct a survey of highway agencies. The expected outcome from the survey was to identify overall trends in prime and tack coating, and evaluate the scope for potential improvement.

The developed questionnaire (Appendix A) was sent to various state highway departments and agencies for their responses. Information collected was

- whether prime coat was required for new construction,
- rate of its application,
- relation of prime coat to asphalt pavement thickness,
- curing time,
- laboratory tests for prime coats,
- field performance tests
- difference between pavements with and without prime coats,
- merits of emulsified asphalts versus cutback asphalts
- types of materials used for tack coats and their application rates, and
- provisions for emulsion breaking under nighttime paving conditions.

3.2 Survey Responses

In all more than 50 questionnaires were sent out and 26 replies have been received to date. The responses of the survey are summarized in Appendix B, and the observations are summarized below:

1. The following states responded to the questionnaire: Alabama, Alaska, Arkansas, Arizona, Connecticut, Florida, Georgia, Idaho, Illinois, Kansas, Kentucky, Maine, Minnesota, Mississippi, Missouri, Nebraska, New Hampshire, New Jersey, New York,

Oklahoma, Rhode Island, South Carolina, Tennessee, Texas, West Virginia, and Wyoming.

2. Ten of the 26 states reported that there is no requirement of prime coat for new construction of the pavement. Two highway agencies, Oklahoma and Alaska, leave it to the individual designers and state that it depends on the location in the state.
3. Of the remaining sixteen states using prime coats, seven (AL, AR, NJ, WY, OK, and IL) reported using only cutbacks for prime coat as opposed to emulsions. For the remaining nine states, most of them used a combination of emulsions (diluted or undiluted) and cutbacks; there were states that preferred only emulsions, e.g. WV, CT, KY and TN.
4. For prime coats,
 - (a) Cutbacks that are currently used in practice are: MC-30, MC-70, MC-250, RC-30, RC-70, and RC-250; and
 - (b) The emulsions used are: AE-90, AE-150, AE-200, AE-P, CAE-P, CMS-2h, CSS-1, CSS-1h, EA-1, EAP-1, EAP&T, EP, EPR-1, MS-2h, PCE, SS-1, SS-1h and Primer-L.
5. In most of the cases, it was reported that cutbacks penetrated better than emulsions. The coverage offered by cutbacks was greater than emulsions. However, there are states that have noted the following in preference to emulsion over cutbacks as prime coats:
 - MS (emulsions, when applied properly, are easier to work with),
 - MO (emulsions have more pickup versus cutback),
 - IL (emulsions for resurfacing projects) and
 - TX (emulsions good for open bases)

The cutbacks did not have any curing problems and hence were preferred where it was not possible to wait for the emulsions to break.

6. The rates of application of the prime coat are from 0.03 gal/yd² to 3.44 gal/yd². In some cases, there was dilution of the emulsion before applying, thus reducing the concentration of the emulsion (e.g. Florida). The rates of application depended on the type of base, as was the case with Mississippi and Alabama. For Maine, the rate was 0.02 gal/yd² for overlays, 0.04 gal/yd² for milled, and 0.01 gal/yd² for new mixes.
7. No specific basis was reported for the curing time of prime coats. In most of the cases, the states did not consider curing time. For those states that required curing, the criteria were subjective such as “tacky to touch” or duration ranging from 1 hour to 3 days. For

Oklahoma the condition was stated as “sufficient to allow proper penetration and hardening of prime coat,” which is quite difficult to assess without testing. Texas requires that the emulsions be worked into the top one inch of the layer and the layer re-compacted.

8. The thickness of the pavement layer is considered by some states in specifying use of prime coats. Georgia and New Jersey require it if the AC thickness is 125-mm (5 inch) or less whereas the limit for Missouri is 100-mm (4 inch). Illinois requires prime coat only for full depth pavements. In spite of variation in the prime coat requirement, all agencies require it where either the thickness is too low or there are lot of horizontal shearing forces on the surface or where interlayer bond failure is likely to occur.
9. The laboratory tests needed to be performed on the emulsions and cutbacks are the viscosity tests (kinematic), distillation, solubility in trichloroethylene, residue test and float test. Most of the agencies do not have any field performance testing procedures or requirements.
10. While a few of the agencies reported that prime coat does improve performance, there was a significant number (50%) who did not see any difference in performance. Some of the reasons cited for better performance were:
 - (a) Water proofing and creating an impervious barrier to moisture.
 - (b) Erosion control of the base.
 - (c) Reduction in shearing and tearing of thinner pavements - < 2-inch thick - on curves and on grades (Idaho). Less delamination, and inability to separate the layers without a saw. In Oklahoma, absence of prime coat had lead to significant plane slippage problems.
 - (d) Ease of densification of SUPERPAVE™ mixes (New Jersey).
 - (e) Maintenance of optimal moisture content levels in the base thus maintaining the base strength at a constant level.
11. The materials used as tack coat are: AC, AE-60, CMS-1, C-70, C-250, C-800, CMS-2, CRS-1, CRS-2, CRS-2h, CSS-1, CSS-1h, HFE-60, HFE-90, HFMS-1, HFMS-2, HFMS-2h, HFMS-2s, MC-250, MC-800, MS-1, MS-2, MS-2h, PG58-22, PG64-22, PG67-22, RC-70, RC-T, RS-1, RS-2, SS-1, and SS-1h. Thus, a larger variety of materials can be

used as tack coats than prime coats. To reduce the concentration of asphalt, the emulsions used for tack coats were diluted with water before application.

12. Tack coats are applied at the rate of 0.03 - 0.2 gal/yd². In cases, where there is dilution with water, the effective rate of application is within the above range. In South Carolina, the rate of application is based on residual asphalt.
13. Nighttime paving: Most states require that the emulsion should break before the placement of new layer, there has been no concrete method to verify such condition. For a few states, the verification of the breaking of emulsion is done based either on touch - tacky touch - or by observation of the inspector. Some states (OK) disallow use of emulsions after sunset whereas states like Alabama are eliminating the use of emulsions because of difficulty in determining the state of the emulsion (broken or not).

In summary, more than 38% of the responding highway agencies do not require prime coats to be used, and some agencies only use it for relatively thin pavement sections (less than 4 to 5 inches). The current practice of using tack coat in the form of emulsion varies widely depending on the highway agencies. Clearly, there is a vast possibility of error in construction technique that may result in poor performance, especially for night time paving operations. Some of these difficulties have been mitigated by various highway agencies by substituting PG64-22 as a tacking agent over emulsion tack coats.

4 Rheological Evaluation

4.1 Introduction

One of the concerns with respect to asphalt mixtures in NCDOT Division 13 was with regards to the variable amount of baghouse fines purged intermittently in the production of the field mixtures. This chapter deals with:

- the evaluation of the gradation of baghouse fines using the state-of-the-art particle analyzer at FHWA Turner Fairbank Highway Research Center;
- the influence of fines on the rheological properties of asphalt cement using mastics was also evaluated using the DSR; and
- the properties of residual asphalts and emulsions

4.2 Selection of Fines

For this study, the mineral filler and baghouse fines with materials passing #200 sieve were obtained from Buncombe and Rutherford counties. The fines selected for analysis were:

- Buncombe County:
 - passing #200 sieve fraction from wet screenings
 - baghouse fines
- Rutherford County
 - Passing #200 sieve fraction from dry screenings
 - 'fine' baghouse fines
 - 'coarse' baghouse fines.

In all, five different types of fines were analyzed using the particle analyzer.

4.3 Gradation Analysis of Fines using FHWA Particle Analyzer

4.3.1 Method Description

The gradation analysis of mineral fillers was carried out at the Turner Fairbank Highway Research Center, McLean, Virginia. The material was separated using a small splitter then further separated using a micro splitter to obtain a representative sample. To run the test, a small amount of material was mixed in a medium to create a suspension. For baghouse fines, distilled water with 1-percent sodium hexametaphosphate was used. Experience showed that this was adequate for most of the mineral fillers.

The testing process consisted of taking a 'blank' measurement of the medium to establish a baseline. The material was then slowly introduced and mixed with the medium until an 'optimum' intensity was found. In order to prevent particle agglomeration, agitation by cavitation was induced by a high intensity ultrasonic processor for 2 minutes. The particle analyzer automatically converted different light intensity measurements into particle size distribution. The average of three different samples was obtained and the results were found to be consistent with each other. The results, however, necessarily need not match with the sieve analysis. The main reason for this is the fact that the gradation obtained from the laser particle analyzer is a volume gradation based on the projection of particles. The device showed the differences that were otherwise difficult to capture.

4.3.2 Results and Discussion

In all two sets of analyses were performed within the duration of this study. Figure 4-1 and Figure 4-2 show the gradations of the mineral fillers and bag-house fines obtained from the two counties. Figure 4-2 presents the particle analysis performed on the first set of fines received before the entire set of materials was requested so that a decision could be made about the further analysis to be performed. Figure 4-1 presents the particle size analysis that was carried out on fines received in the latter batch of materials from which the samples for laboratory testing were actually fabricated.

For Rutherford County, the 'coarse' baghouse fines appeared to be 'sandy' and hence their size distribution was measured using a slightly more viscous medium. The two media

used for Rutherford County 'coarse' bag-house fines were distilled water (W) and 90-percent distilled water plus 10-percent glycerin (G). In Figure 4-2, the particle analysis results using the two different media are fairly different. However, both media show that this sample is the coarsest.

Figure 4-1 and Figure 4-2 show that the 'coarse' baghouse fines from Rutherford County is the coarsest material passing #200 sieve. Although it was anticipated that the baghouse fines, in general, would be finer than the regular fines passing #200 sieve, the particle size analysis indicated for both set of materials that the baghouse fines from both counties had more or less similar particle size distribution as the regular fines. Table 4-1 shows the properties of the fines based on the second set of materials which was used for mixture performance testing in this study. The mean particle size of regular fines from Buncombe and Rutherford counties are both 30.5- μm . The baghouse fines from Buncombe County has the mean particle size 40- μm and the Rutherford County 'fine' baghouse fines has a mean particle size of 31- μm . The 'coarse' baghouse fines from Rutherford County have a mean particle size of 88- μm , more than twice the mean size of any other regular or baghouse fines.

The particle size analysis suggests that based on gradation, the mixture performance should not be affected whether the mineral filler used is regular fines or from baghouses. However, as the particle shape and/or perhaps the mineral content distribution may be different for the baghouse fines, it may have different effect on the rheological behavior of the asphalt cement and mixtures in general. This effect is investigated in the following section where the performance of baghouse and regular fines are studied using asphalt-fines mastics in an aged and unaged condition. In Chapter 5, this effect is also evaluated based on the performance of the asphalt mixtures.

4.4 Analysis of Asphalt-Fines Mastics using DSR

The objective of this task was to evaluate the rheological properties of the binders and mastics containing baghouse fines at intermediate to high temperatures. Testing was conducted in accordance with AASHTO TP5-93 [5].

4.4.1 Specimen Preparation

The asphalt cement used for the preparation of mastics was a PG64-22 supplied by NCDOT. Four mastics were prepared using the fines received from Buncombe and Rutherford counties. The asphalt cements and each of the mastics were tested in an unaged and aged condition with at least three replicates. The following asphalt and mastic combinations were used:

- Binder (virgin and RTFO-aged, PG64-22 for both counties)
- Mastic (virgin and aged) from the baghouse fines. Only the 'fine' baghouse fine was used from Rutherford County.
- Mastic (virgin and aged) from the regular mineral filler (fraction passing #200 sieve).

The prepared mastic was a mixture of the filler/fines with asphalt from the corresponding county. The proportion of asphalt was 50-percent by weight of the total mastic. For preparation of mastics, the fines and the asphalt binder were pre-heated to a temperature of 160°C. The fines were then added slowly to the heated binder with constant stirring until uniform, consistent agglomerate free 'batter' was obtained.

The asphalt binders were aged in an RTFO oven, while the mastics were aged in an air draft oven due to the higher consistency of the mastics. Due to high consistency of mastics, problems were encountered in recovery from the RTFO bottles. The mastics, therefore, were poured in a PAV dish and were kept in an oven for a period of 85 minutes at 163 °C for aging to simulate the RTFO aging effect. One problem encountered with handling the mastics was segregation of fines. Hence while pouring into the molds; it was necessary to stir vigorously so as to have a uniform consistency for the DSR specimens.

4.4.2 Test Parameters

The asphalt cement and mastics were evaluated at three temperatures – 58, 64, and 70°C. For the asphalt binder, the DSR spindle diameter of 25-mm with 1-mm gap was used. As the mastics were more viscous, a spindle diameter of 8-mm with 2-mm gap was used.

Testing at 10 radians per second and at different strain levels (strain sweep) was conducted to establish for each asphalt binder and mastic, the linear viscoelastic region in the strain domain (defined by AASHTO TP5 to be a range of strain values where the test measurement $|G^*|$ does not vary more than 95-percent of the $|G^*|$ estimated at zero strain). Based on the strain sweep test, the strain levels for unaged and aged binders selected was 12 and 10-percent, respectively. For the mastics, the strain levels selected were typically in the range of 1 to 2-percent for both aged and unaged binders.

Frequency sweep tests were conducted on the asphalt binders and mastics at the frequencies of 0.01, 0.05, 0.1, 0.15, 0.5, 1.0, 1.59, 5.0, 10.0 and 20.0 Hz. The measured parameters from the test results were the dynamic shear modulus $|G^*|$ and phase angle δ . These results were then used to generate master curves at 64°C for dynamic shear modulus $|G^*|$ and $|G^*|/\sin\delta$.

4.4.3 Test Results and Discussion

Figure 4-3 and Figure 4-4 show the dynamic shear modulus as function of reduced frequency at 64°C for Buncombe and Rutherford counties. The raw DSR testing data is presented in Appendix E. These figures show that in general:

- 1) aging tends to increase the $|G^*|$ values for both the asphalt binder and the mastics as compared to the unaged condition;
- 2) $|G^*|$ values for the mastics are much higher than the asphalt binder (this trend is expected as the mastics contain 50-percent fines);
- 3) in case of Buncombe County, the mastic containing baghouse fines have higher $|G^*|$ values over the range in frequency as compared to the mastic containing regular mineral filler material;
- 4) in case of Rutherford County, the mastic containing baghouse fines show similar $|G^*|$ values over the range in frequency as compared to the mastic containing regular mineral filler material.

Figure 4-5 through Figure 4-8 show the Superpave rutting parameter, $|G^*|/\sin\delta$, as function of reduced frequency at 64°C. For Buncombe County, mastic containing baghouse fines shows higher $|G^*|/\sin\delta$ values both in aged and unaged condition as compared to the mastic containing regular fines. For Rutherford County, the mastic containing baghouse fines shows higher $|G^*|/\sin\delta$ values in unaged condition but about similar values in aged condition compared to the mastic containing regular fines.

In summary, therefore, it appears that Buncombe County baghouse fines show different effect on aging of asphalt as compared to the Rutherford County baghouse fines.

4.5 DSR Testing of Emulsions

In order to evaluate the properties of the residual binders in the emulsions, DSR testing was conducted. As emulsions contain a large amount of water, they were broken prior to being tested in the DSR. The following two approaches were used to break the emulsions:

- *Rolling Thin Film Oven:*

The rolling thin film oven, commonly referred to as RTFO, is commonly used to simulate the short term aging of asphalt in laboratory. The oven uses a temperature of 163 °C for testing purposes. The emulsions were broken in RTFO at lower temperature of 85 °C in order to prevent excessive aging of AC. At the end of the 85 minute test it was found that there was substantial presence of moisture indicated by soft and fluid nature of residual asphalt as well as by presence of typical brown coloration on the inner walls of the RTFO bottles. In the second round, the RTFO temperatures were increased to 105 °C, however there was not a significant improvement in the results.

- *Open heating:*

Due to non-conclusive outcome of the earlier approach, it was decided to break the emulsions using the shallow, flat pressure aging vessel (PAV) pans. The heating temperature was raised to 135 °C (to ensure complete evaporation of water component) with constant stirring at regular intervals (roughly 15 minutes). The total heating period was 85 minutes, same as the duration of the RTFO test. The temperature of 135 °C was chosen because it is the highest temperature that asphalt can be subjected to without a

significant risk of aging. Most of the emulsions broke satisfactorily using this approach. The emulsion EA-P, however, did not break because of its polymeric nature. This emulsion, therefore, was heated to a temperature of 155 °C and it broke after extensive heating for 2 hours.

The DSR testing was carried out on the residual binders at the following temperatures: 52, 58, 64 and 70 °C. Using a 25-mm diameter spindle and 1-mm thick specimens, the testing was carried out at a frequency of 1.592 Hz. Two tests were performed: a stress sweep test to determine the linear range of the binder and an oscillation test at 1.592 Hz.

4.5.1 Test Results and Discussion

The results are summarized in Figure 4-9 through Figure 4-11 and Table 4-2. The following conclusions can be drawn:

1. It can be seen that with increase in temperature, there is a continuous fall in $|G^*|/\sin\delta$ values. The results yield a straight line when plotted on a log-linear scale. All the curves had an R^2 value of one indicating a very good fit.
2. The CRS-1H is the hardest (stiffest) residual binder and the CMS-2 has the softest residual binder of all. These results are as expected.
3. The testing of CRS-1H binder posed problems at a temperature of 52 °C because the binder was too stiff. The deformation caused by the applied stresses was too small to be accurately recorded by the DSR.
4. The residual binders of CRS-1H, EA-P and I.A.S. emulsions have a ‘reported’ high temperature PG rating of PG70 but their actual PG ratings are PG73.7, PG74.7 and PG70.7 respectively. Similarly, CRS-Koch has a ‘reported PG rating’ of PG64 but the actual PG rating is PG65.1 and CMS-2 has a ‘reported PG rating’ of PG52 but the actual PG rating is PG57.1. The DSR testing, therefore, provides a more accurate classification of the emulsions. Thus, the emulsions can be listed in the following order (of decreasing stiffness):
 - CRS-1H
 - EA-P
 - I.A.S.

- CRS-Koch, and
 - CMS-2.
5. The polymeric nature of the EA-P emulsion, combined with the high ‘actual PG grade’ of residual binder, explains the stability of the emulsion at elevated temperatures.
 6. Based on the DSR results, it can be hypothesized that the tacking strength of the emulsions would be directly proportional to their respective PG temperatures.

4.6 Brookfield Viscosity

A rotational viscometer determines the flow characteristics of the asphalt binder and its ability to be pumped and handled at the hot mix plant. Testing of binders was conducted in accordance with ASTM D4402 (Standard Method for Viscosity Determinations of Unfilled Asphalts using the Brookfield Thermosel Apparatus). It measures the amount of torque required to maintain a constant speed of a cylindrical spindle immersed in liquid binder at a given temperature. The number of replicates for Brookfield Viscometer testing was three. The testing was carried out at two temperatures of 150 and 135 °C.

From Figure 4-12 and Figure 4-14, it can be seen that the EAP emulsion exhibits a rapid decrease in viscosity compared to other emulsions. Further, CRS-1 and CMS-2 emulsions have relatively similar consistency at 150 and 135 °C whereas for all other emulsions under consideration, there is a rapid drop in viscosity with increase in temperature. This could suggest that CRS-1 and CMS-2 are preferable compared to their counterparts. This is further reinforced by the fact that their viscosities are relatively independent of the spindle RPM. The CRS-1H and IAS emulsions have comparable values however, IAS seems more temperature susceptible than CRS-1H. Based on the test results, the acceptability in the order of preference is CMS-2, CRS-1, CRS-1H, IAS and EAP.

4.7 Conclusions

It was originally hypothesized that the one of the contributory factor to the delamination and shoving distress observed in Buncombe County was the intermittent purging of the baghouse fines in the field asphalt mixes. Results of the gradation analysis show that the baghouse fines have similar, or in some cases coarser, gradation as compared

to the regular mineral filler used in these respective counties. The dynamic mechanical analysis of the mastics using the DSR suggests that inclusion of baghouse fines in asphalt mixtures may not have any detrimental effect. On the contrary, for Buncombe County, the inclusion of baghouse fines appears to enhance the rut resistance of the asphalt mixture as will be shown to be the case in chapter 5. However, the effect of moisture sensitivity on the mixtures containing baghouse fines needs to be evaluated before any final conclusion can be made.

Table 4-1 Properties of fines from particle size analysis (set 2) [23]

Particle Property	Buncombe Baghouses	Buncombe Passing #200	Rutherford 'Coarse' Fines	Rutherford 'Fine' Fines	Rutherford Passing #200
Fineness Modulus (F.M.)	5.72	5.40	7.10	5.43	5.31
Coefficient of Uniformity (C_U)	10.20	7.60	4.00	9.11	8.67
Coefficient of Curvature (C_C)	1.73	2.15	1.72	1.96	2.28
Skewness Indicator (σ_1)	2.25	2.31	1.14	2.60	2.30
Skewness Indicator (σ_2)	4.40	2.90	2.75	3.88	3.59
Mean Particle Size (μm)	40.0	30.5	88.0	31.0	30.5

Table 4-2 Temperatures for residual binders when $|G^*|/\text{sin} \delta \approx 1.0$ kPa

Emulsion	Temp. ($^{\circ}\text{C}$)	PG rating
CRS-1H	73.7	PG70
EA-P	74.7	PG70
IAS ¹	70.7	PG70
CRS-Koch	65.1	PG64
CMS-2	57.1	PG52

¹ The testing was performed at **four** temperatures and the results were extrapolated to determine the appropriate 1-kPa temperature. Extra testing was not felt necessary because the results were almost a straight line when graphed.

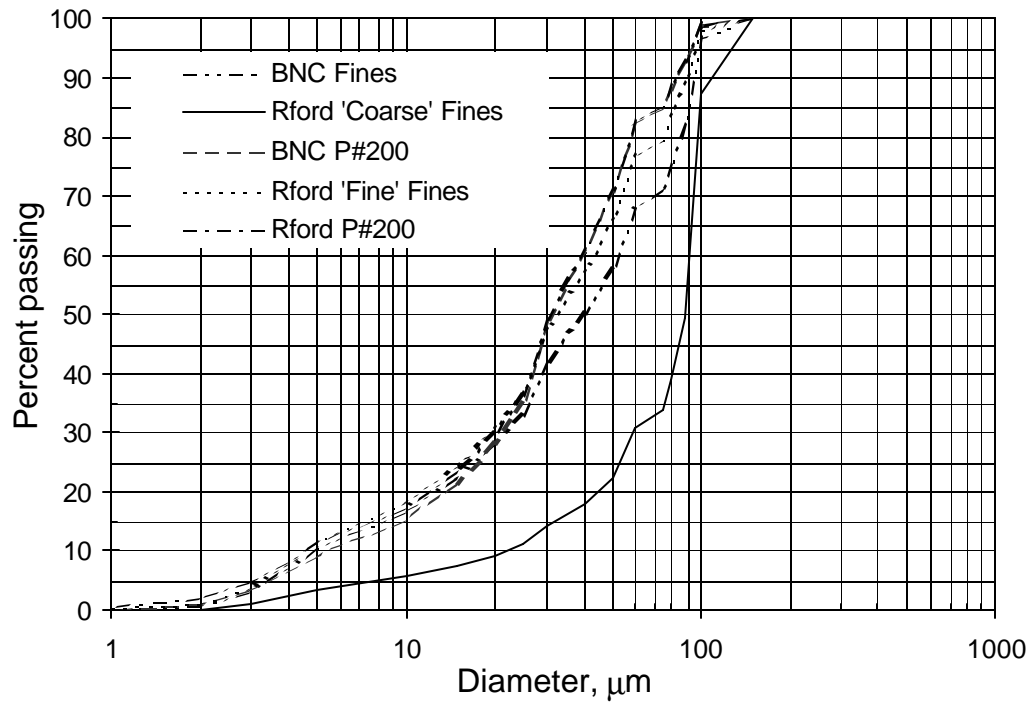


Figure 4-1 Gradation analysis of fines using FHWA particle analyzer, set 2

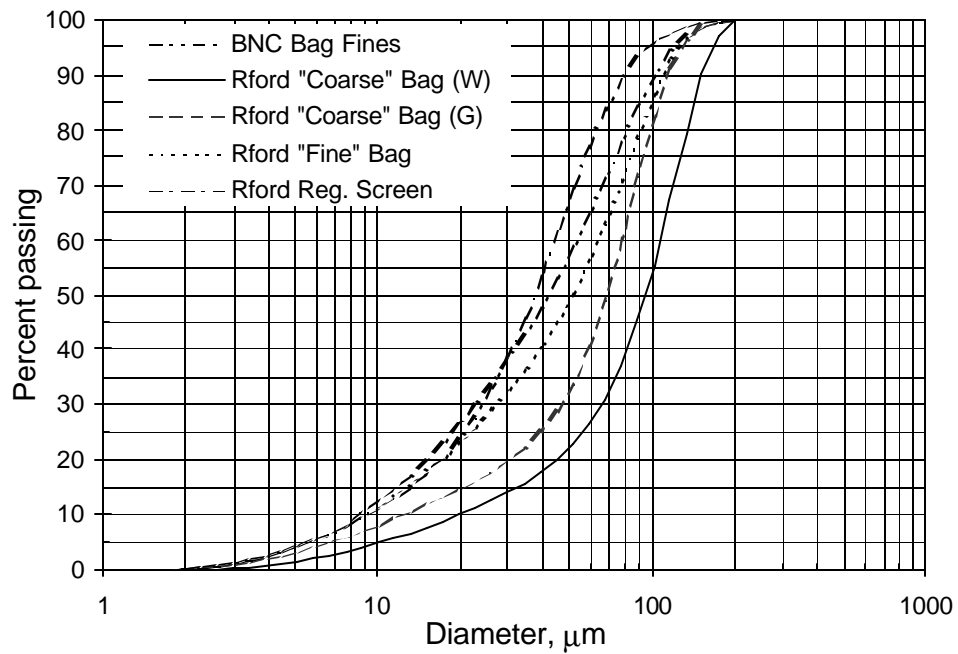


Figure 4-2 Gradation analysis of fines using FHWA particle analyzer, set 1

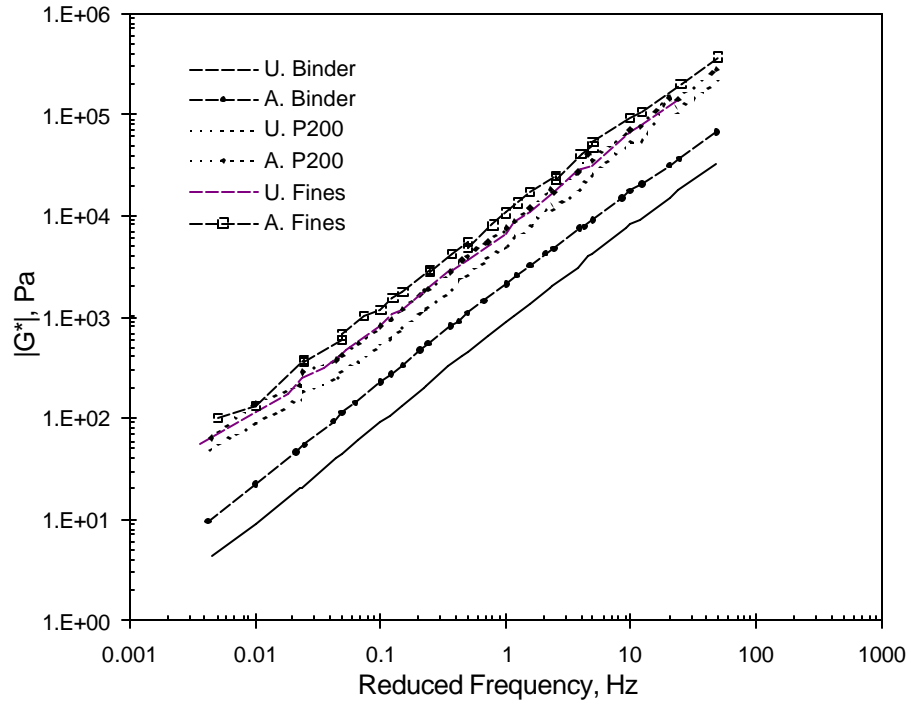


Figure 4-3 Master curves ($|G^*|$) for Buncombe County, 64°C

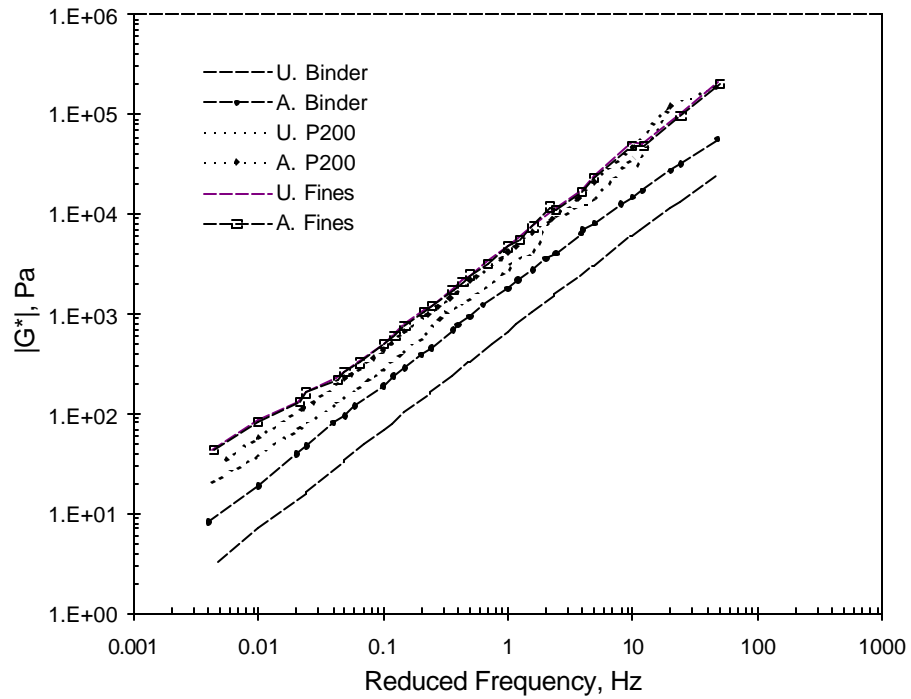


Figure 4-4 Master curves ($|G^*|$) for Rutherford County, 64°C

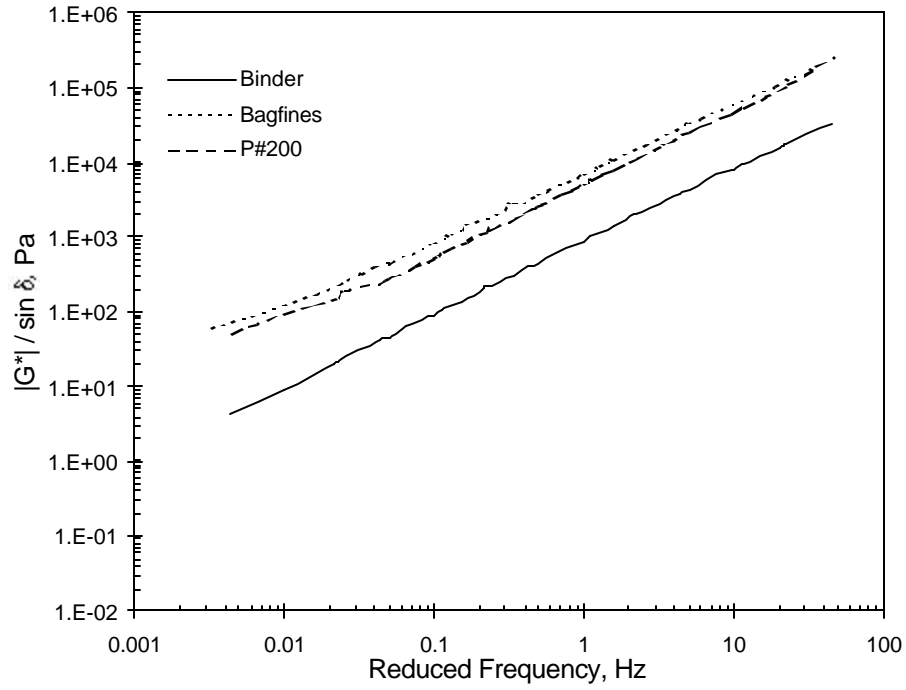


Figure 4-5 Master curves ($|G^*|/\sin \delta$) for Buncombe County, unaged, 64°C

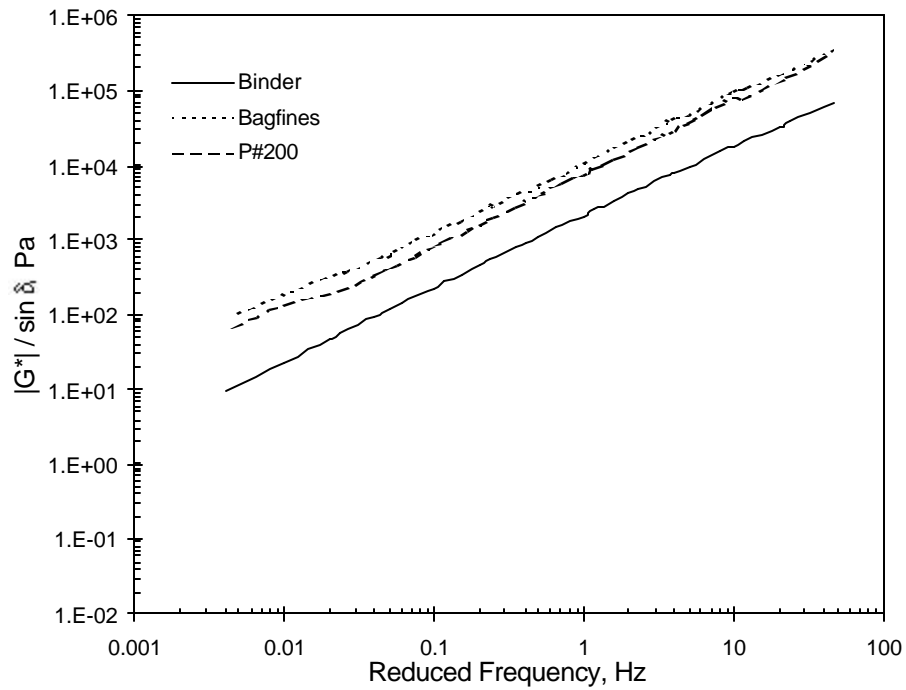


Figure 4-6 Master curves ($|G^*|/\sin \delta$) for Buncombe County, aged, 64°C

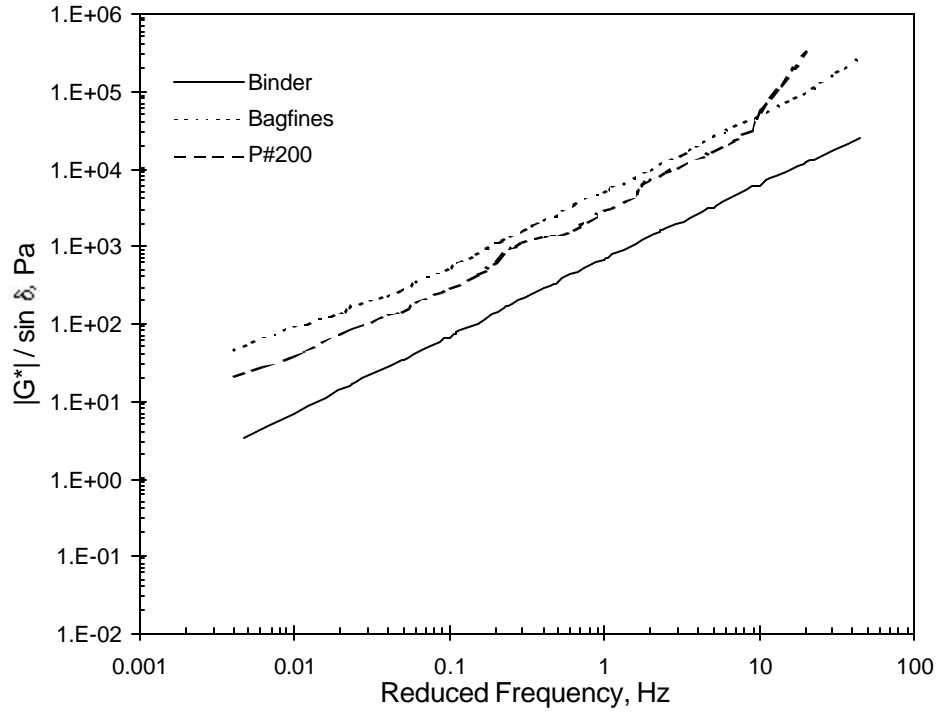


Figure 4-7 Master curves ($|G^*|/\sin \delta$) for Rutherford County, unaged, 64°C

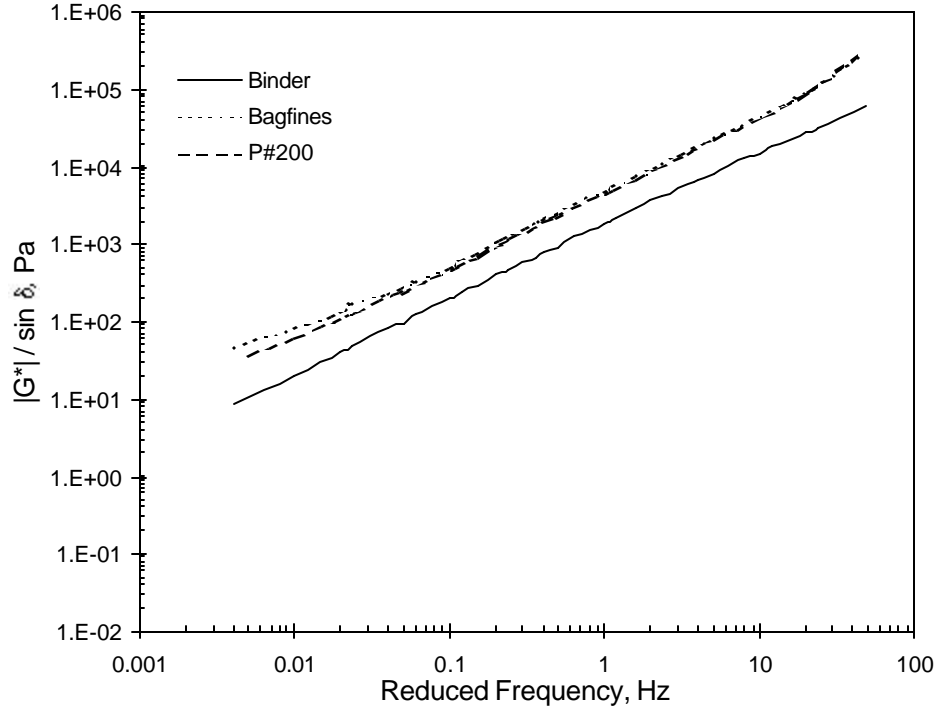


Figure 4-8 Master curves ($|G^*|/\sin \delta$) for Rutherford County, aged, 64°C

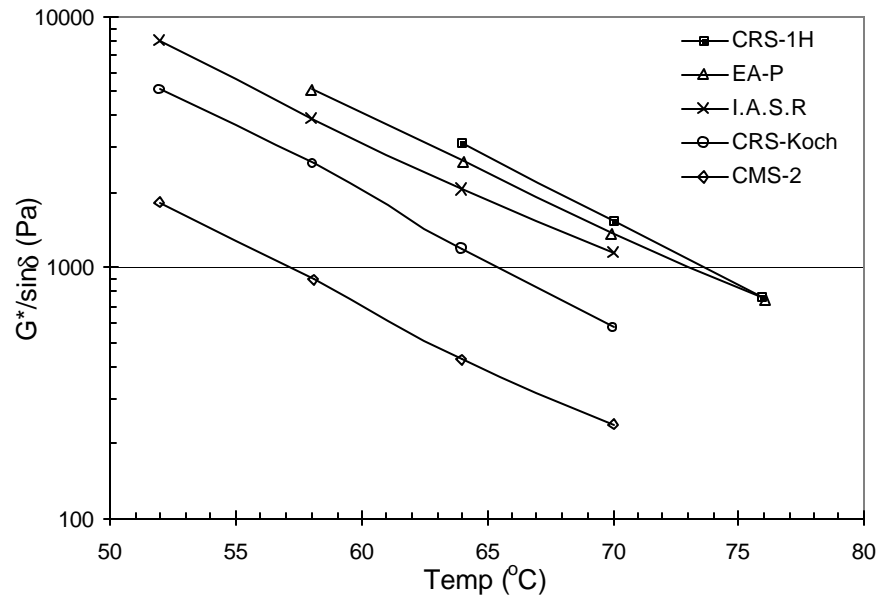


Figure 4-9 Comparison of $|G^*/\sin(d)|$ at various temperatures for residual binders

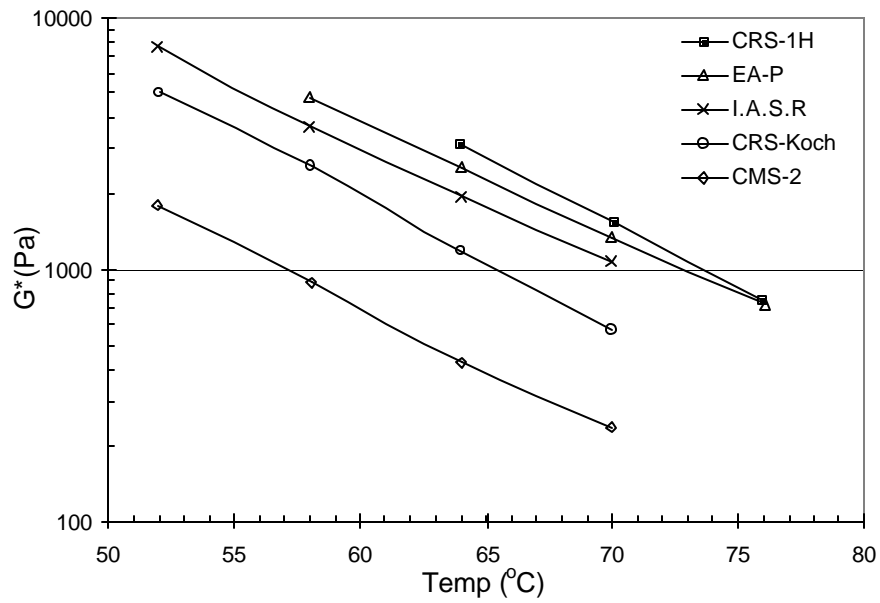


Figure 4-10 Comparison of $|G^*|$ at various temperatures for residual binders

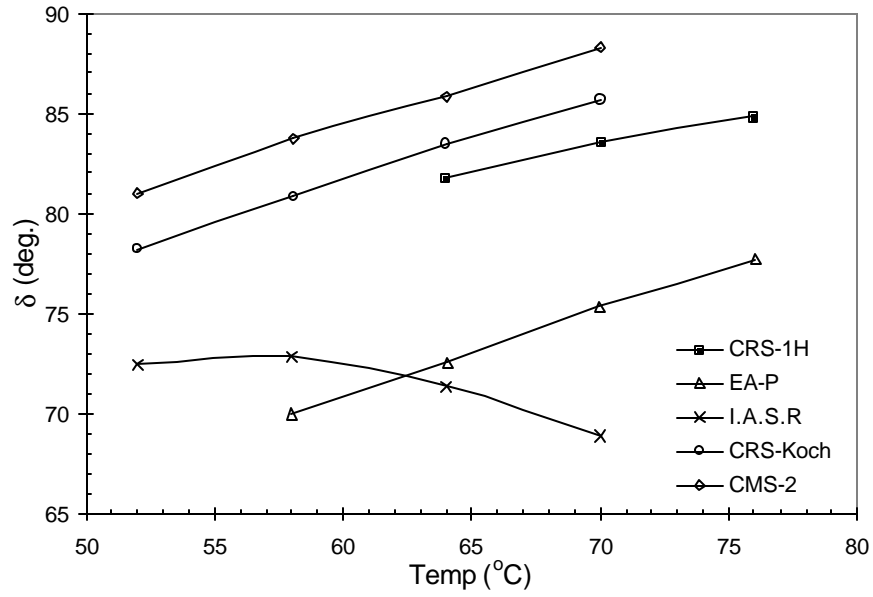


Figure 4-11 Comparison of δ at various temperatures for residual binders

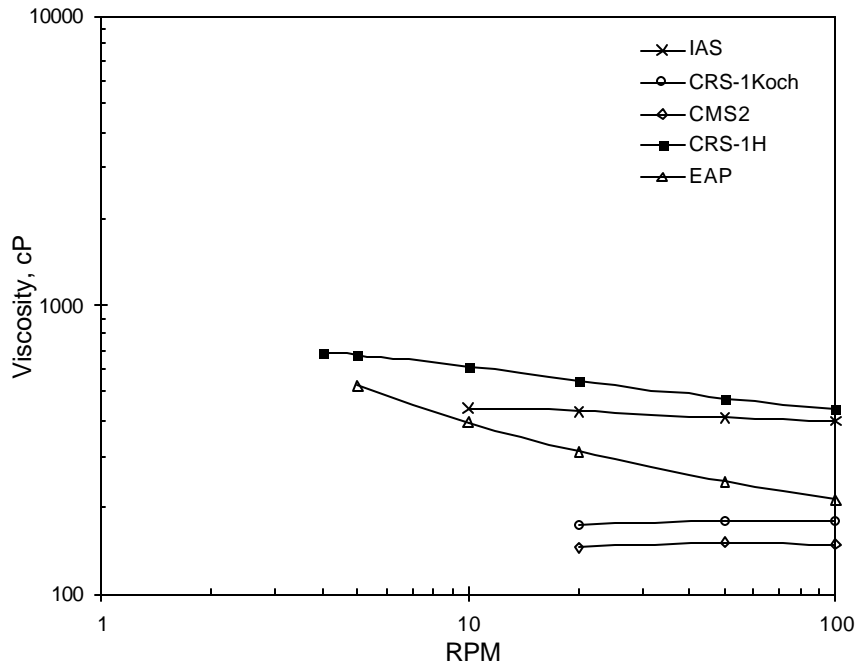


Figure 4-12 Viscosity vs. RPM, 150 °C

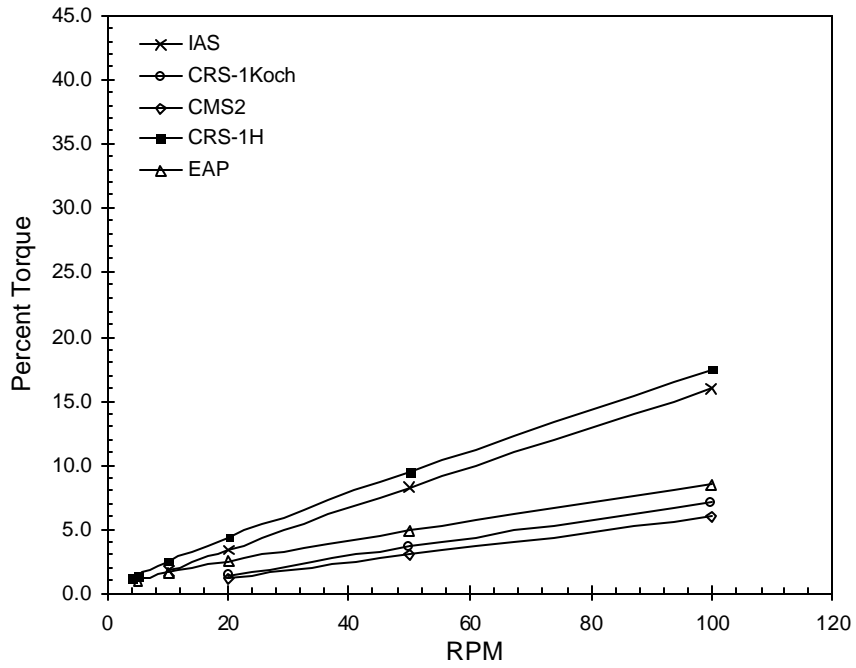


Figure 4-13 Percent torque vs. RPM, 150 °C

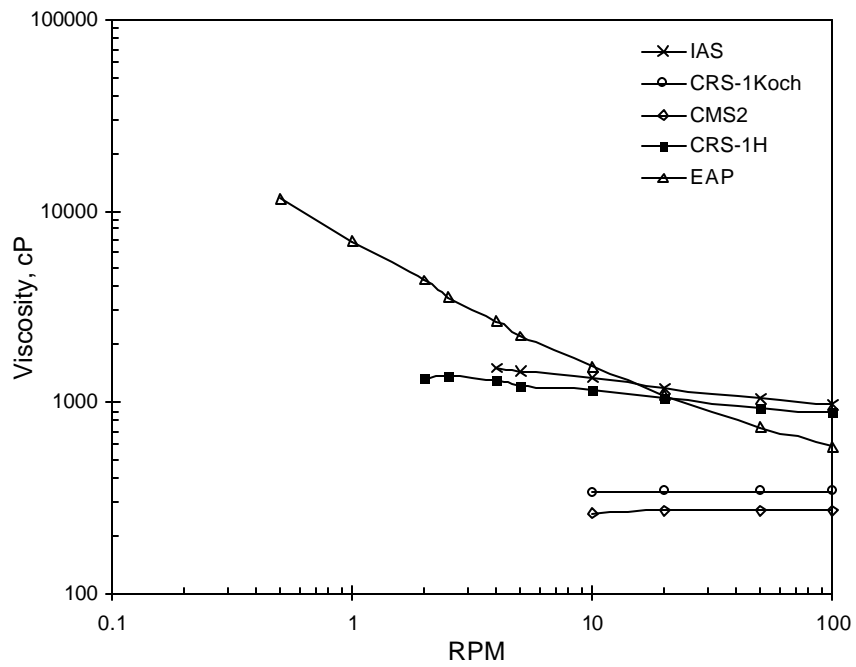


Figure 4-14 Viscosity vs. RPM, 135 °C

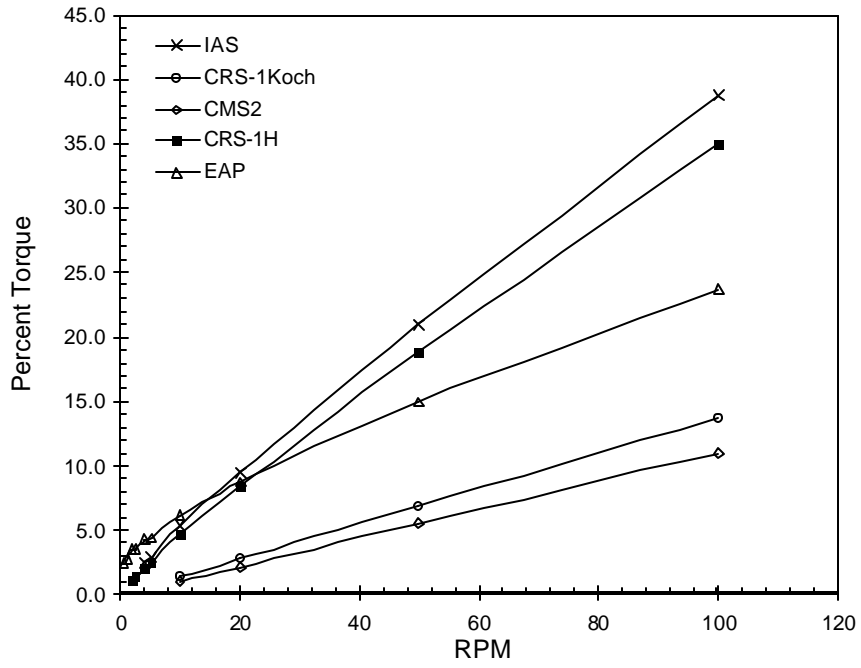


Figure 4-15 Percent torque vs. RPM, 135° C

5 Performance Testing of SGC Specimens

5.1 Introduction

The main objective of this task was to evaluate the performance of laboratory samples, prepared using the Superpave Gyrotory Compactor (SGC). These samples were tested for performance characteristics using SST, APA and TSR moisture sensitivity tests.

5.2 Test Parameters

For a given test system, the results of the performance test are governed by several parameters including reliability and repeatability of the test system, and the mix and test parameters. For the mix parameters, the asphalt type and content, and the aggregate type and gradation was fixed based on the job mix formula for the given pavement section. The only mix parameter that varied was the air void content of the laboratory mixes. Table 5-1 shows the air void content of the laboratory prepared specimens with and without the baghouse fines. For these mixes, the air void content of 5 ± 0.5 -percent was targeted based on the JMF requirement of 5-percent voids.

The major test parameters considered in this study were: 1) test temperature, 2) applied stress or strain, 3) test frequency, and 4) test duration. As per the research methodology presented in Chapter 2, the following tests were conducted on laboratory mixes from both Buncombe and Rutherford counties with testing broadly classified in the following two categories:

- Shear testing
 - FSCH (Frequency Sweep at Constant Height Test)
 - RSCH (Repeated Shear at Constant Height Test)
- APA test
- TSR tests

The shear testing consisted of a shear frequency sweep at constant height (FSCH) and repeated shear at constant height (RSCH) tests. Each of these test methods is described in the

latter sections. Laboratory specimens 150-mm in diameter were compacted using the SGC and were sawed to the required height of 50 mm.

5.3 Test Temperature

5.3.1 Selection of Testing Temperature

Temperature plays an important role in the design of asphalt mixes. The properties of binder depend significantly on the temperature and, consequently, the mix properties such as resistance to rutting and fatigue vary with temperature. In order to evaluate the load associated performance of the pavement it is imperative that the testing be carried out at a temperature representing the actual field conditions. One of the procedures for determining the pavement temperatures is recommended by AASHTO TP7 - Procedure F (Repeated Shear at Constant Height Test) [6]. This procedure requires conducting the RSCH test at the maximum seven-day pavement temperature at the selected pavement depth. The recommended depth at which the maximum seven-day pavement temperature is calculated is 20-mm from the top surface. The data for this temperature is normally obtained from the weather data at the paving site using the SHRPBIND program [36] developed within the SUPERPAVE™ program.

5.3.2 Temperature Zones

SHRP report (SHRP-A-415) [37] outlines an elaborate procedure for computing the critical and maximum pavement temperatures. It has divided the continental United States into nine climatic regions based on the temperature and humidity of the soils. The nine temperature zones are shown in Figure 5-1. Table 5-2 lists the effective, maximum, and critical temperatures for the nine zones as reported in SHRP-A-415 [37]. The effective temperature is the temperature at which loading damage accumulates at the same average rate in service as in laboratory. Thus, there is a one-to-one correspondence between the laboratory and in-service loading cycles at the effective temperature. The critical temperature is the temperature at which the maximum amount of damage occurs in service. This temperature can be considered as an ideal temperature for laboratory testing because it

minimizes errors due to variations in the mix temperature sensitivity due to its accelerated rate of damage accumulation. North Carolina falls in regions IB and IC with both Buncombe and Rutherford counties being in region IC with critical and maximum temperatures in the range of 35 to 38 °C.

5.3.3 Selection of Depth for Computation of Testing Temperature

The job mix formulae for the mixes from both the counties indicated that there were two 50-mm lifts of HDS asphalt course. Ideally, the testing temperatures for mixes from both the counties should have been 38 °C, but the actual layer thickness' are much lower than 50-mm. The average depths to the uppermost interface measured from the field core surfaces are summarized in Table 5-3 for both counties. Since the parameter under investigation was the tack coat properties, it was necessary that the laboratory test temperature corresponded to that of the tack coats in the field. Consequently, testing temperatures were selected corresponding to the depth of the tack coat (approximately 33-mm for both counties).

5.3.4 Reliability Factors

AASHTO provisional standard TP-7 [6] specifies that the RSCH test be conducted at the maximum seven-day pavement temperature for the selected depth. However, it does not specify the reliability level at which this temperature should be computed. A reliability level of 50-percent was selected for this study.

5.3.5 Temperature Selection Method

The seven-day maximum air temperatures were computed based on the following equations used within the SHRPBIND [36] software:

$$T_{surf} - T_{air} = -0.00618 \times (lat.)^2 + 0.2289 \times (lat.) + 24.4 \quad (5.1)$$

Where T_{surf} and T_{air} are the air and surface temperatures respectively in degree Celsius and $lat.$ is the latitude in degrees. From the surface temperature, the pavement temperature is computed using:

$$T_d = T_{surf} \times (1 - 0.063 \times d + 0.007 \times d^2 - 0.0004 \times d^3) \quad (5.2)$$

Where T_d and T_{air} are the temperatures at depth d and at surface, respectively, in °F with the depth, d , in inches. In this study, the pavement temperatures were calculated by two different ways. In the first method, the temperature was calculated at the required depth from the air temperature using Equations 5.1 and 5.2. In the second method, the pavement temperature was calculated using the SHRPBIND program. It was found that the temperatures calculated by the two different methods differed by approximately 3 °C. Hence, an average of the two was taken as the critical test temperature. Table 5-3 summarizes the temperatures calculated by the two methods.

Based on an average value, the testing temperatures for Buncombe and Rutherford counties were 50.2 and 54.0 °C, respectively at 33-mm depth and 50-percent reliability. However, in order to compare different tack coats (CRS-2.5 and PG64-22) a single test temperature of 50.2 °C was selected.

5.4 Performance Test Results of Lab Mixes with Baghouse Fines

The objective of this task was to evaluate the effect of baghouse fines on laboratory mixes. Laboratory specimens were fabricated using the SGC. Performance of the specimens containing baghouse fines versus crushed mineral filler (passing #200 sieve) was evaluated using the FSCH and the RSCH tests.

5.4.1 Specimen Fabrication

The specimens were fabricated using the SGC (Superpave Gyratory Compactor). The aggregates received from NCDOT were separated into various fractions depending on their sieve sizes and were then blended to the appropriate NCDOT specified JMF (Appendix C) gradations. The exception to this procedure was that the Rutherford County sand and all the baghouse fines were added in bulk as received. Specimens with zero percent baghouse fines were fabricated with mineral filler (fraction passing #200 sieve) whereas, specimens with 100% baghouses had their fraction passing #200 sieve substituted completely by the

baghouse fines. For Rutherford County, there were two types of baghouses: the 'fine' baghouse fines and the 'coarse' baghouse fines. For the purpose of laboratory testing, only the 'fine' baghouse fines were used. The asphalt contents for Rutherford and Buncombe Counties were 6.2 and 5.7-percent, respectively, and the non-strip additive requirement was 0.5-percent for both the counties.

The mixing and compaction was carried out at a temperature of 285 °F, and before compaction, the mixes were aged at a temperature of 275 °F for 2 hours. The 6-inch diameter RSCH test specimens were compacted to a height of approximately 3-inches with target air voids of 5±1-percent. Both ends were then sawed to achieve the required height of 2-inches. Table 5-1 shows the air void content of the specimens used for the RSCH test. It may be noted that the specimen identification for Buncombe and Rutherford counties consists of 'W' for the specimens containing baghouse fines, and 'WO' for specimens without the baghouse fines.

5.4.2 FSCH Test

The FSCH test measures the viscoelastic shear properties (dynamic shear modulus, $|G^*|$ and the phase shift, δ) over a range of testing frequencies and at different temperatures. Testing is conducted in a semi-confined condition in which the specimen dilation due to application of shear load is prevented by an axial force – hence, the acronym “constant height” test.

In this study, testing was conducted in accordance with AASHTO TP7 Procedure E [6] in which a sinusoidal shearing strain of amplitude ± 0.005 -percent (0.0001 mm/mm peak-to-peak strain) was applied at frequencies of 10, 5, 2, 1, 0.5, 0.2, 0.1, 0.05, 0.02 and 0.01 Hz. At each frequency, the stress response is measured along with the phase shift between the stress and strain. The dynamic shear modulus ($|G^*|$) was computed as the ratio of the peak stress over the peak strain. Testing was conducted at 50.2°C.

Data presented in Table 5-4 through Table 5-9, and Figure 5-2 through Figure 5-7 show the FSCH test results for the mixtures from Buncombe and Rutherford counties. Based on these figures, and, in particular, Table 5-6 and Table 5-9 it may be noted that the baghouse

finer particles have a stiffening effect on the mixtures. That is, on an average, specimens containing baghouse fines have higher shear modulus values $|G^*|$ and $|G^*|/\sin\delta$ compared to those specimens without the baghouse fines. The percentage difference is approximately 30-percent for the Buncombe County mixes and 20-percent for the Rutherford County mixes. These results are consistent with the results obtained for the mastics using the DSR presented in chapter 4. Moreover, for both mixes with and without the baghouse fines, the Buncombe County mixes generally show very similar performance to the Rutherford County mixes for the air voids and test temperature used in this study. Based on these results, it is expected that rutting performance will also be in line with the results obtained from FSCH test.

5.4.3 RSCH Test

The RSCH test measures the rutting potential of the mix over a range of temperatures. In this study, the RSCH test was conducted in accordance with AASHTO TP-7, Procedure F [6]. A controlled cyclic sinusoidal shearing stress was applied for a period of 0.1 s followed by a rest period of 0.6 s with a peak shear stress of 68 ± 5 kPa. The test duration was defined to correspond with permanent shear strain accumulation of 5-percent, or 100,000 loading cycles. The measured response was in terms of permanent shear strain accumulation as a function of the number of loading cycles.

The laboratory compacted specimens with and without the baghouse fines were first subjected to the FSCH test described earlier in this chapter. Following the FSCH test, these specimens were then subjected to RSCH test to evaluate the mixture resistance to rutting. Testing was conducted at 50.2°C.

Table 5-10, Figure 5-8, and Figure 5-9 show the RSCH test results. The accumulated plastic shear strain at 100,000 cycles shown in Table 5-10 confirm the results from FSCH test: 1) for both counties specimens containing baghouse fines show lower accumulated plastic shear strain compared to specimens without the bag house fines with a percentage difference of approximately 15-percent; and 2) respective mixes from Buncombe and Rutherford counties show similar performance. As the accumulated plastic strain for all mixtures are less than 5-percent, it is expected that these mixtures should not show in-situ accumulated rut depth more than 0.5-inch under normal traffic loading.

5.5 Asphalt Pavement Analyzer Tests

The effect of baghouse fines on the rutting resistance of asphalt mixtures was also evaluated using the Asphalt Pavement Analyzer (APA). NCDOT Materials and Tests Unit conducted the tests.

“Accelerated pavement testing is defined as the controlled application of a prototype wheel loading, at or above the appropriate legal load limit to a prototype or actual, layered, structural pavement system to determine pavement response and performance under a controlled, accelerated, accumulation of damage in a compressed time period [30].” The APA measures rutting susceptibility by rolling a steel wheel over a pressurized rubber hose pressing against a rectangular asphalt concrete slab or a 6-inch diameter circular specimen. The test is normally performed at 40.6 °C and with the rubber hoses pressurized to 0.69 MPa (100 psi). The wheel passes over the hoses and slab at approximately 2.0 km/h (33±1 cycles/min) and the specimen is subjected to 8,000 cycles with each cycle defined as two passes of the wheel back and forth across the specimen. The deformation of the slab or specimen is measured at three points across the specimen and averaged. The Georgia Department of Transportation (GDOT) defines a mixture as susceptible to rutting if the average rut depth for replicate specimens is greater than 7.6-mm. However, the FHWA recommends that the maximum rut depth criteria be set to 5-mm.

Since the APA is a ‘proof’ test or a ‘pass / fail test,’ many variations of the test temperatures and rut depth acceptance criteria exist based on local experience. NCDOT normally conducts these tests corresponding to the asphalt cements high PG rating with rut depth acceptance criterion of 0.25-inches (6.25-mm). In this study, APA test temperature of 50 °C was selected for consistency with the temperatures used for other performance tests. The 6-inch diameter specimens for APA test were fabricated at NCSU materials laboratory using the SGC (Superpave Gyrotory Compactor). The specimens were compacted to a height of 3 inches with a target air void content of 7±1-percent. Table 5-11 shows the air voids content of specimens used for the APA tests. APA testing was carried out at NCDOT. Two cylindrical specimens were used for each test and an average rut depth was determined.

5.5.1 APA Test Results

Test results obtained from NCDOT (Appendix D) indicate that the materials from Buncombe County with and without the baghouse fines had an average rut depth of 6.15-mm and 6.12-mm, respectively. For the Rutherford County, specimens with and without the baghouse fines had an average rut depth of 12.33-mm and 12.78-mm, respectively, two times those observed for the Buncombe County.

Based on the test results obtained, it appears that the Buncombe County mixes would be acceptable based on the GDOT criterion but would fail based on the NCDOT criterion. It should be noted that GDOT requires testing to be conducted at 40.6°C, whereas NCDOT requires a testing temperature of 64°C as these mixtures contain a PG64-22 asphalt binder. For Rutherford County, both mixtures with and without the baghouse fines would fail.

APA test results indicate that mixtures from both counties are susceptible to excessive rutting. However, it should be noted that pavement sections in these counties have not shown excessive rutting to date. Pavement sections in Buncombe County were observed to have slightly more rutting (which was also evident from the field cores received [43]) compared to the cores from Rutherford County, contrary to the APA test results. Nevertheless, the objective in this study was not to estimate the rutting susceptibility of the mixtures per-se, but to evaluate the effect of baghouse fines on the mixture performance. In this regard, the APA test shows that the baghouse fines used in this study do not have any effect on the performance of the asphalt mixtures from either county, a result consistent with all prior performance test results presented in earlier sections.

5.6 Effect of Baghouse Fines on Moisture Sensitivity

NCDOT Materials and Tests Unit, in accordance with their procedure, conducted the TSR tests. It may be noted that NCDOT does not require the specimens to be subjected to freeze-thaw cycle as required under AASHTO T283 procedure. Four inch diameter specimens compacted using Marshall procedure were manufactured at NCSU and tested at NCDOT. In all, 8 specimens were made for each asphalt mixture with and without the

baghouse fines for both counties. The results of the TSR tests are presented in Table 5-12 through Table 5-16.

Table 5-16 shows the summary of TSR test results for the asphalt mixtures with and without baghouse fines for the Buncombe and Rutherford counties. Test results show that the tensile strength ratio for asphalt mixtures containing baghouse fines for Buncombe and Rutherford counties are 78-percent and 84-percent, respectively, which fails the NCDOT 85-percent tensile strength ratio requirement for surface mixtures. It may be noted that these mixtures do contain anti-strip additive with a dosage suggested in the respective NCDOT JMFs. Mixtures without the baghouse fines meet or exceed the NCDOT requirement with mixtures from Buncombe and Rutherford counties showing an 85-percent and 92-percent tensile strength ratio, respectively. Later, an in-depth study conducted by Tayebali et al [42] based on 6 inch diameter specimens also confirmed the finding of this investigation.

5.7 Summary and Conclusion

The main objective of this task was to evaluate the performance of laboratory mixes containing baghouse fines. FSCH and RSCH test results for laboratory mixes containing baghouse fines show the following:

- Baghouse fines have a stiffening effect on mixtures from both counties;
- Mixtures containing baghouse fines are more resistant to rutting as compared to mixtures not containing baghouse fines;
- Respective mixtures from both counties show similar dynamic shear stiffness and rutting characteristics.

The APA test results indicate that mixtures with and without baghouse fines from both counties are susceptible to excessive rutting. However, for both Buncombe as well as Rutherford counties, it was observed that the baghouse fines did not have an effect in comparison to the mixtures containing regular mineral filler materials. This observation is in agreement with other SST performance test results. However, the TSR test results clearly show that mixtures containing baghouse fines are sensitive to moisture and fail the NCDOT

tensile strength ratio requirement. The mixture moisture sensitivity may therefore be one of the contributory factors in the shoving distress observed in Buncombe County; the other reason being either failure of tack coat itself due to inadequate bond strength, non-uniform application, or improper breaking of emulsions. It should be noted that remaining moisture due to inadequate curing of tack coat may adversely affect the overlaid asphalt layer in terms of moisture damage especially for those mixes containing excessive baghouse fines.

Table 5-1 Air voids and G_{mm} of 150-mm diameter laboratory mix specimens

Buncombe County				Rutherford County			
Sample ID	Height (mm)	Air voids (%)	Avg. Air Void (%)	Sample ID	Height (mm)	Air void (%)	Avg. Air Void (%)
BW11	50.2	4.9	4.7	RW41	50.5	5.5	5.5
BW12	49.3	4.5		RW42	47.5	5.5	
BWO11	50.4	4.9	4.9	RWO41	47.4	5.6	5.5
BWO12	48.6	4.8		RWO42	48.6	5.3	
G_{mm} – mixes w/baghouse fines			2.511	G_{mm} – mixes w/baghouse fines			2.513
G_{mm} – mixes wo/baghouse fines			2.505	G_{mm} – mixes wo/baghouse fines			2.509

Table 5-2 Nationwide pavement temperatures, [37]

Region	Temperature in °C		
	Effective	Critical	Maximum
I A	27.7	35	37.6
I B	33.0	40	41.8
I C	29.3	35	37.5
II A	28.3	36	38.4
II B	34.2	42	43.7
II C	36.0	43	45.7
III A	30.1	36	38.6
III B	37.2	44	46.6
III C	35.1	42	44.3
Mean	32.3	39.2	41.6

Table 5-3 Average depths and test temperatures

County	Weather Station.	Depth (mm)	Equation Temp.	SHRPBIND Temp.	Average Temp.
Buncombe	Asheville	33	51.4 °C	48.9 °C	50.2 °C
Rutherford	Caroleen	32	55.4 °C	52.5 °C	54.0 °C

Table 5-4 |G*| (Pa) versus frequency (Hz) for lab mixes, 50.2 ° C, Buncombe County

Frequency	BW11	BW12	BWO11	BWO12
10	1.44E+08	1.90E+08	9.18E+07	1.62E+08
5	1.10E+08	1.41E+08	6.69E+07	1.17E+08
2	7.94E+07	9.88E+07	4.66E+07	8.02E+07
1	6.38E+07	7.71E+07	3.67E+07	6.17E+07
0.5	5.23E+07	6.15E+07	2.93E+07	5.12E+07
0.2	4.24E+07	4.83E+07	2.30E+07	3.66E+07
0.1	3.78E+07	4.11E+07	2.00E+07	3.08E+07
0.05	3.16E+07	3.49E+07	1.65E+07	2.72E+07
0.02	2.87E+07	3.30E+07	1.48E+07	2.44E+07
0.01	2.71E+07	2.66E+07	1.38E+07	2.10E+07

Table 5-5 d (degrees) versus frequency (Hz) for lab mixes, 50.2 ° C, Buncombe County

Frequency	BW11	BW12	BWO11	BWO12
10	41.11	45.80	49.68	47.84
5	40.46	45.47	48.20	47.79
2	39.37	44.07	46.92	46.45
1	38.41	42.59	43.19	45.93
0.5	36.08	40.72	44.05	43.55
0.2	33.70	37.97	40.55	41.28
0.1	32.40	36.07	37.35	39.46
0.05	29.00	33.47	35.30	35.01
0.02	29.26	34.25	34.74	34.25
0.01	25.68	25.39	29.56	29.78

Table 5-6 Average |G*|, d, and |G*|/sin d values, 50.2 ° C, lab mixes Buncombe County

Frequency	G* (Pa.) (With)	G* (Pa.) (W/o)	d (deg.) (With)	d (deg.) (W/o)	G* /sin d (With)	G* /sin d (W/o)
10	1.67E+08	1.27E+08	43.46	48.76	2.42E+08	1.69E+08
5	1.25E+08	9.21E+07	42.97	48.00	1.83E+08	1.24E+08
2	8.91E+07	6.34E+07	41.72	46.69	1.34E+08	8.73E+07
1	7.04E+07	4.92E+07	40.50	44.56	1.08E+08	6.97E+07
0.5	5.69E+07	4.03E+07	38.40	43.80	9.15E+07	5.82E+07
0.2	4.53E+07	2.98E+07	35.83	40.91	7.74E+07	4.54E+07
0.1	3.94E+07	2.54E+07	34.23	38.40	7.02E+07	4.07E+07
0.05	3.32E+07	2.19E+07	31.24	35.16	6.42E+07	3.80E+07
0.02	3.08E+07	1.96E+07	31.75	34.50	5.87E+07	3.47E+07
0.01	2.68E+07	1.74E+07	25.54	29.67	6.23E+07	3.52E+07
Average	6.85E+07	4.86E+07	3.66E+01	4.10E+01	1.09E+08	7.02E+07

Table 5-7 |G*| (Pa) versus frequency (Hz) for lab mixes, 50.2 ° C, Rutherford County

Frequency	RW41	RW42	RWO41	RWO42
10	2.25E+08	2.02E+08	1.74E+08	1.86E+08
5	1.64E+08	1.46E+08	1.23E+08	1.34E+08
2	1.09E+08	9.68E+07	7.83E+07	8.85E+07
1	8.00E+07	7.16E+07	5.68E+07	4.39E+07
0.5	5.98E+07	5.41E+07	4.19E+07	4.47E+07
0.2	4.18E+07	3.83E+07	2.95E+07	3.68E+07
0.1	3.21E+07	3.09E+07	2.36E+07	2.91E+07
0.05	2.56E+07	2.31E+07	1.80E+07	1.15E+07
0.02	2.00E+07	1.98E+07	1.50E+07	1.21E+07
0.01	1.77E+07	1.84E+07	1.33E+07	1.54E+07

Table 5-8 d (degrees) versus frequency (Hz) for lab mixes, 50.2 ° C, Rutherford County

Frequency	RW41	RW42	RWO41	RWO42
10	43.97	45.61	48.26	46.45
5	45.36	46.81	49.51	47.29
2	46.72	47.28	50.07	47.98
1	47.66	45.66	54.41	28.08
0.5	47.79	47.09	50.10	59.49
0.2	45.93	45.22	47.63	57.29
0.1	43.61	42.52	46.53	48.85
0.05	40.86	39.49	43.78	35.35
0.02	39.28	34.86	37.73	32.52
0.01	37.73	32.08	37.85	33.17

Table 5-9 Average |G*|, d, and |G*|/sin d values, 50.2 ° C, lab mixes Rutherford County

Frequency	G* (Pa.) (With)	G* (Pa.) (W/o)	d (deg.) (With)	d (deg.) (W/o)	G* /sin d (With)	G* /sin d (W/o)
10	2.14E+08	1.80E+08	44.79	47.36	3.04E+08	2.44E+08
5	1.55E+08	1.28E+08	46.08	48.40	2.15E+08	1.72E+08
2	1.03E+08	8.34E+07	47.00	49.03	1.41E+08	1.11E+08
1	7.58E+07	5.03E+07	46.66	41.24	1.04E+08	8.15E+07
0.5	5.70E+07	4.33E+07	47.44	54.80	7.73E+07	5.32E+07
0.2	4.00E+07	3.31E+07	45.58	52.46	5.60E+07	4.18E+07
0.1	3.15E+07	2.64E+07	43.07	47.69	4.61E+07	3.56E+07
0.05	2.44E+07	1.48E+07	40.18	39.57	3.78E+07	2.30E+07
0.02	1.99E+07	1.36E+07	37.07	35.12	3.31E+07	2.35E+07
0.01	1.81E+07	1.44E+07	34.91	35.51	3.18E+07	2.49E+07
Average	7.38E+07	5.87E+07	4.33E+01	4.51E+01	1.05E+08	8.10E+07

Table 5-10 Strain at the end of RSCH test, 50.2 ° C, lab mixes

Specimens 'With' Baghouse Fines			Specimens 'Without' Baghouse Fines		
County	Sample ID	% Strain	County	Sample ID	% Strain
Buncombe	BW11	2.10	Buncombe	BWO11	2.70
Buncombe	BW12	1.59	Buncombe	BWO12	1.57
Average % Strain		1.85	Average % Strain		2.14
Rutherford	RW41	1.70	Rutherford	RWO41	2.18
Rutherford	RW42	1.89	Rutherford	RWO42	2.15
Average % Strain		1.80	Average % Strain		2.17

Table 5-11 Air voids and heights of 6-inch diameter laboratory specimens for APA test

Buncombe County				Rutherford County			
Sample ID	Height (mm)	Air voids (%)	Avg. Air Void (%)	Sample ID	Height (mm)	Air void (%)	Avg. Air Void (%)
BW02	75.6	6.5	6.5	RW05	75.6	7.7	7.6
BW03	75.5	6.5		RW06	75.4	7.4	
BWO1	75.5	6.4	6.5	RWO5	75.4	6.9	6.8
BWO2	75.5	6.6		RWO6	75.5	6.6	

Table 5-12 Buncombe County (With baghouse fines) TSR results (4-inch specimens)

Unconditioned Specimens				Conditioned Specimens			
Sample ID	Height (mm)	Air voids (%)	Max. Load (N)	Sample ID	Height (mm)	Air voids (%)	Max. Load (N)
BW01	63.9	6.9	2200	BW02	64.0	7.0	1600
BW03	63.9	6.8	2060	BW06	63.8	6.6	1750
BW05	63.8	6.7	2040	BW08	63.7	6.9	1550
BW11	63.8	7.0	2270	BW10	63.8	6.9	1700
Average		6.9	2142			6.9	1650

Table 5-13 Buncombe County (W/out baghouse fines) TSR results (4-inch specimens)

Unconditioned Specimens				Conditioned Specimens			
Sample ID	Height (mm)	Air voids (%)	Max. Load (N)	Sample ID	Height (mm)	Air voids (%)	Max. Load (N)
BWO03	64.0	6.6	1980	BWO01	63.6	6.9	1600
BWO06	63.7	6.8	2050	BWO02	63.8	6.5	1750
BWO08	63.9	6.3	2080	BWO05	63.8	6.3	1760
BWO09	63.9	6.8	1900	BWO07	63.8	6.7	1810
Average		6.6	2002			6.6	1730

Table 5-14 Rutherford County (With baghouse fines) TSR results (4-inch specimens)

Unconditioned Specimens				Conditioned Specimens			
Sample ID	Height (mm)	Air voids (%)	Max. Load (N)	Sample ID	Height (mm)	Air voids (%)	Max. Load (N)
RW03	63.7	6.9	2450	RW01	63.8	7.1	2050
RW06	63.7	7.1	2400	RW02	63.8	6.8	2050
RW07	63.8	7.0	2450	RW04	63.7	6.9	2050
RW08	63.8	6.7	2500	RW10	63.8	6.8	2050
Average		6.9	2450			6.9	2050

Table 5-15 Rutherford County (W/out baghouse fines) TSR results (4-inch specimens)

Unconditioned Specimens				Conditioned Specimens			
Sample ID	Height (mm)	Air voids (%)	Max. Load (N)	Sample ID	Height (mm)	Air voids (%)	Max. Load (N)
RWO02	63.9	6.5	2150	RWO01	63.7	6.4	1950
RWO04	63.9	6.4	2100	RWO03	63.9	6.4	2050
RWO07	63.8	6.2	2300	RWO05	64.0	6.3	2025
RWO08	63.8	6.4	2250	RWO06	63.9	6.4	2100
Average		6.4	2200			6.4	2031

Table 5-16 Summary of TSR results

County	Type of Mix	QA/QC Comparative TSR	Average Tensile Strength (kPa)		Tensile Strength Ratio (%)
			Dry	Wet	
Buncombe	With bag-fines	Minor	209.3	162.9	77.8
	Without bag-fines	Minor	203.0	172.8	85.1
Rutherford	With bag-fines	Minor	244.6	204.7	83.7
	Without bag-fines	Minor	219.4	202.5	92.3

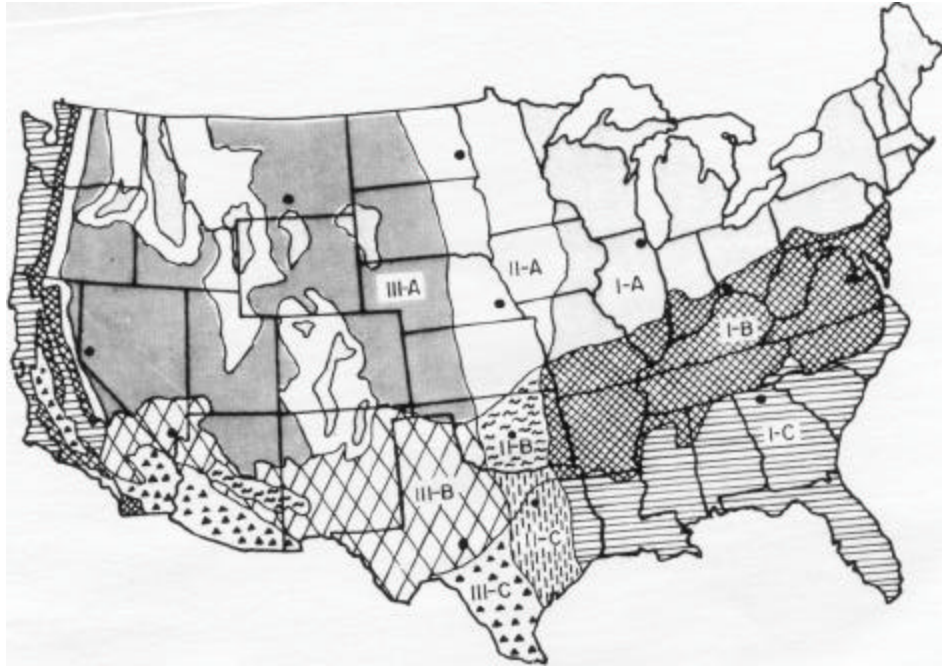


Figure 5-1 Nine climatic regions in US

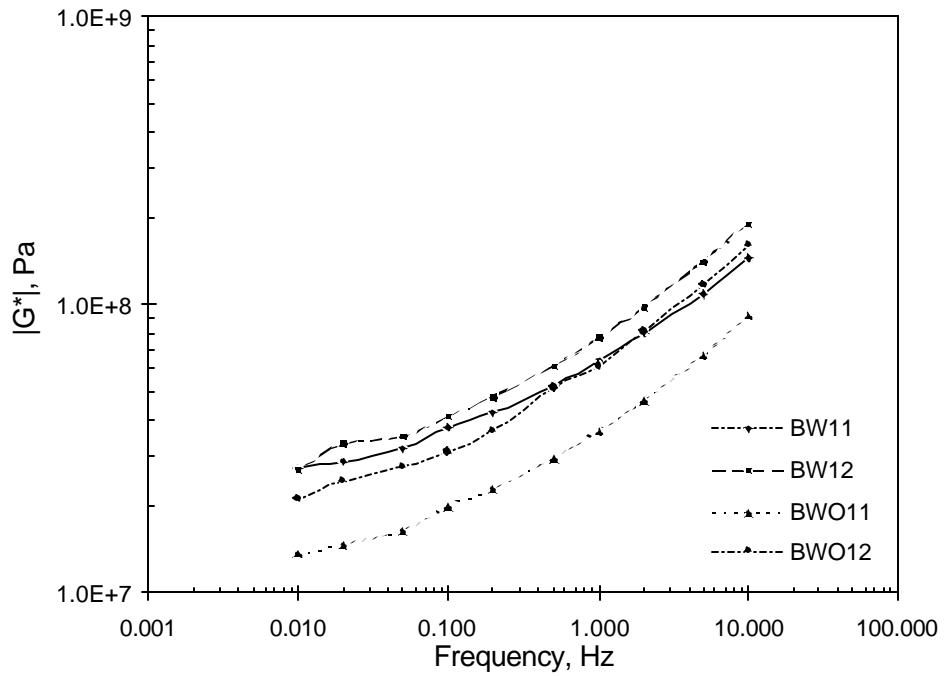


Figure 5-2 Dynamic Shear Modulus ($|G^*|$) vs. freq., 50.2°C, Buncombe, lab mixes

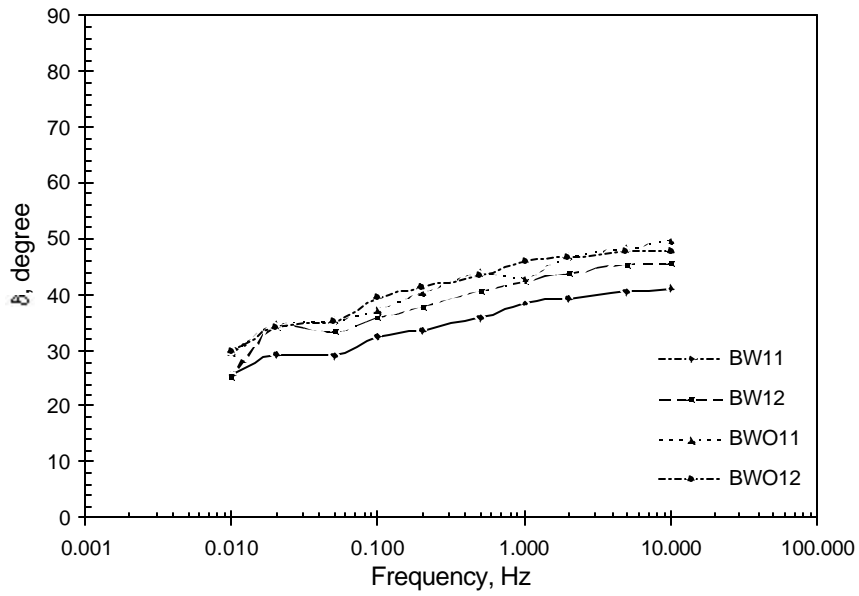


Figure 5-3 Phase angle (δ) versus frequency, 50.2°C, Buncombe, lab mixes

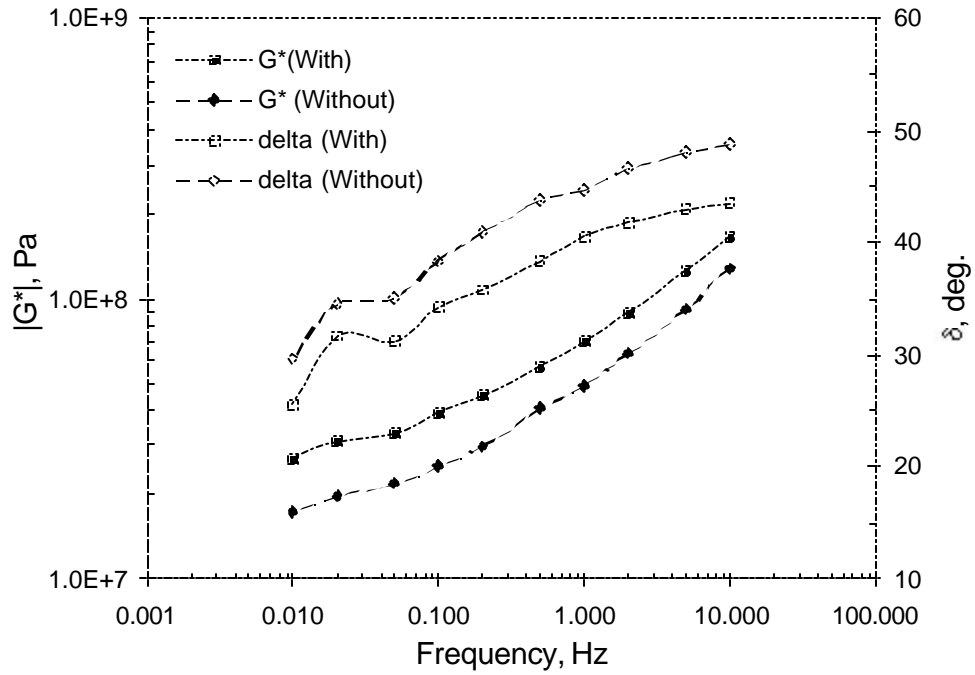


Figure 5-4 Average $|G^*|$ and δ values vs. freq., 50.2°C, Buncombe, lab mixes

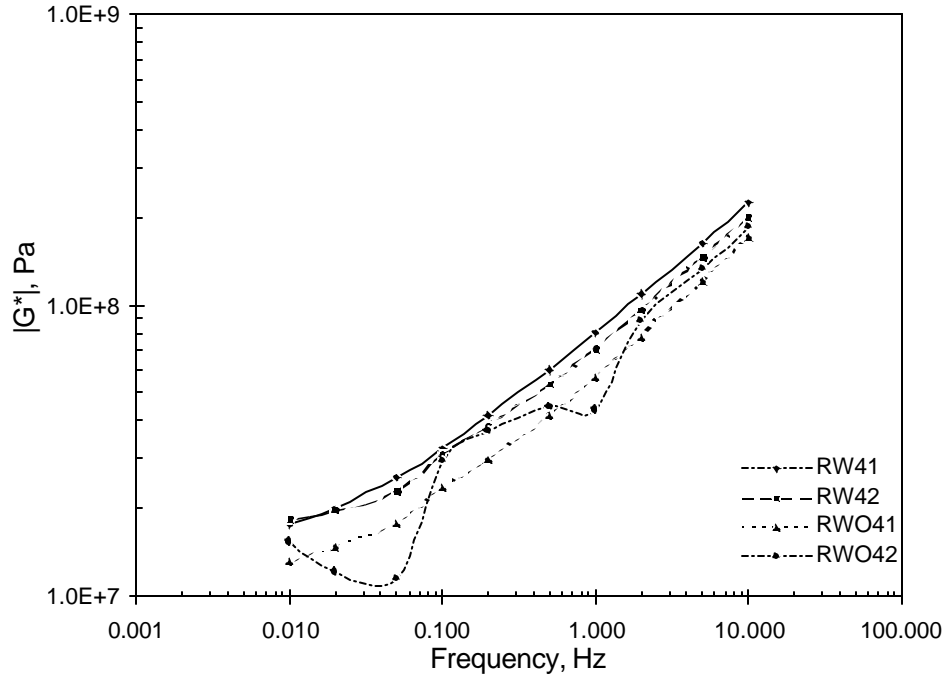


Figure 5-5 Dynamic Shear Modulus ($|G^*|$) vs. freq., 50.2°C, Rutherford, lab mixes

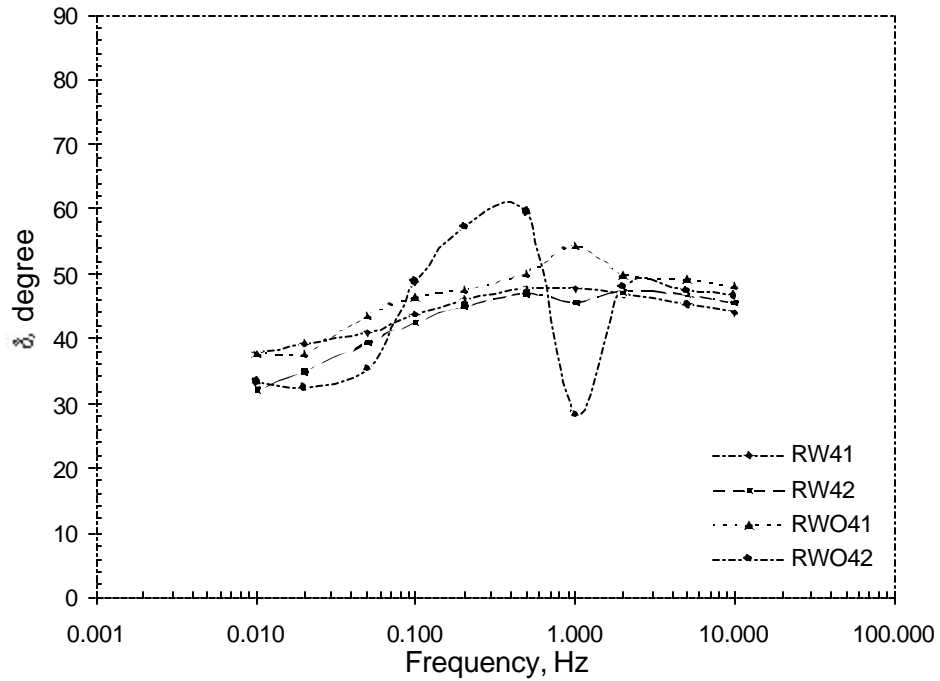


Figure 5-6 Phase angle (δ) vs. frequency, 50.2°C, Rutherford, lab mixes

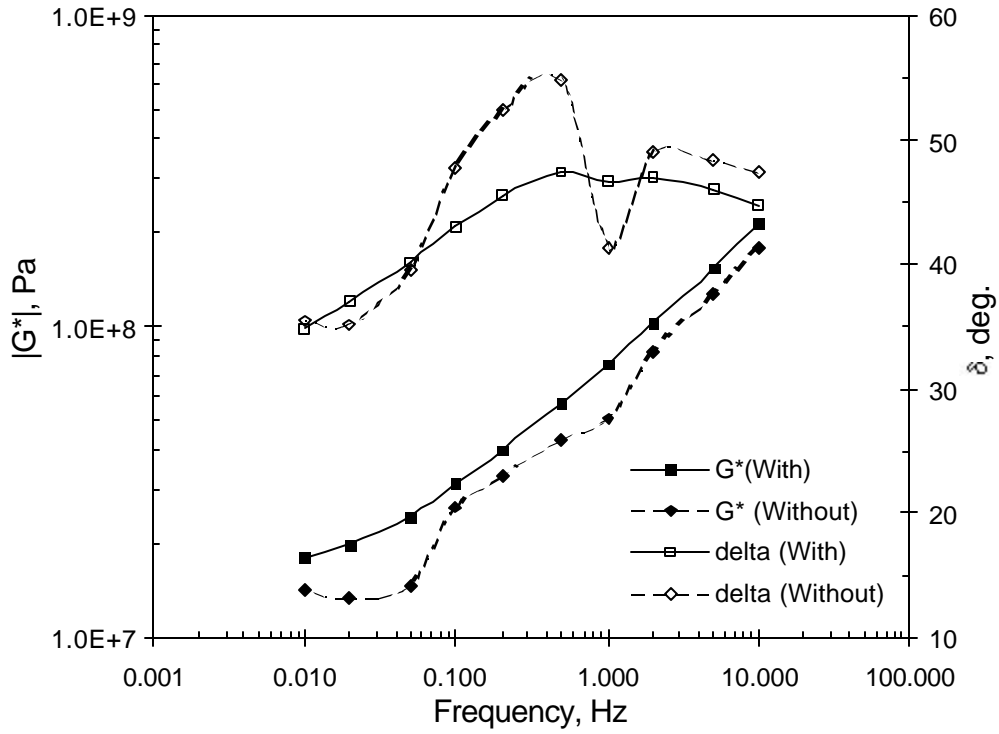


Figure 5-7 Average $|G^*|$ and δ values vs. freq., 50.2°C, Rutherford, lab mixes

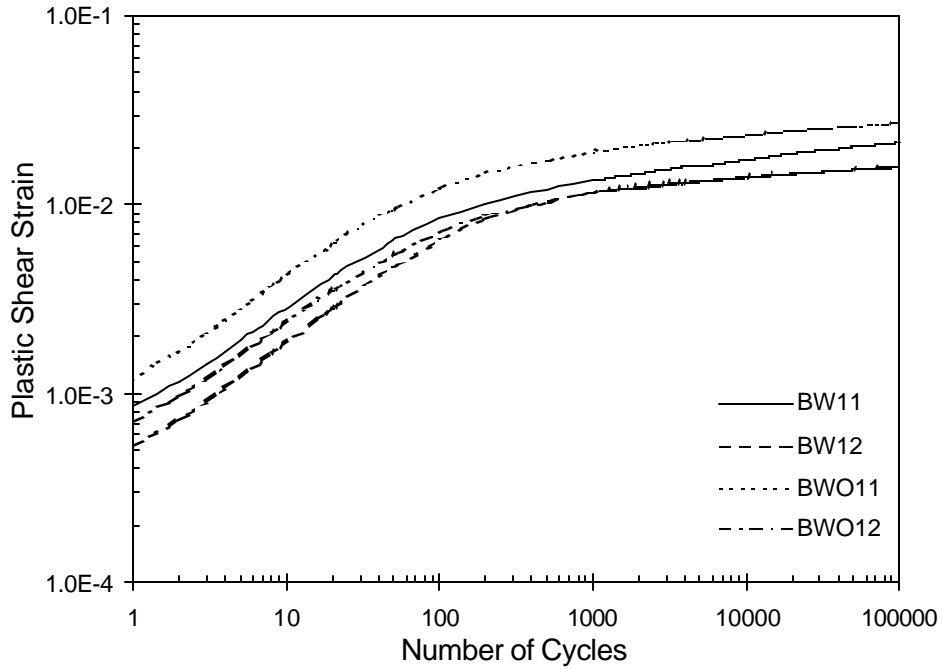


Figure 5-8 Plastic shear strain vs. RSCH cycles, 50.2°C, Buncombe County, lab mixes

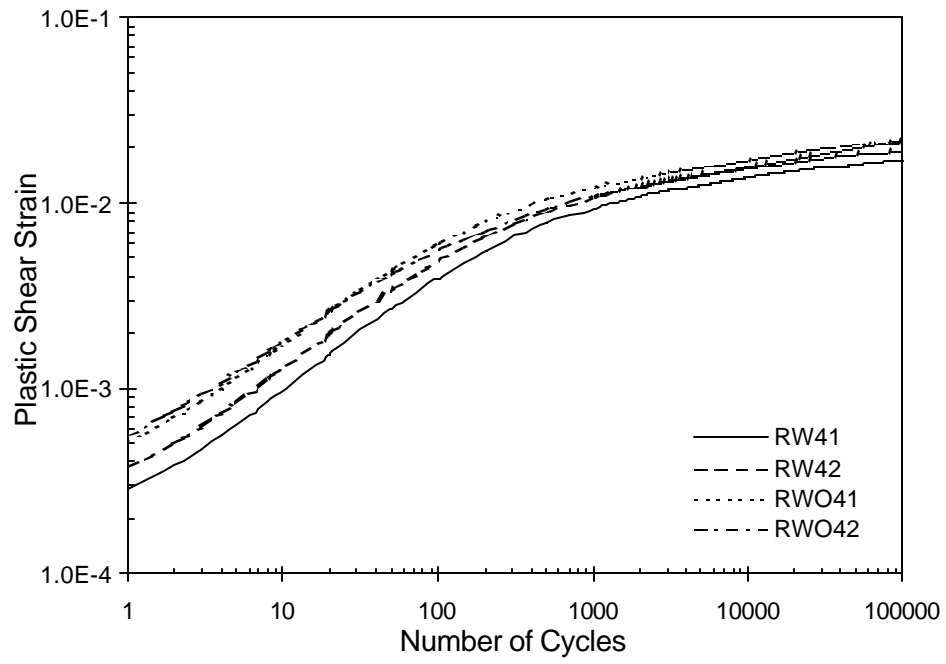


Figure 5-9 Plastic shear strain vs. RSCH cycles, 50.2°C, Rutherford County, lab mixes

6 Specimen Fabrication Using Rolling Wheel Compactor

6.1 Introduction

This chapter discusses the method used for manufacturing specimens in the laboratory. The testing is to be carried out using SST machine and the specimens would be 6-inch in diameter. The goal was to fabricate specimens closest to the field conditions. Mohammad et al [31] have fabricated specimens in a gyratory compactor in multiple layers. The bottom portion was compacted in a SGC first, followed by application of tack coat and then reinserting the specimen in the mold and compacting loose mix on top of it. This method would have given the best control over the air voids, but would not be close to field conditions where roller based compaction is used.

The alternative was to prepare slabs using a rolling wheel compactor (Figure 6-2 and Figure 6-4) to simulate the field conditions. The equipment used for compaction was gasoline powered rolling wheel compactor that had two drum rollers. The approximate weight was about 2 tons and the roller width was 25 inches. The engine provided the thrust for moving the roller in forward and reverse direction; however the steering had to be done manually. The roller had two tanks of water that can be used to vary the weight and moisten the drums. The wetting of drums is necessary to prevent the sticking of asphalt mix to the drums.

6.2 Fabrication of Steel Molds

Steel molds (Figure 6-7 through Figure 6-10) were fabricated at NCSU to make the slabs. Steel was preferred to wood because it was stronger, less likely to warp or get deformed, and could be heated to the compaction temperature immediately prior to the assembly. The goal was to have molds that would be adjustable so that slabs (specimens) can be made with different heights with a fairly accurate tolerance. To allow uniform compaction inside the mold, the sides along the direction of rolling were sloped inwards. The mold was assembled on a base plate consisting of a plywood laminate topped with an aluminum plate. Figure 6-1 and Figure 6-2 show the picture of assembled molds in and perpendicular to the direction of compaction. On the surface of the aluminum plate were four L-sections to which

the molds were anchored using steel bolts. If a taller specimen was desired, the mold extensions (shown in Figure 6-7 and Figure 6-9) were placed on the bottom portion, and were anchored using steel bolts. The compaction was achieved by rolling the compactor over the loose mix put in the molds. The effect of compaction was most visible at the edge of the roller. In order to operate the roller in a level position, a wooden platform was constructed all around the mold. In addition, wooden ramps were designed to raise or lower the roller from the wooden platform.

6.3 Specimen Fabrication

6.3.1 Asphalt Concrete Slabs

The material for making the asphalt concrete slabs was received from NCDOT. The material was heated to 160 °C in a convection oven for 4-5 hours. The molds were also heated at the same temperature. Depending on the situation, the heated molds were assembled either on the base plate or were placed as extensions over the existing mold. After securing the molds with steel bolts and nuts, the wooden platforms were placed on all sides of the mold to make the compactor flush with top surface of the mold.

A predetermined amount of the heated mix was, subsequently, poured into the mold and spread uniformly. The weight of the mix added to the mold was obtained iteratively to get a target air void of 4%. The mix was rodded with a spatula for initial compaction to remove air pockets and obtain a uniform spread throughout. The compaction process started immediately with the roller drums being moistened with water. The passes were made only in one (longitudinal) direction as is done in the field. At the end of every pass, the roller was turned slightly so as to cause the edge of the roller to move progressively from left end of the mold to right. After every few passes, the flatness of the top surface was checked using a water level. This process continued till a fairly flat profile was obtained. After compaction, the slab was cooled for 24 hours before placing a tack coat, or performing any cutting and coring operation.

6.3.2 Portland Cement Concrete Slabs

Garner granite aggregate, natural sand, and Portland cement were used to cast slabs. The mold was assembled and bolted to the base plate. It was coated with a thin layer of oil to prevent the sticking of hardened cement to the mold. After thorough mixing in the cement mixer, the mix was poured into the molds. The mix was then rodded to remove air cavities from the mold and leveled using a wooden float. It was allowed to stand for 30-45 minutes so that the bleed water rose to the surface. The excess bleed water on the surface was removed and, the surface was made smooth with a magnesium trowel (Figure 6-3).

The slab was then allowed to sit for 24 hours before the mold was disassembled. After removal from the mold, the slab was covered with wet cotton towels and was sealed in a polythene plastic sheet (Figure 6-3 top part). Water was added daily to keep the towels moist and aid the hydration of the slab. To accelerate specimen fabrication for laboratory testing, the slab was hydrated for 7 days and kept in sun (summer time) for about 48 hours to dry and shrink before applying the tack coat.

6.3.3 Cement Treated Base Slab

The procedure used to make cement treated base slabs was similar to the PCC slabs mentioned earlier. The material was mixed in a mixer and poured into the mold. Using a metal rod, the mix was rodded and leveled using a float. It was then covered with a slightly damp cloth to retain the moisture. After 24 hours the mold was disassembled; however, as the cement content in the CTB slabs was about 5%, the strength of the slabs was very low. The slabs could not withstand the normal handling stresses and crumbled as soon as they were removed from the mold.

After two unsuccessful attempts to fabricate the CTB slabs, it was decided to fabricate the CTB specimens in smaller 6-inch diameter mold and follow the procedure similar to that outlined by Mohammad et al [31]. The CTB material was poured in a 6-inch diameter modified proctor metal mold to a height of about 4.584 inches. It was then compacted in 5 layers using 56 blows per layer of the Modified Proctor Test hammer. Immediately after compaction, the specimen was covered with a damp towel to retain moisture. After about 8-10 hours, the specimens were extruded from the molds and wrapped in cotton towels and

plastic. The towels were kept wet to cure CTB for 7 days. After 7 days, the specimens were cut to a height of 1-inch (Figure 6-5). These 1-inch CTB ‘discs’ were coated with prime coat on one side (Figure 6-6). After breaking of the prime coat, the ‘discs’ were inserted in the gyratory compactor molds with the coated side facing up. The problem with this approach was that the ‘discs’ expanded after extrusion from the molds and could not be reinserted. So, using a metal file, the sides of the ‘discs’ were filed to slightly reduce the diameter of the discs. Then hot loose asphalt mix was poured in the mold and compacted to a height of 1 inch. The target air void for this overlying layer was 4%. The samples were extruded and allowed to cool before testing. Figure 8-22, on page 130, shows a picture of composite CTB-AC specimen.

6.4 Tack / Prime Coat Application

NCDOT specifications (§605 of Standard Specifications for Roads and Structures, 2002) require the placement of tack coat beneath every layer of asphalt plant mix. The required rate of application is 0.04 to 0.08 gallons per square yard. The tack coat rate chosen for preparing the laboratory samples was 0.06 gallons per square yard, which is in the middle of the range. In consultation with the NCDOT, PG64-22 binder and CMS-2 emulsion were chosen as tack coat materials.

The tack coat was applied 24 hours after rolling the asphalt slab. This would allow adequate time for cooling of the mix. For PCC, the slabs were left in sun for 48 hours to ensure that the shrinkage cracks do not occur after applying tack coat. The surface of the asphalt (or PCC) slab was cleaned with a wire brush and blasted with pressurized air to remove the loose dust particles. The CMS-2 emulsion was stirred and applied using a regular paint brush. The weight of the CMS-2 container was monitored to ensure the correct rate of application. After application, the slab was kept in a draft of fan air for 24 hours to ensure the breaking of the emulsion. In most cases, the surface was adequately ‘tacky’ to touch.

A similar procedure was followed for applying PG64-22 binder as tack coat, except that the binder was heated to about 185 °C on a hot plate. The application surface was heated with heat lamps to ensure easier application of tack coat. The weight of the binder was

monitored frequently to get to the correct rate of application. Although no ‘breakage’ of tack coat was required for PG64-22 asphalt, the next layer was paved about 24 hours after applying tack coat to maintain consistency in relation to the CMS-2 emulsion.

Section 600 of NCDOT Standard Specifications for Roads and Structures specifies the rate of application of prime coat as 0.2 to 0.5 gallons per square yard. The maximum amount of emulsion applied to the CTB specimens without overflow constrained the application rate to 0.24 gallons per square yard, which is within the permissible range. CSS-1, EPR-1 and EA-P were used as prime coat materials. The procedure for application of prime coat was similar to that of tack coat. The individual CTB ‘discs’ were weighed on a balance and were ‘painted’ with emulsions to get to the required application rate. The prime coat was allowed to break for 24 hours before another layer was compacted on top of the discs.

In case where no tack coat or prime coat was desired, the next layer was paved without prime or tack coat.

6.5 Coring and Cutting Samples

For material characterization, a three inch slab was used. The dimension of the slab used for acquiring specimens was 2 ft × 2 ft. In all, nine cores (each of 6 inch diameter) were drilled from the slab with a spacing of 1½ inches between two adjacent cores. Subsequently, the 3 inch thick cores were reduced to a height of 2 inches by shaving off the top and bottom ½ inch portions.

Composite slabs (AC over AC and AC over PCC) were 4 inch in thickness. Nine cores were drilled from these slabs, each core spaced 1½ inches apart from adjacent cores. The interface was kept at midway by removing the top and bottom portions of the core. The final height of the specimen was 2 inches, as required for SST testing.

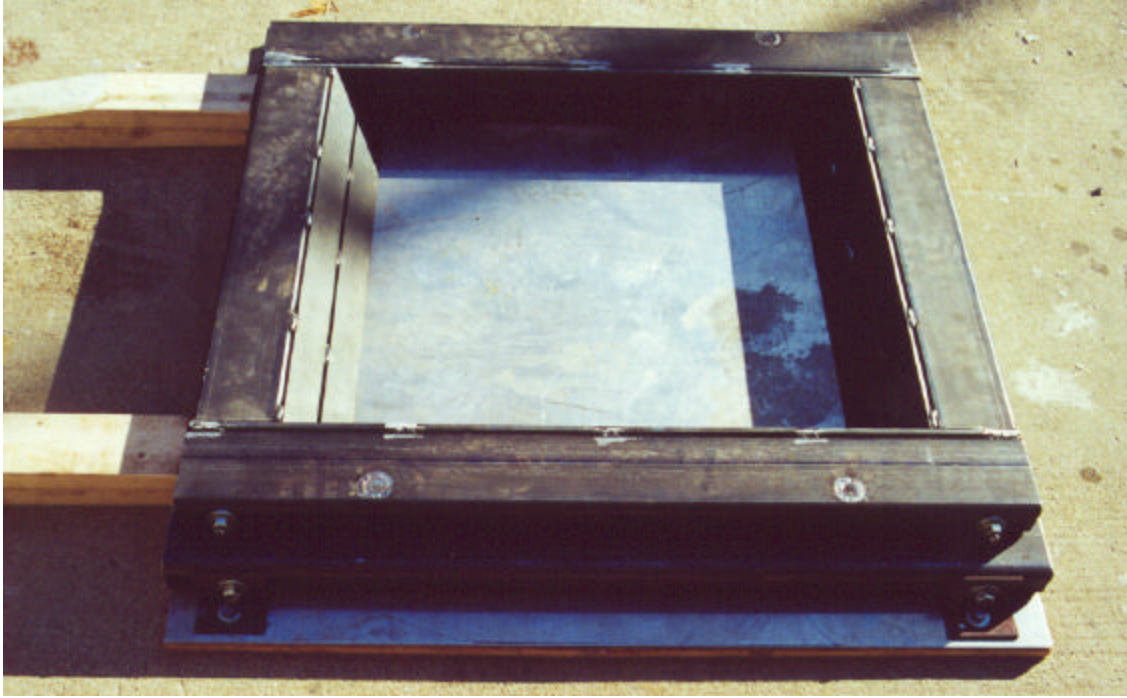


Figure 6-1 View of mold with adjustable ramps (on left)



Figure 6-2 Mold with roller

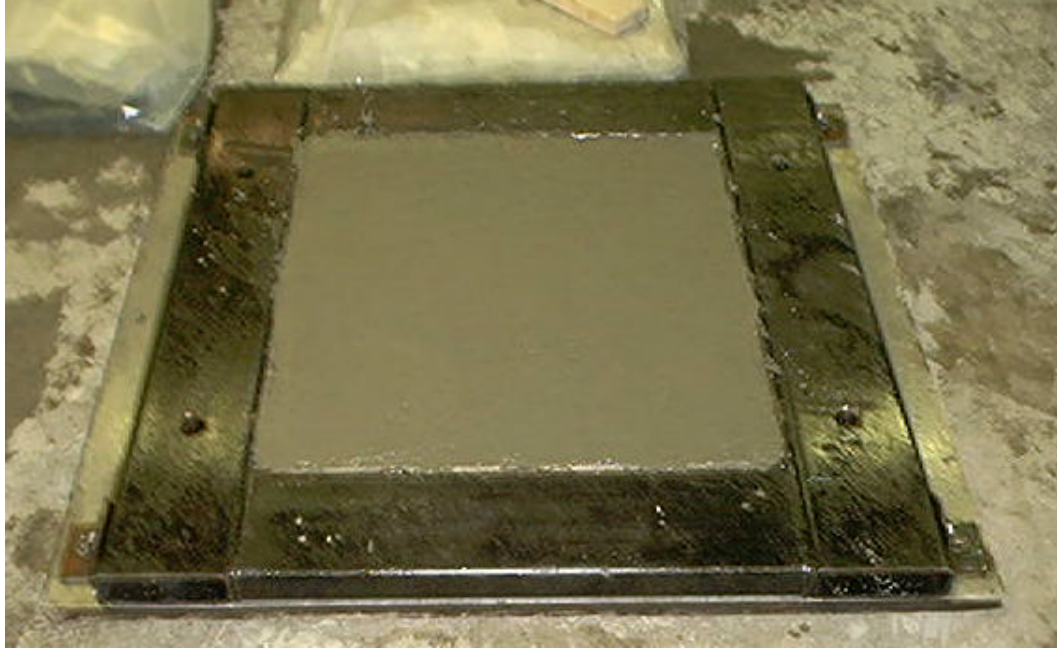


Figure 6-3 Freshly cast PCC slab



Figure 6-4 Side view with roller on the mold



Figure 6-5 Photo of a 1-inch thick CTB ‘disk’

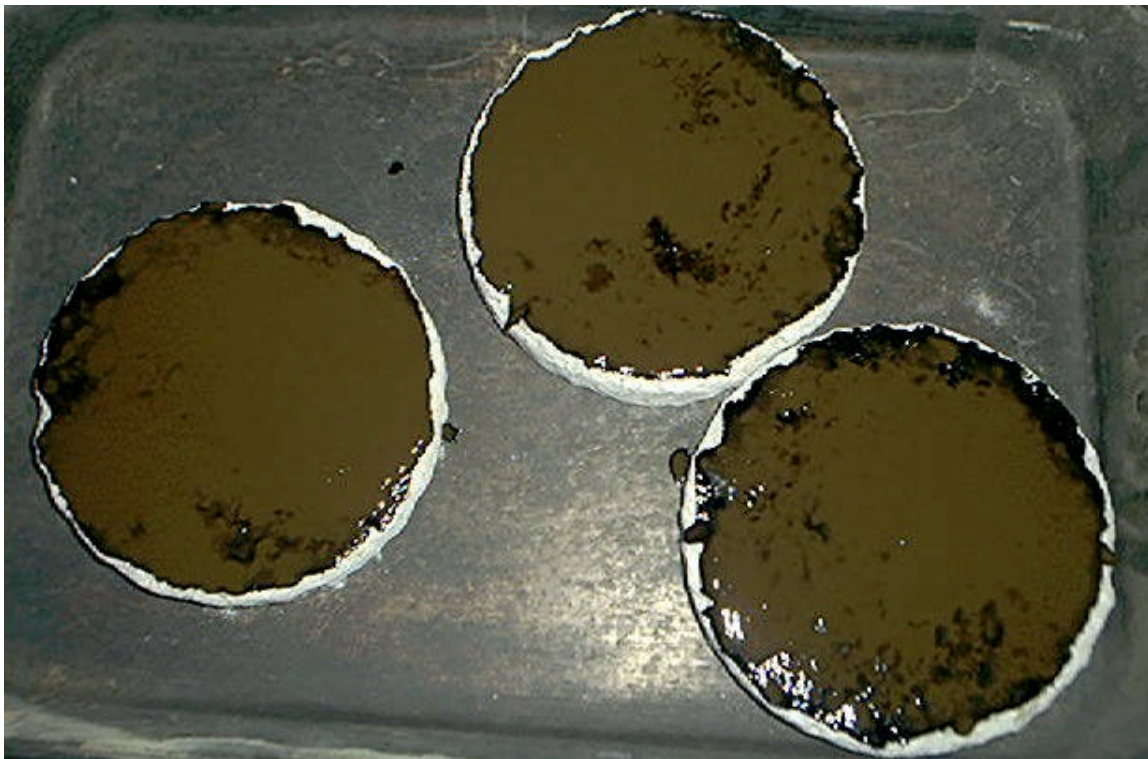
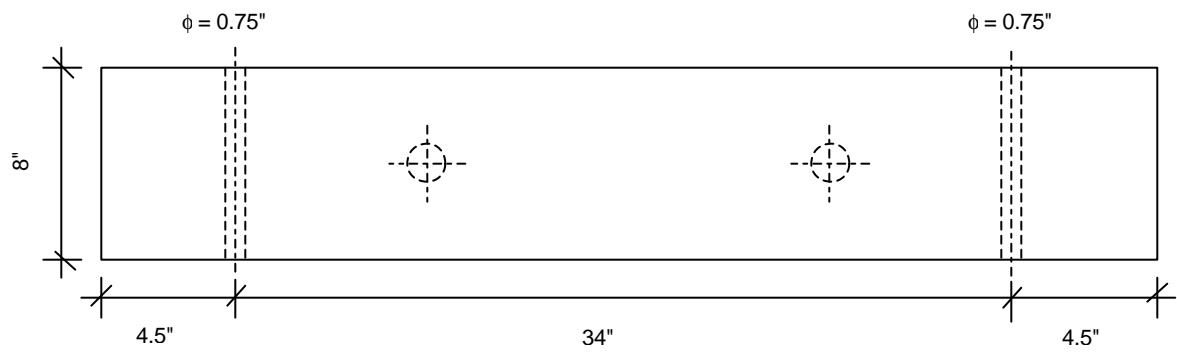
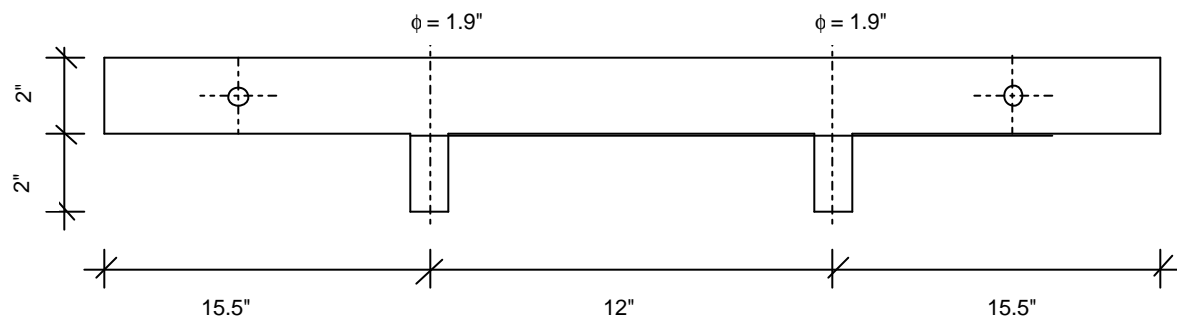


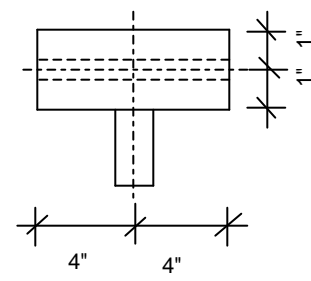
Figure 6-6 CTB ‘disks’ coated with emulsion



PLAN

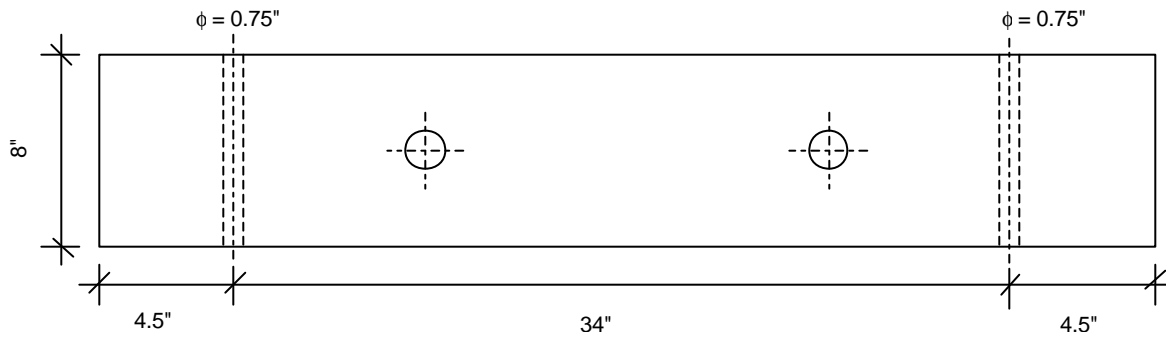


FRONT VIEW

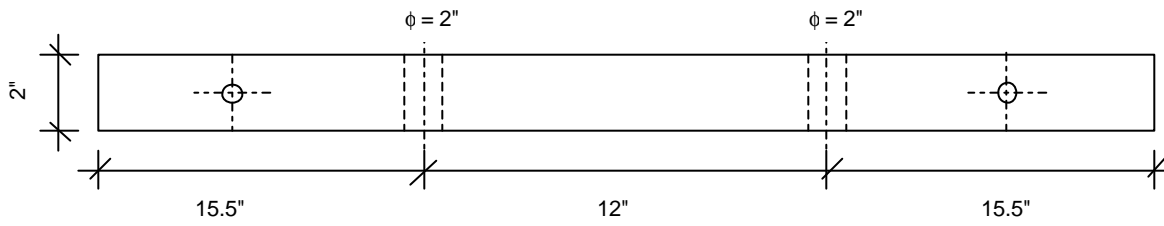


SIDE VIEW

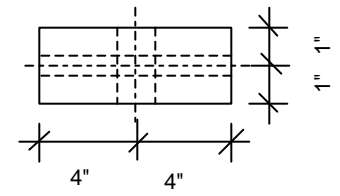
Figure 6-7 Mold Top – Part I



PLAN

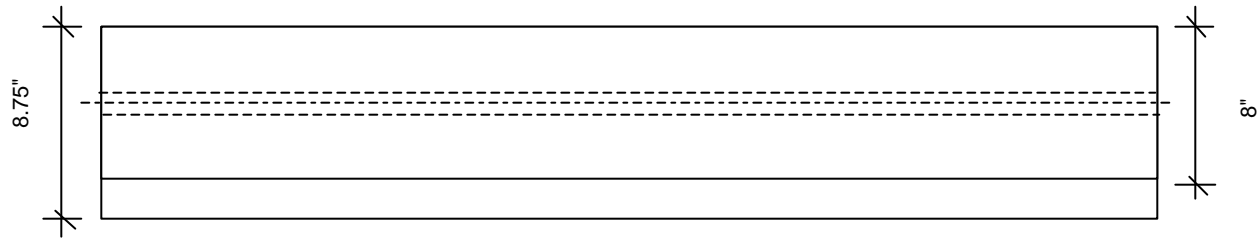


FRONT VIEW

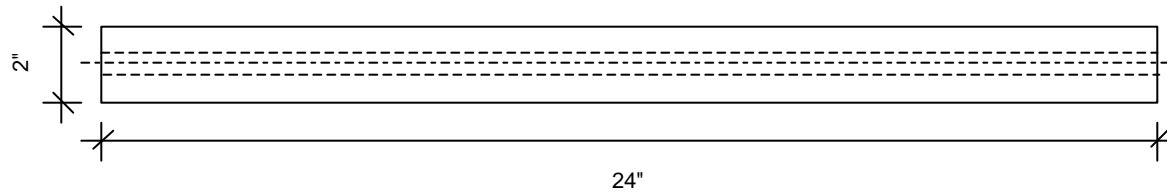


SIDE VIEW

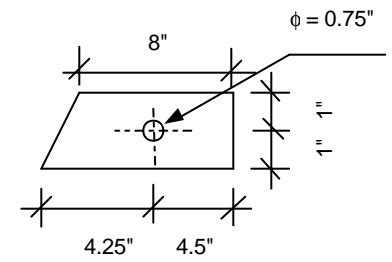
Figure 6-8 Mold Bottom – Part I



PLAN

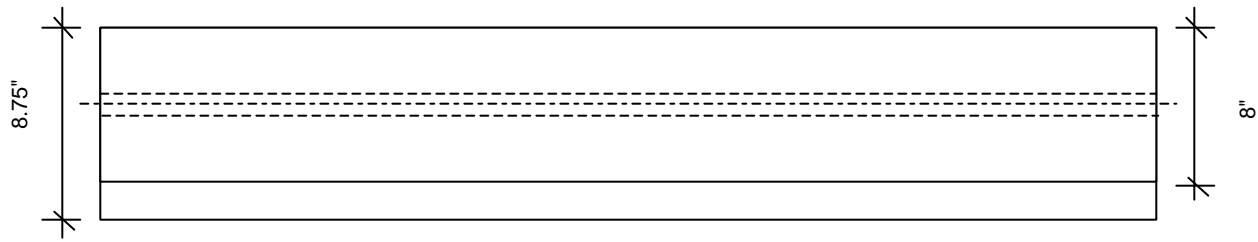


FRONT VIEW

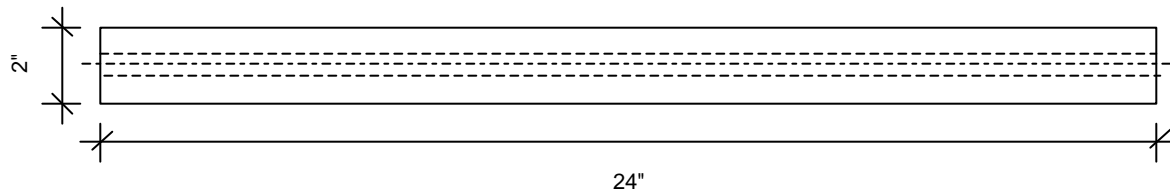


SIDE VIEW

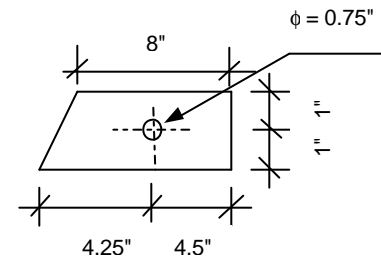
Figure 6-9 Mold Top – Part II



PLAN



FRONT VIEW



SIDE VIEW

Figure 6-10 Mold Bottom – Part II

7 Material Characterization

7.1 Introduction

The objective of this task was to obtain material characteristics needed for the mechanistic analysis of the pavement sections. In this section, the properties of asphalt mix, PCC and CTB were evaluated using the SST (Simple Shear Tester) tests and UTM (Universal Testing Machine). Test methods utilized for measuring the properties were Shear Frequency Sweep Test at Constant Height (FSCH), Axial Frequency Sweep Test (AFST), and unconfined compressive tests for PCC and CTB specimens.

7.2 Asphalt Mix Characterization

The asphalt mix (JMF enclosed in Appendix C, page 218), received from NCDOT, was characterized by the following performance tests:

- Shear tests
 - Frequency Sweep Test at Constant Height (FSCH),
 - Repeated Shear Test at Constant Height (RSCH),
- Axial tests
 - Frequency Sweep Test (AFST), and
 - Repeated Axial Test.

Specimens for the shear tests were fabricated using rolling wheel compaction (Section 6.3.1), and cored and cut (Section 6.5) to a height of 50 mm. After coring and cutting, the specimens were fan dried to remove the residual water and bulk specific gravity (ASTM D 2726) was determined. The target air void content of the specimens was 4.0 ± 0.5 %. The G_{mm} (maximum theoretical specific gravity) determined according to ASTM D 2041 was **2.442** for the loose mix. Table 7-1 lists the air void contents of the samples obtained.

Specimens for the axial tests were fabricated in the laboratory using the Servopac™ gyratory compactor. The mix was preheated to a temperature of 160 °C in the ovens for 3

hours. A known quantity of the mix was then poured into the compactor molds and compacted to a target air void content of 5.5%. The targeted air void content was slightly higher so that after coring and cutting the final air void content would be 4%, which is the desired air void content. The average height of the specimens was 17.8 cm. The specimens were extruded and, after the mix was cooled, each specimen was cored to a 4-in diameter and the top and bottom portions shaved to give a final height of 6-in (15.2 cm). The specimens used for axial testing were 4×6 inch in dimensions with an air void of 4±0.5%.

7.2.1 Frequency Sweep Test at Constant Height (FSCH)

The FSCH test measures the viscoelastic shear properties over a range of testing frequencies and temperatures. The testing was carried out at 20, 30, 40 and 60 °C. Table 7-2 through Table 7-9 show the FSCH test results for AC mixes. The results are graphically presented in Figure 7-1 through Figure 7-10. The mix shear stiffness ($|G^*|$) reduces with increasing temperature or lowering of frequency. The results for shear phase angle (δ) are a slightly different. It is expected that with increasing frequency, the phase angle would reduce but this is not the case at 60 °C (Figure 7-8). The phase angle increases with increasing frequency at this relatively high temperature. Further, at 40 °C, the phase angle curve (Figure 7-6) is shaped ‘concave downwards.’ The phase angle, at 40 °C, increases with frequency (at lower frequencies) and then reduces with increasing frequency (higher frequencies). This behavior is summarized in the phase angle master curves shown in Figure 7-12 and Figure 7-14. At higher frequencies the mix is more elastic than viscous; hence the phase angle reduces with increasing frequency. At lower frequencies, however, the binder (in the mix) is mostly viscous and the aggregate, being elastic, contributes primarily to the mix strength. The relative contribution of aggregate to strength increases causing phase angle to reduce (alternatively, more elastic mix) with reducing frequency. The master curves at 30 and 40 °C (Figure 7-11 through Figure 7-16) characterize the behavior of asphalt mix over a range of frequencies.

7.2.2 Repeated Shear Test at Constant Height (RSCH)

The rutting potential of a mix is characterized by the RSCH test (details in §5.4.3). As rutting is more likely to occur at higher temperatures, the tests were carried out at temperature of 40 and 60 °C. The purpose of this test was to ensure that the mix did not fail prematurely during the shear ramp test. The test results are given in Table 7-10 and Figure 7-17. The tests were conducted to a maximum of 100,000 cycles or 5.0% strain whichever happened earlier. It was observed that specimens tested at 60 °C failed at an average of 20,000 cycles compared to specimens tested at 40 °C. The 60 °C test results (Figure 7-17) indicate an accumulation of tertiary strain in the samples. The specimens at 40 °C accumulated an average total strain of 1.05% at the end of test. This indicates the mix has a significant ability to resist rutting at 40 °C. Based on the information at 40 °C the testing at 20 °C would have yielded lower plastic strain at 100,000 cycles. The plastic shear strain at 5,000 RSCH cycles is a good indicator of the mix behavior. It can be observed that at 60 °C, the accumulated plastic strain is 2.95% compared to 0.67% at 40 °C. Given the low accumulation of plastic strain at 40 °C, the mix is expected to perform well at this temperature.

7.2.3 Axial Frequency Sweep Test (AFST)

In the earlier two sections (Sections 7.2.1 and 7.2.2), the performance of the AC mix was evaluated using FSCH and RSCH tests. In those tests, the shear properties were evaluated. This section describes the evaluation of axial stiffness modulus and the phase angle of the mix.

The AFST test is similar to the FSCH test except that a dynamic uniaxial loading is applied as opposed to shear. The test was conducted in a controlled strain mode of loading with a sinusoidal axial strain of amplitude of $\pm 0.005\%$ (0.0001 mm/mm peak to peak strain) applied at 10, 5, 2, 1, 0.5 and 0.2 Hz. At each frequency, the stress response was measured along with the axial phase shift (δ) between the stress and strain, and the dynamic axial modulus ($|E^*|$) was computed as the ratio of peak stress over peak strain. This test was attempted in two ways: unglued specimens, and glued specimens. In case of unglued

specimens, the specimens were sandwiched between two platens without gluing. A variable seating load (from 30 psi at 20 °C to 10 psi at 60 °C) was applied to keep the platens from losing contact with the specimen during testing. The results obtained had high variability and were unpredictable. To reduce the variability, it was decided to glue the specimens to the platens. The specimens were tested with zero seating load. The air void contents of the axial test specimens are given in Table 7-11.

Figure 7-18 through Figure 7-20, and Table 7-12 through Table 7-15 list the results of the axial frequency sweep test. It can be seen that with increasing test temperature, the axial stiffness decreases and the phase angle increases. The trend is similar to the shear behavior. The results are not reported at low frequencies at 60 °C as they are highly variable.

7.2.4 Repeated Axial Test

The repeated axial test, similar to the RSCH test, (details in §5.4.3) was used to characterize the axial deformation of the mix. The loading pattern was similar to the RSCH tests, except that the load was applied axially instead of shear. A controlled cyclic sinusoidal axial stress was applied for a period of 0.1 s followed by a rest period of 0.6 s with a peak axial stress of 68 ± 5 kPa. The test duration was defined to correspond with permanent axial strain accumulation of 1-percent, or 100,000 loading cycles. The measured response was in terms of permanent axial strain accumulation as function of the number of loading cycles.

Figure 7-21 and Table 7-16 show the results of the test. It can be seen that at 60 °C, the mix is more prone to axial deformation than at 40 °C. The number of cycles at 60 °C average to 11400 for 1.4% axial strain, whereas at 40 °C the cycles average to more than 100,000 for 0.18% strain. Figure 7-21 shows the plot of accumulated plastic strain versus the number of cycles. The shape of the curve is concave upward and the rate of accumulation increases with number of cycles at 60 °C. However at 40 °C it can be said that the rate of accumulation starts decreasing after initial 1000 cycles. Figure 7-22 shows the overall relationship between $|G^*|$ and $|E^*|$ values across test temperatures and frequencies. It can be seen that the relationship is linear; however the value of Poisson's ratio based on the equation of the best fit line is 0.69 – a theoretical impossibility. This aberration could be due to

different sized samples used for shear and axial tests. Similarly, Figure 7-23 shows the relation between shear and axial phase angle for AC mixes. In this case, it can be said that the shear phase angle is almost the same axial phase angle. The relationships between shear and axial properties can be used to determine one if the other is known regardless of the frequency and test temperature.

7.3 Portland Cement Concrete (PCC) Characterization

A PCC mix was made using locally available aggregate, natural sand, and Type I cement. The composition was a typical 3:2:1 (rock:sand:cement) proportioning with a target water-cement ratio of 0.40. The aggregates used were classified as #67 according to AASHTO M43 specifications and were obtained from Garner quarry of Martin Marietta. The goal was to design a typical concrete for testing the bond strength of PCC overlaid with asphalt mix.

The natural sand and aggregate properties were determined according to procedures outlined in standards AASHTO T84 (Standard Method of Test for Specific Gravity and Absorption of Fine Aggregate) and AASHTO T85 (Standard Method of Test for Specific Gravity and Absorption of Coarse Aggregate) respectively. Table 7-17 lists the moisture contents and bulk specific gravities obtained for the materials used. The specific gravity of cement was *assumed* to be 3.15, a commonly used value, in most concrete calculations. To allow for air entrainment and adequate time to cast the mix into samples (or slabs) air entraining agent (AEA) and set-retarder were used. The target yield to prepare required number of test samples or slabs was 1.5 ft³. The actual finalized batch weights, including the amounts required to make a cubic yard of concrete, are listed in Table 7-18.

7.3.1 Mixing, Casting and Curing of Specimens

The mixing process started with wetting the inside of the mixer with water and draining it completely. All the materials, including the AEA and set-retarder, were weighed out before starting the process. Then about half of the rock, sand and water were added to the concrete mixer and mixed for 2 minutes. The AEA was added, followed by about a quarter of

rock and the sand. The mixing process was continued till small bubbles could be seen in the aggregate sand slurry. The bubble formation was due to the addition of the AEA to the slurry. This process took an additional minute of mixing. The set-retarder was added at this point to the mixer. After 1 minute of mixing, the mixer was stopped, and cement was added. The cement was covered with remaining sand and aggregate to prevent the loss of cement due to mixing process. The mixing was started and the remaining water was added slowly through the side walls of the mixer. The mixing continued for about 3-4 minutes before the mix was dumped out of the mixer.

Immediately after mixing ended, a cone slump test (AASHTO T119 – Standard Method of Test for Slump of Portland Cement Concrete) was performed on the plastic mix. The slump cone was moistened and placed on a moist rigid surface. The cone was held down by standing on the two foot pieces and plastic concrete, about 1/3 of the cone volume, was poured into the cone. It was tamped 25 times by a tamping rod and a second layer, about the same volume, was poured into the mold. After tamping 25 times, a third layer was added and the mix was tamped 25 times. Afterwards, the top surface was leveled and the cone lifted vertically. The vertical difference between the top of the mold and the original center of the concrete specimen is the slump of the concrete. The average of three slump tests was 4.75 in.

The unit weight of fresh concrete was determined according to procedure outlined in standard ASTM C138 (Standard Test Method for Density, Yield and Air Content of Concrete). In this procedure, an aluminum alloy bucket was used to consolidate the concrete. The volume of the bucket was 0.25 ft³. The concrete was placed in this bucket in three layers of equal volume. After placing every layer, it was rodded using a metal rod 25 times. After rodding, the sides of the container were tamped 10 times by a mallet to remove the air bubbles that might have been trapped due to rodding. After rodding and tamping the final layer, the excess concrete was struck off the surface of the bucket with a straight edge, and floated to get a flat and smooth surface. The outside walls of the bucket were washed with clean water and wiped dry. The entire bucket was weighed. The mass of the concrete was divided by the volume of the bucket to give the unit weight. The average unit weight of the concrete was 138 pcf.

The fresh concrete was cast into 4×8 and 6×12 inch cylinders and 4×4×16 inch beams according to procedure in AASHTO T23 (Standard Method of Test for Making and Curing Concrete Test Specimens in the Field). Before casting the mix, the insides of the molds were coated with a thin layer of industrial grease. For casting the cylinders, plastic molds were used and the material was compacted in three equal layers, each layer being rodded 25 times before addition of the second layer. For beam specimens, cast into metal molds, the compaction was done in two layers. Each layer was rodded uniformly 32 times before adding the next layer. After rodding the topmost layer, the excess concrete was struck off the top of the mold and the surface floated. Thin polythene sheets were used to cover the exposed surface of fresh concrete to prevent loss of moisture during the initial curing phase. Twenty four hours after casting, the cylinders were extruded from the plastic molds using compressed air. The metal molds were disassembled and the beams removed. Immediately after removal from molds, the specimens were immersed in a water bath and allowed to cure. Immediately prior to testing, the specimens were removed from the water bath. This was done to reduce the chances of having lower strength due to drying cracks. This was important, especially for flexural specimens, where surface cracks could cause tensile stresses in extreme fibers causing lower strength. Testing was carried out at 7, 14 and 28 days.

7.3.2 Compressive Strength of Cylindrical Concrete Specimens

The basic test to characterize concrete is the compressive strength of concrete. The test was conducted in accordance with standard ASTM C39 (Standard Test Method for Compressive Strength of Cylindrical Concrete Specimens) procedure. The standard states that this test is applicable for concrete mixes having a density of at least 50 pcf. For this test, 4×8 inch specimens were used. Neoprene caps were placed at the top and bottom to enclose the specimen. This was necessary to ensure that the load was applied axially and any non-uniformity on the surface would be leveled out. The moist specimens were placed in a UTM and were subjected to an axial compressive load at a rate of 20 – 50 psi/s until failure. The peak load was recorded and the failure stress computed by dividing with the cross-sectional area of the cylinder. The results, an average of three tests, are listed in Table 7-19. The average 7, 14 and 28 day strengths were 4810, 5250, and 5750 psi respectively. Most of the

specimens tested had a biaxial failure near the edge, a characteristic of testing performed using neoprene caps.

7.3.3 Modulus of Rupture for Concrete Specimens

The flexural strength of PCC was determined using the third point loading test on concrete beams. In this test, a beam of dimensions 4×4×16 inches, was loaded according to specifications in ASTM C78 (Standard Test Method for Flexural Strength of Concrete – Using Simple Beam with Third-Point Loading). The span of the beam between two supports was three times the depth, i.e. 12 inches, with 2 inch overhang on either support. Two point loads were applied at 1/3 and 2/3 length of the span. A three point loading test would cause the middle third of the beam span to be in pure uniform bending with no shear. Thus it would measure the resistance of concrete to pure flexure. The rate of loading was such that the stresses in the extreme fiber increased at a rate of 125 to 175 psi/min. For all the three replicates, the samples failed in the middle third span. The test was conducted at 7 days and the average value for modulus of rupture was 635 psi.

7.3.4 Splitting Tension Test for Concrete Specimens

The tensile strength of PCC was determined using the splitting tensile test. The test was conducted in accordance with AASHTO T198 (Standard Method of Test for Splitting Tensile Strength of Cylindrical Concrete Specimens) at 7 days on 6×12 inch cylinders. The cylinders were tested on their sides and were split diametrically by compressive load. The rate of loading was 100 to 200 psi/min. The peak load at which the failure occurred was used to calculate the splitting tensile strength of the specimen. Based on an average of three tests, the 7 day splitting tensile strength was 410 psi.

7.3.5 Elastic Modulus Test for Concrete Specimens

The elastic modulus of concrete was determined at 7 days in accordance with ASTM C 469 (Standard Test Method for Static Modulus of Elasticity and Poisson's Ratio of Concrete in Compression). A deflection measuring jig was mounted on a 6×12 inch cylinder

to measure the deformation of the cylinder under compressive load. Figure 7-24 shows the sketch of the assembly. The jig consisted of two rings attached to the cylinder by means of screws. The spacing between the two rings was 8 inch. Thus the effective height of the cylinder was 8 inches. The jig was such that one end of the rings was fixed, whereas the diametric end had a dial gauge mounted on it. By geometry, a unit deformation of the cylinder would be recorded as two units on the dial gauge. The strain would, therefore, be half the dial gauge reading divided by the 8, which is the effective height of the cylinder. Based on the result of the compressive strength of the concrete, the maximum stress to which the specimen was loaded was 40%. In this region, the stress versus strain curve is almost a straight line and its slope is the elastic modulus of concrete. Figure 7-25 and Table 7-20 show the results of the elastic modulus test performed. The E-value of concrete as obtained from the plot is 3×10^6 psi.

7.4 Cement Treated Base (CTB) Characterization

Base course is a layer below the surface course in a pavement section and is constructed above the subbase or directly on the subgrade. This section deals with preparing CTB samples and determining their properties. Stabilized bases have higher strength and provide better support to the overlying HMA layer than unbound granular materials. Stabilization can be done either by adding cement, lime or asphalt to crushed aggregate to increase the strength. Type I cement was used for stabilization of the bases tested.

7.4.1 CTB Composition

Aggregates from Garner quarry of Martin Marietta and Type I Portland cement were used to prepare CTB samples. Blending was achieved by combining #67 aggregate, washed screenings and material passing #200 sieves in 70:25:5 proportions. Sieve analysis was performed on individual aggregate stockpiles to obtain gradation of each fraction. Table 7-21, Table 7-22, and Figure 7-26 show the results of the individual stockpiles and the final blend. After batching aggregate, 5% cement by weight of aggregate was added.

7.4.2 Atterberg Limits for CTB Aggregates

Section 1010, subsection 4 (§1010-4) of NCDOT Standard Specifications for Roads and Structures specifies the gradation and Atterberg limits for aggregates used to make (Portland) cement treated base (CTB). In accordance with requirements of AASHTO T 89 or ASTM D 4318 (Standard Test Methods for Liquid Limit, Plastic Limit, and Plasticity Index of Soils), the aggregate blend was sieved on a #40 (0.425 mm) sieve. The fraction passing #40 was used to conduct this test. About 200 g of material was sampled and the test was performed using the standard liquid limit device (Casagrande cup). In this case, the maximum number of blows on the Casagrande cup was about 10 over a range of moisture contents. Thus, it was concluded that the material was non-plastic.

This required the use of the modified method for liquid limit for non-plastic materials as per NCDOT specifications. The modified test required mixing the soil with water to form a uniform mass of stiff consistency. The mass was then spread in a dish, similar to the Casagrande cup procedure, but without grooving. A clean dry spatula was pressed firmly on the soil mass and lifted without dragging. The surface of the spatula in contact with soil was observed for water. This process was repeated with increasing water content till water just started to adhere to the spatula in the form of beads. The water content, at this consistency, is called as the liquid limit. Table 7-24 shows the liquid limit value obtained; the average is 29. This falls within the DOT specified range of 0-30. The plastic limit could not be determined as the material could not be rolled into threads on a glass plate. The plasticity index for the CTB is NP (non-plastic).

7.4.3 Modified Proctor Density Test

This section describes the modified proctor density test conducted in accordance with ASTM D1557 (Standard Test Methods for Laboratory Compaction Characteristics of Soil using Modified Effort). The aggregates and cement were blended proportion before adding water. The compaction was done in a standard modified proctor mold having dimensions of 6×4.58 inches (volume 0.075 ft³). The compaction was done in five layers with each layer having about the same volume. After putting in a layer in the mold, it was compacted by applying 56 blows with a modified proctor hammer. The excess material was scraped out

from the top of the mold and the sides. The weight of the empty mold and the mold with specimen were determined. The wet density of the specimen could be obtained by dividing the weight of the specimen by the volume of the mold. Table 7-23 shows the results obtained for the test. The water content was continuously increased from 3.5 to 7%. A small representative part from the larger sample was dried and the moisture content determined. The dry density was calculated and the results are presented graphically in Figure 7-27. The peak dry density as seen from the plot is 146 pcf and the optimum moisture content is 5.6%. The CTB specimens used to make the composite samples were compacted with 6.0% moisture content, slightly higher than the optimum moisture content. (NCDOT specifications - §540 of Standard Specifications for Roads and Structures - state that the compaction of CTB should occur between optimum and optimum + 1.5% moisture content.)

An estimate of 7-day unconfined compressive strength of 600 psi for CTB was obtained in consultation with NCDOT. Based on the nomograph presented in Figure 7-28, the modulus corresponding to 600 psi unconfined strength was estimated to be 6.9×10^5 psi. This value was used for layered analysis in Chapter 9.

Table 7-1 Air voids of AC mix samples

Sample ID	Height (mm)	Air voids (%)
M1	50.36	4.3
M2	48.93	4.4
M3	49.20	4.3
M4	47.68	4.3

Table 7-2 |G*| vs. frequency for AC mix, 20 ° C, in Pa

Frequency (Hz)	M1	M2	M3	M4	Average
10	1.87E+09	1.65E+09	1.70E+09	1.79E+09	1.75E+09
5	1.63E+09	1.46E+09	1.52E+09	1.59E+09	1.55E+09
2	1.29E+09	1.16E+09	1.20E+09	1.27E+09	1.23E+09
1	1.14E+09	1.07E+09	1.22E+09	1.15E+09	1.15E+09
0.5	8.60E+08	8.73E+08	8.29E+08	9.01E+08	8.66E+08
0.2	6.45E+08	6.51E+08	6.90E+08	6.76E+08	6.66E+08
0.1	4.98E+08	5.25E+08	6.02E+08	5.27E+08	5.38E+08
0.05	3.13E+08	3.33E+08	2.03E+08	3.95E+08	3.11E+08
0.02	2.28E+08	2.50E+08	1.91E+08	2.77E+08	2.37E+08
0.01	1.76E+08	2.49E+08	2.78E+08	2.18E+08	2.30E+08

Table 7-3 Shear phase angle (degrees) vs. frequency for AC mix, 20 °C

Frequency (Hz)	M1	M2	M3	M4	Average
10	17.14	15.71	16.12	14.46	15.86
5	19.14	17.45	17.27	16.21	17.52
2	22.49	19.19	25.63	19.71	21.76
1	22.79	20.98	23.79	19.91	21.87
0.5	27.15	26.12	26.36	22.89	25.63
0.2	32.00	30.97	32.18	28.40	30.89
0.1	35.61	36.69	37.60	31.29	35.30
0.05	28.85	31.52	18.33	30.84	27.39
0.02	35.99	38.49	29.88	34.90	34.82
0.01	38.49	47.24	49.96	37.78	43.37

Table 7-4 |G*| vs. frequency for AC mix, 30 °C, in Pa

Frequency (Hz)	M1	M2	M3	M4	Average
10	9.62E+08	9.49E+08	1.00E+09	9.05E+08	9.55E+08
5	7.70E+08	7.65E+08	8.01E+08	7.23E+08	7.65E+08
2	5.57E+08	5.66E+08	5.78E+08	5.20E+08	5.55E+08
1	4.18E+08	4.12E+08	4.42E+08	3.91E+08	4.16E+08
0.5	3.14E+08	3.23E+08	3.25E+08	2.91E+08	3.13E+08
0.2	2.08E+08	2.17E+08	2.18E+08	1.94E+08	2.09E+08
0.1	1.54E+08	1.59E+08	1.61E+08	1.46E+08	1.55E+08
0.05	1.01E+08	1.09E+08	1.10E+08	9.60E+07	1.04E+08
0.02	6.89E+07	7.74E+07	6.92E+07	6.61E+07	7.04E+07
0.01	5.08E+07	5.74E+07	5.31E+07	5.03E+07	5.29E+07

Table 7-5 Shear phase angle (degrees) vs. frequency for AC mix, 30 °C

Frequency (Hz)	M1	M2	M3	M4	Average
10	27.80	26.33	27.45	28.87	27.61
5	30.58	29.17	30.25	31.64	30.41
2	33.88	33.03	34.01	35.15	34.02
1	37.70	33.21	40.61	38.23	37.44
0.5	39.73	38.67	39.44	41.25	39.77
0.2	43.92	42.65	43.75	44.51	43.71
0.1	46.39	44.68	45.50	46.41	45.75
0.05	45.39	43.61	46.71	43.77	44.87
0.02	46.98	50.20	46.32	47.60	47.78
0.01	47.87	49.21	52.98	45.99	49.01

Table 7-6 $|G^*|$ vs. frequency for AC mix, 40 ° C, in Pa

Frequency (Hz)	M1	M2	M3	M4	Average
10	4.55E+08	4.46E+08	4.45E+08	4.54E+08	4.50E+08
5	3.40E+08	3.37E+08	3.29E+08	3.37E+08	3.36E+08
2	2.29E+08	2.34E+08	2.26E+08	2.26E+08	2.29E+08
1	1.66E+08	1.72E+08	1.67E+08	1.66E+08	1.68E+08
0.5	1.22E+08	1.21E+08	1.20E+08	1.21E+08	1.21E+08
0.2	8.21E+07	8.15E+07	7.95E+07	8.06E+07	8.09E+07
0.1	6.30E+07	5.82E+07	5.91E+07	6.02E+07	6.01E+07
0.05	4.68E+07	3.81E+07	4.25E+07	4.57E+07	4.32E+07
0.02	3.61E+07	2.92E+07	3.19E+07	3.46E+07	3.29E+07
0.01	2.93E+07	2.56E+07	2.72E+07	2.81E+07	2.75E+07

Table 7-7 Shear phase angle (degrees) vs. frequency for AC mix, 40 ° C

Frequency (Hz)	M1	M2	M3	M4	Average
10	37.57	37.21	38.35	37.66	37.70
5	40.26	39.59	40.84	40.50	40.30
2	42.85	40.19	44.88	43.25	42.79
1	45.02	47.16	44.91	44.42	45.38
0.5	45.79	45.83	46.66	46.50	46.19
0.2	45.92	47.46	47.32	46.16	46.72
0.1	43.78	45.27	45.47	44.02	44.63
0.05	42.58	43.38	41.62	43.55	42.78
0.02	40.49	40.29	39.96	40.64	40.34
0.01	37.62	40.91	40.00	40.61	39.79

Table 7-8 $|G^*|$ vs. frequency for AC mix, 60 ° C, in Pa

Frequency (Hz)	M1	M2	M3	M4	Average
10	1.03E+08	8.75E+07	1.04E+08	1.03E+08	9.95E+07
5	7.84E+07	6.84E+07	7.79E+07	7.89E+07	7.59E+07
2	5.99E+07	5.22E+07	6.95E+07	5.73E+07	5.97E+07
1	4.85E+07	4.38E+07	4.91E+07	4.79E+07	4.73E+07
0.5	4.04E+07	3.78E+07	3.96E+07	4.04E+07	3.96E+07
0.2	3.34E+07	3.23E+07	3.09E+07	3.35E+07	3.25E+07
0.1	3.02E+07	2.90E+07	2.62E+07	2.96E+07	2.88E+07
0.05	2.59E+07	2.66E+07	2.33E+07	2.70E+07	2.57E+07
0.02	2.35E+07	2.43E+07	2.12E+07	2.39E+07	2.32E+07
0.01	2.19E+07	2.30E+07	1.85E+07	2.19E+07	2.13E+07

Table 7-9 Shear phase angle (degrees) vs. frequency for AC mix, 60 °C

Frequency (Hz)	M1	M2	M3	M4	Average
10	42.21	40.56	41.88	42.37	39.81
5	40.01	38.06	40.37	40.81	39.07
2	39.96	34.87	45.14	36.30	33.94
1	35.08	31.86	33.83	34.99	31.64
0.5	31.54	30.19	32.32	32.50	28.85
0.2	28.85	27.54	29.72	29.29	26.74
0.1	26.13	24.79	29.06	26.97	24.63
0.05	23.87	23.06	27.41	24.17	22.37
0.02	22.90	20.43	22.36	23.78	20.57
0.01	18.24	17.45	26.66	19.93	39.81

Table 7-10 RSCH cycles, at 40 and 60 °C

Sample ID	Test Temperature (°C)	Max RSCH cycles	Max Plastic Strain	Plastic Strain @5000 cycles
M1	60	13000	4.60%	3.05%
M2	60	27000	4.80%	2.84%
M3	40	100000	0.76%	0.52%
M4	40	100000	1.34%	0.82%

Table 7-11 Air voids of axial test samples

Sample ID	Test temperature	Tests	Air voids
SA01	60 °C	Repeated Axial Test	3.8%
SA03			3.9%
SA04	40 °C	Repeated Axial Test	3.8%
SA05			4.0%
SA07	20, 30, 40, 60 °C	Axial Frequency Sweep Test	4.0%
SA12			3.8%

Table 7-12 |E*| vs. frequency for AC mix, 20 and 30 °C, in Pa

Frequency (Hz)	20 C			30 C		
	SA07	SA12	Average	SA07	SA12	Average
10	6.14E+09	5.57E+09	5.86E+09	3.47E+09	3.40E+09	3.43E+09
5	5.40E+09	4.81E+09	5.11E+09	2.83E+09	2.74E+09	2.79E+09
2	4.45E+09	3.87E+09	4.16E+09	2.10E+09	1.99E+09	2.04E+09
1	3.77E+09	3.20E+09	3.49E+09	1.61E+09	1.49E+09	1.55E+09
0.5	3.13E+09	2.58E+09	2.86E+09	1.23E+09	1.11E+09	1.17E+09
0.2	2.37E+09	1.88E+09	2.12E+09	8.18E+08	7.08E+08	7.63E+08

Table 7-13 Axial phase angle (degrees) vs. frequency for AC mix, 20 and 30 ° C

Frequency (Hz)	20 C			30 C		
	SA07	SA12	Average	SA07	SA12	Average
10	16.84	18.74	17.79	25.17	26.84	26.00
5	18.49	20.74	19.61	27.66	29.79	28.72
2	21.01	23.76	22.38	31.24	33.95	32.60
1	23.10	26.30	24.70	33.87	37.62	35.75
0.5	25.79	29.12	27.45	36.76	40.62	38.69
0.2	29.44	33.11	31.27	40.12	44.91	42.51

Table 7-14 |E*| vs. frequency for AC mix, 40 and 60 ° C, in Pa

Frequency (Hz)	40 C			60 C		
	SA07	SA12	Average	SA07	SA12	Average
10	1.87E+09	1.69E+09	1.78E+09	5.46E+08	3.36E+08	4.41E+08
5	1.42E+09	1.28E+09	1.35E+09	3.94E+08	2.28E+08	3.11E+08
2	9.57E+08	8.53E+08	9.05E+08	2.83E+08	1.57E+08	2.20E+08
1	6.90E+08	6.11E+08	6.51E+08	2.07E+08	1.02E+08	1.55E+08
0.5	4.85E+08	4.40E+08	4.63E+08	–	–	–
0.2	2.97E+08	2.76E+08	2.87E+08	–	–	–

Table 7-15 Axial phase angle (degrees) vs. frequency for AC mix, 40 and 60 ° C

Frequency (Hz)	40 C			60 C		
	SA07	SA12	Average	SA07	SA12	Average
10	33.19	34.42	33.81	41.14	44.23	42.69
5	35.79	36.29	36.04	40.81	44.73	42.77
2	39.24	38.87	39.05	38.06	43.64	40.85
1	41.34	39.87	40.60	37.17	42.72	39.95
0.5	43.04	40.90	41.97	–	–	–
0.2	44.72	41.20	42.96	–	–	–

Table 7-16 Repeated axial test cycles, at 40 and 60 ° C

Sample ID	Test Temperature (°C)	Max axial cycles	Max Plastic Strain
SA01	60	8800	1.37%
SA03	60	14000	1.44%
SA04	40	100000	0.19%
SA05	40	100000	0.17%

Table 7-17 Aggregate moisture contents and specific gravities

Property	Sand	Rock	Cement
SG (SSD)	2.630	2.632	3.15 ²
Total moisture	0.40%	0.40%	0%
Absorption	0.60%	0.66%	0%

Table 7-18 Batch weights for PCC

Material	Trial Weight (lb)	Batch Weight (pcy)	SSD Weight (pcy)
Cement	35.5	622	622
Sand	66.6	1166	1168
Rock	95.5	1672	1676
Water	15.2	266	259
AEA	6 ml	0.56 oz/cwt	0.56 oz/cwt
Retarder	20 ml	1.88 oz/cwt	1.88 oz/cwt

Table 7-19 Properties of concrete

Property	Value
w/c ratio	0.42
Slump	4.75 in
Unit wt	138 pcf
7d strength	4810 psi
14d strength	5250 psi
28d strength	5750 psi
7d Elastic modulus	3.0E+06 psi
7d Splitting tension	410 psi
7d Modulus of rupture	635 psi

Table 7-20 Elastic modulus for PCC

Load (lb)	Stress (psi)	Dial (in)	Strain
4800	169.8	8.00E-04	5.00E-05
5775	204.2	8.00E-04	5.00E-05
24000	848.8	4.00E-03	2.50E-04
24000	848.8	4.30E-03	2.69E-04
27000	954.9	4.70E-03	2.94E-04
31000	1096.4	5.60E-03	3.50E-04
31000	1096.4	5.60E-03	3.50E-04

² The cement specific gravity has been assumed to be 3.15. The absorption and total moisture content of cement is assumed to be 0%.

Table 7-21 Gradation (% passing) for aggregate piles used for CTB

Sieve size	#67	Screenings	P #200	Blended	DOT Specs
1.5"	100.0	100.0	100.0	100.0	
1.0"	100.0	100.0	100.0	100.0	76-100
0.5"	77.0	100.0	100.0	83.9	54-86
#4	15.2	99.0	100.0	40.4	35-64
#10	6.9	75.0	100.0	28.6	24-54
#40	3.9	29.1	100.0	15.0	12-36
#200	1.1	2.0	100.0	6.3	5-14
Proportion	70	25	5		

Table 7-22 Gradation criteria for material passing #10 sieve (soil mortar)

Sieve Size	Blend	DOT Specs
#40	53%	38-87%
#200	22%	11-36%

Table 7-23 Moisture density determination for CTB

Test No.	Mold Weight (lb)		Mold Volume (ft ³)			0.075	
	13.11	13.11	Wet Unit wt (pcf)	Wt of wet sample (lb)	Wt of dry sample (lb)	Water content (%)	Dry unit weight (pcf)
1	23.73	10.63	141.72	0.810	0.782	3.59	136.81
2	23.94	10.84	144.52	1.045	1.002	4.24	138.65
3	24.40	11.29	150.52	1.149	1.094	5.07	143.25
4	24.66	11.55	153.98	1.041	0.986	5.60	145.82
5	24.60	11.49	153.18	1.186	1.114	6.45	143.90
6	24.53	11.42	152.25	1.118	1.045	6.99	142.30

Table 7-24 Liquid limit property for CTB using DOT modified method

Sample	Wt of can (g)	Wt of can + wet soil (g)	Wt of can + dry soil (g)	Liquid Limit
1	15.60	32.73	28.98	28.0%
2	16.11	37.11	32.32	29.5%
3	15.99	42.99	36.83	29.6%

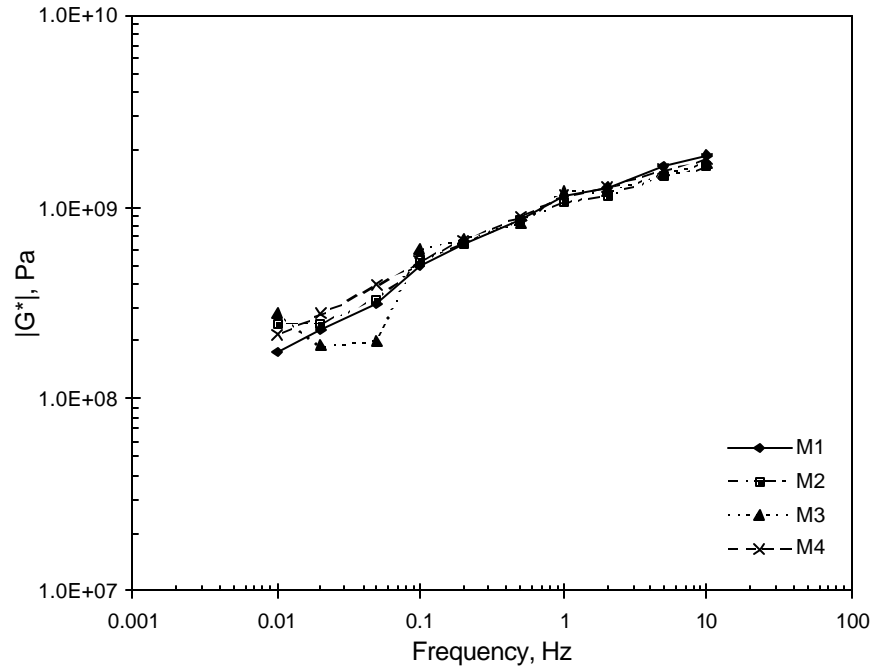


Figure 7-1 Dynamic shear modulus ($|G^*|$) vs. frequency for AC mix, 20 °C

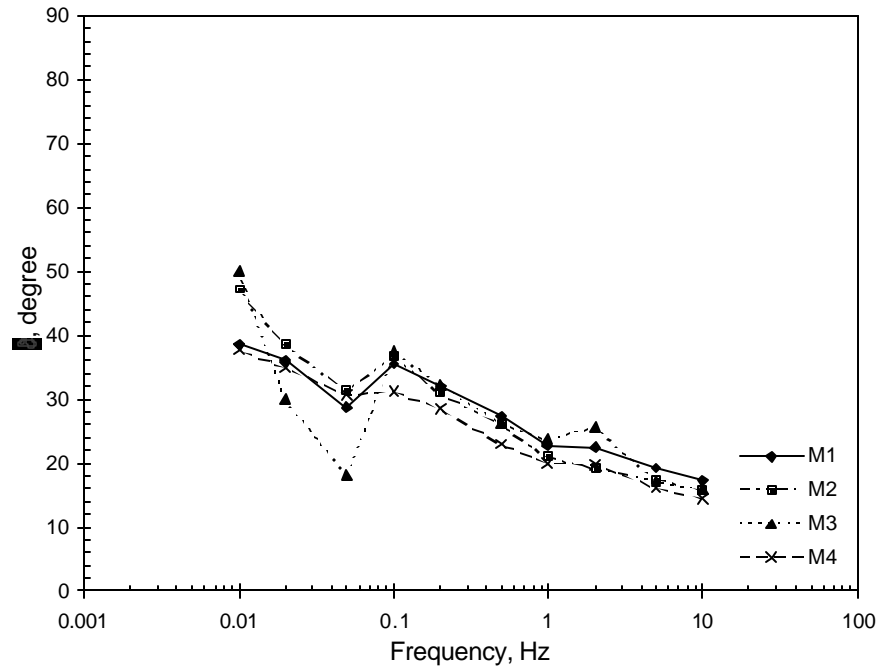


Figure 7-2 Shear phase angle (δ) vs. frequency for AC mix, 20 °C

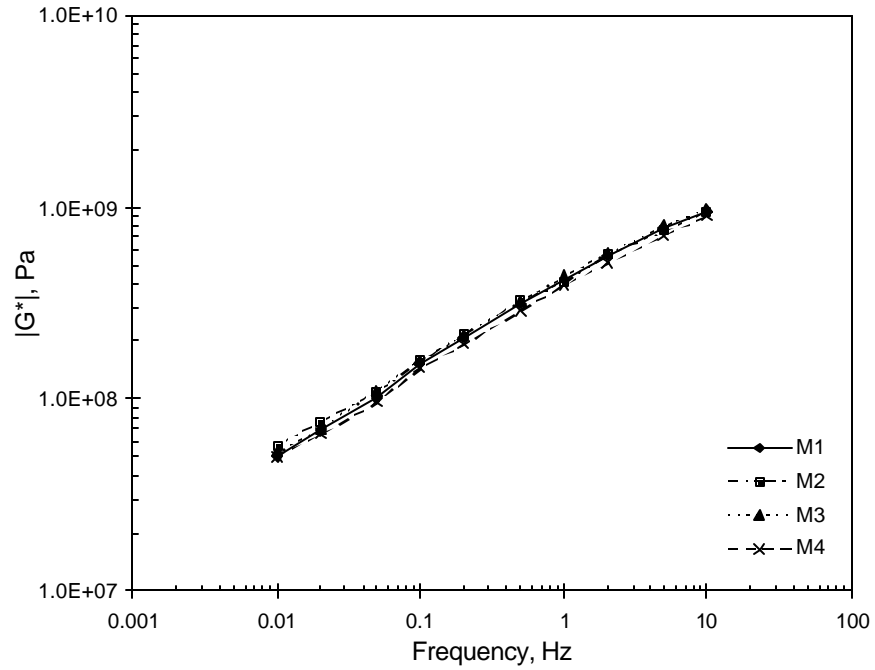


Figure 7-3 Dynamic shear modulus ($|G^*$) vs. frequency for AC mix, 30 °C

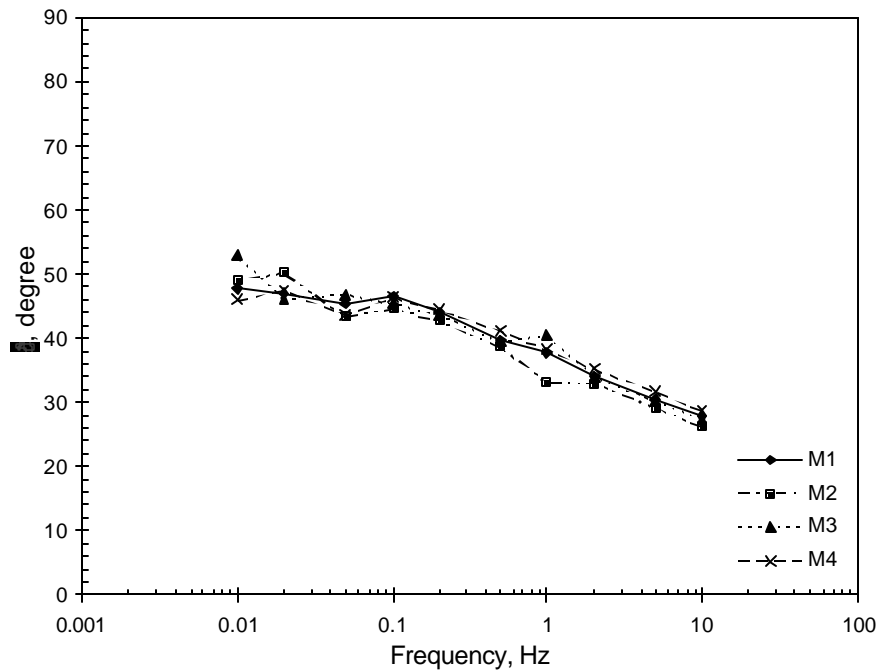


Figure 7-4 Shear phase angle (δ) vs. frequency for AC mix, 30 °C

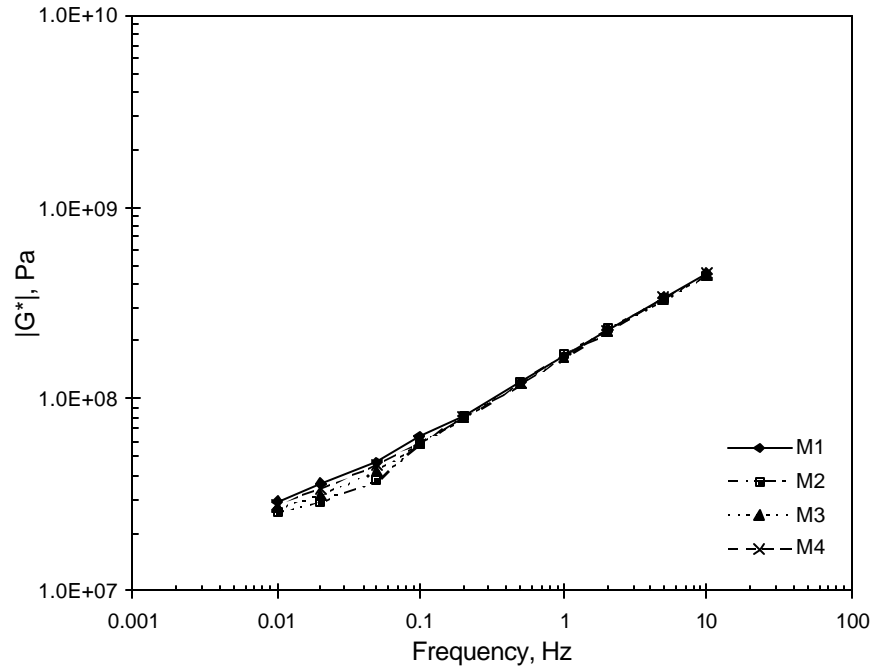


Figure 7-5 Dynamic shear modulus ($|G^*|$) vs. frequency for AC mix, 40 °C

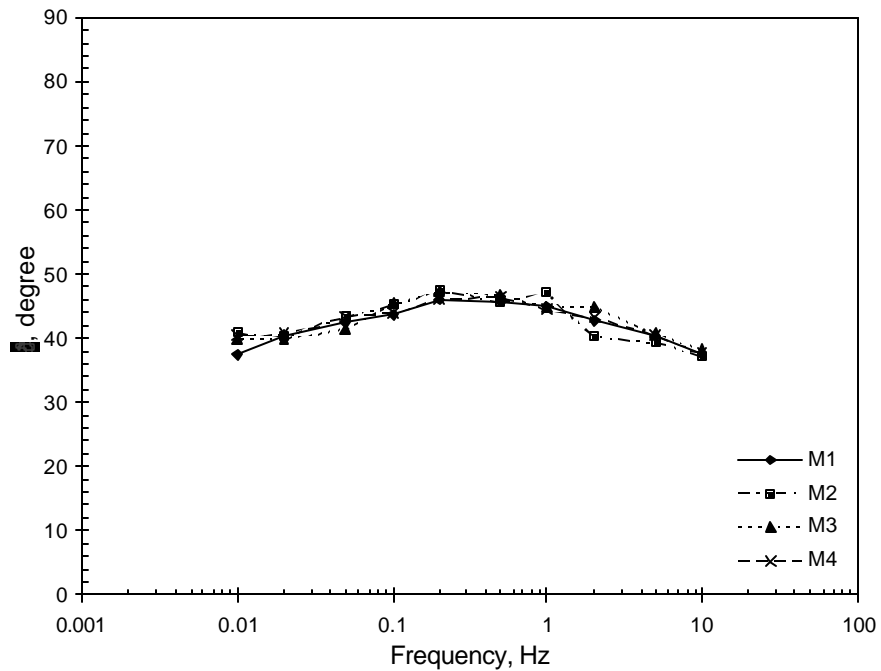


Figure 7-6 Shear phase angle (δ) vs. frequency for AC mix, 40 °C

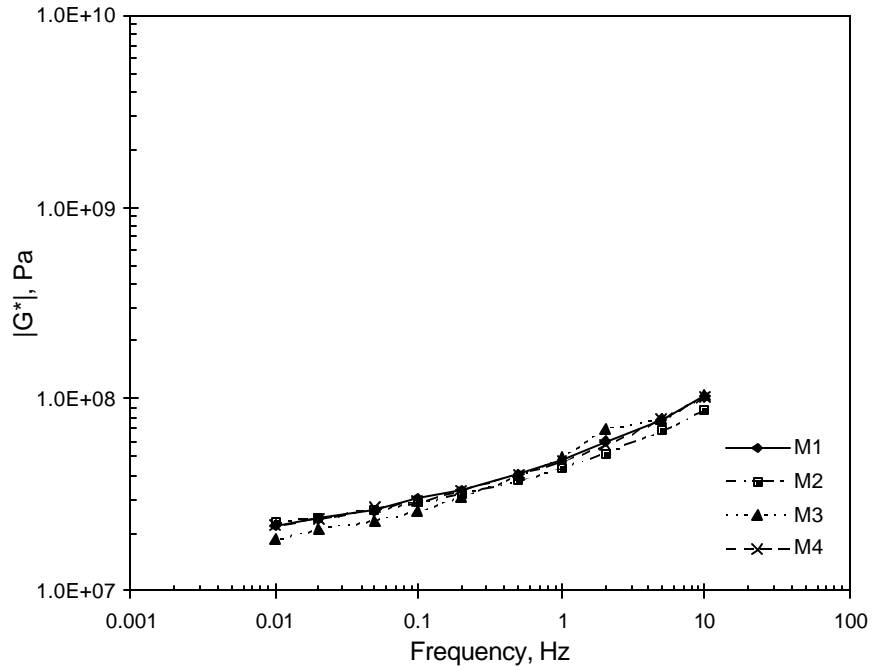


Figure 7-7 Dynamic shear modulus ($|G^*$) vs. frequency for AC mix, 60 °C

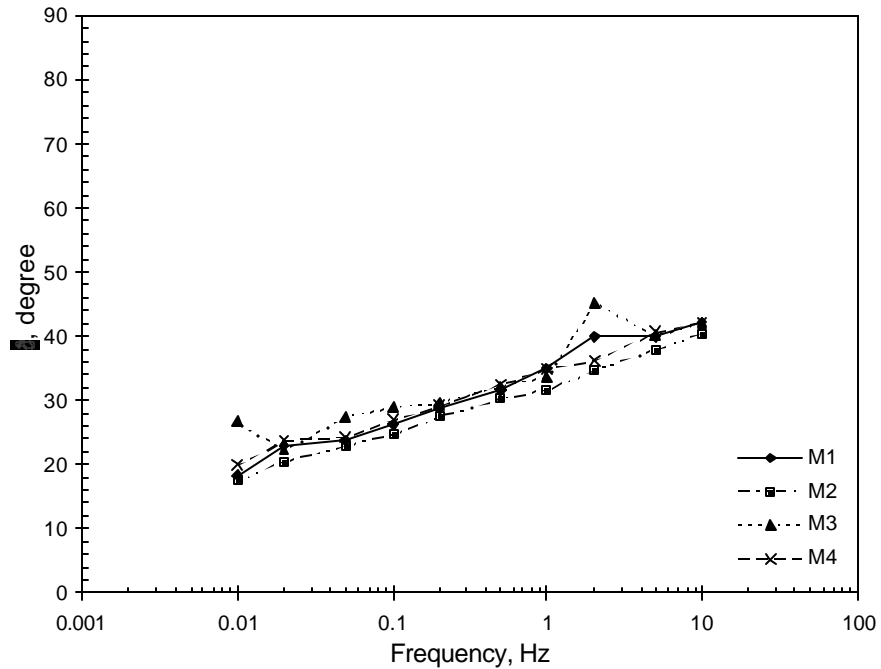


Figure 7-8 Shear phase angle (δ) vs. frequency for AC mix, 60 °C

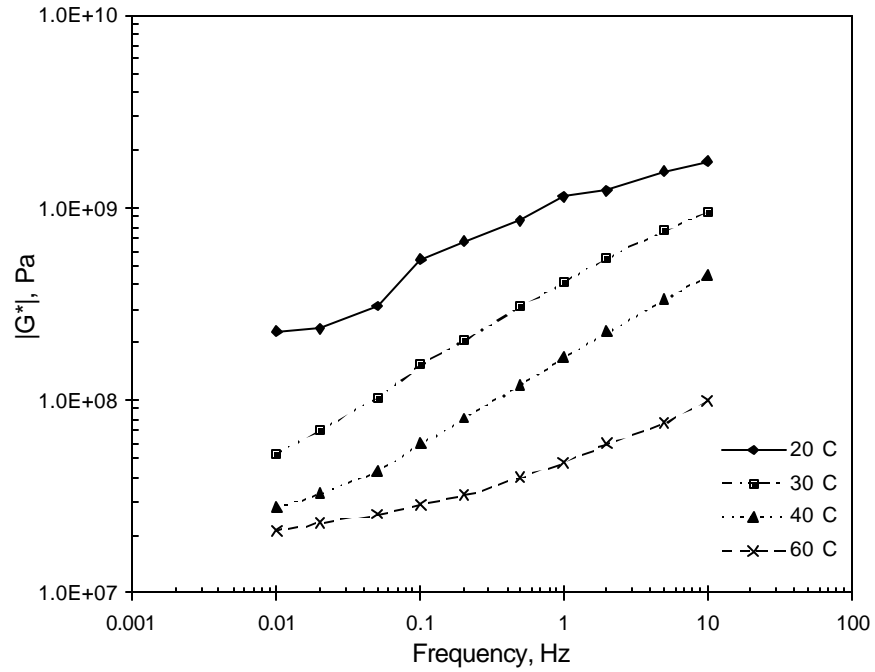


Figure 7-9 Average dynamic shear modulus ($|G^*|$) vs. frequency for AC mix

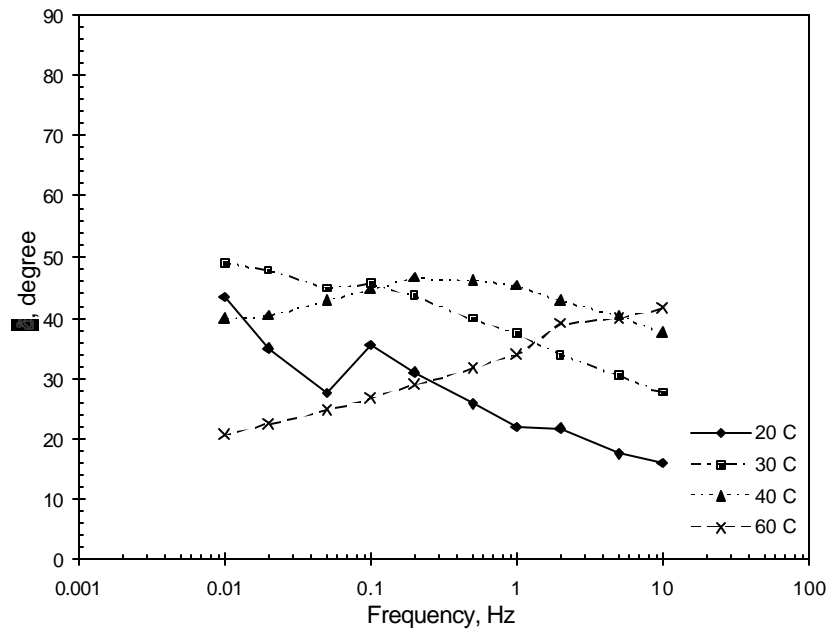


Figure 7-10 Average shear phase angle (δ) vs. frequency for AC mix

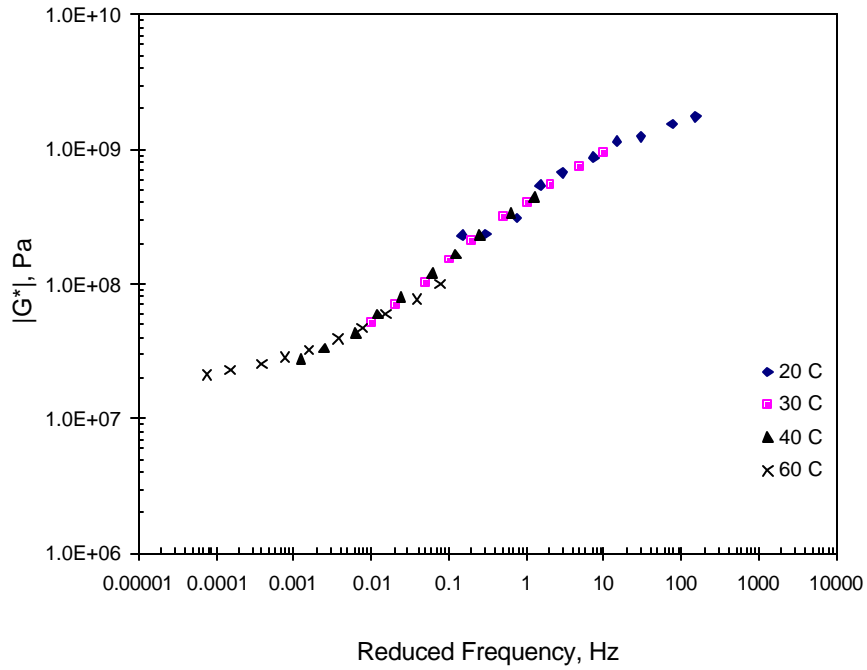


Figure 7-11 $|G^*|$ master curve for AC mix, 30 °C

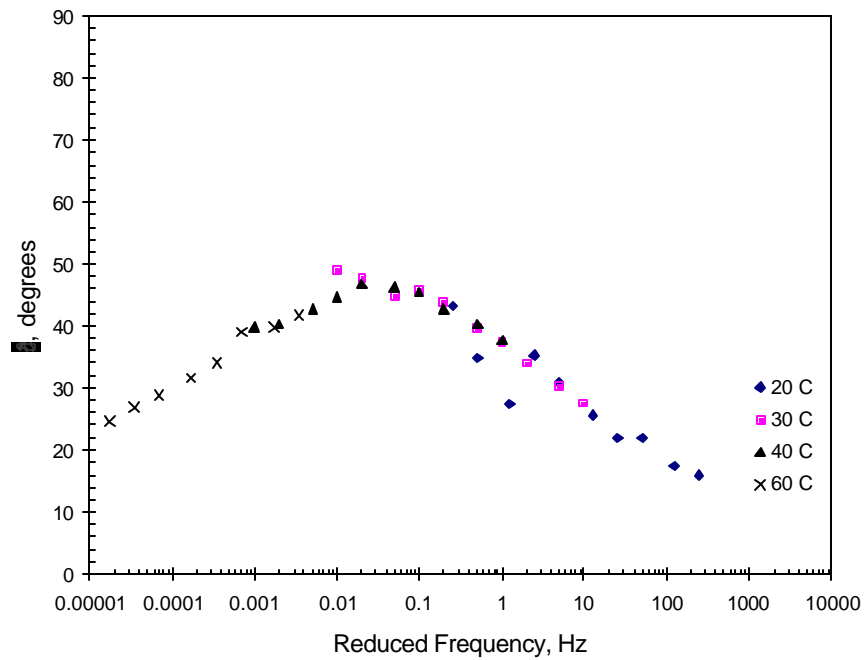


Figure 7-12 Shear phase angle (δ) master curve for AC mix, 30 °C

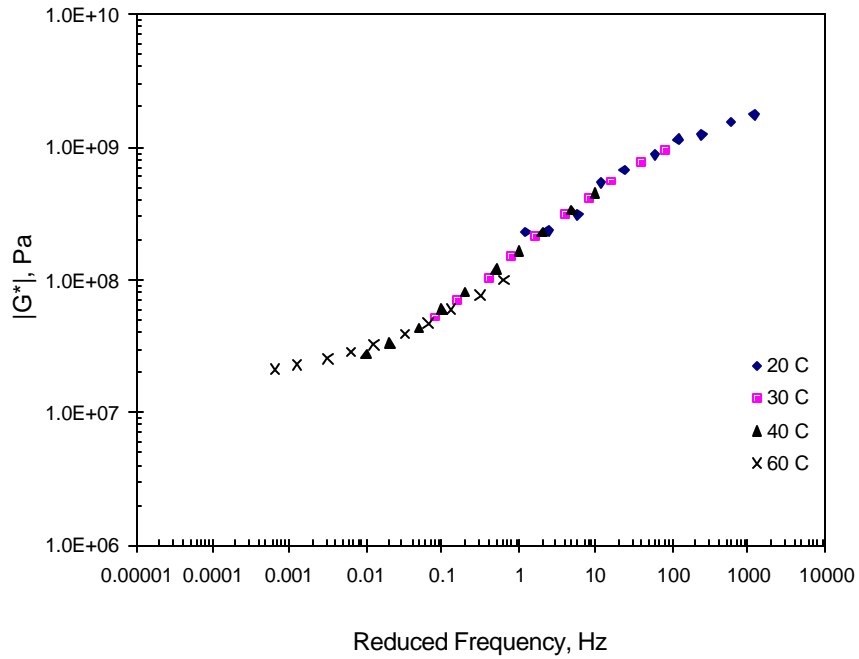


Figure 7-13 $|G^*|$ master curve for AC mix, 40 °C

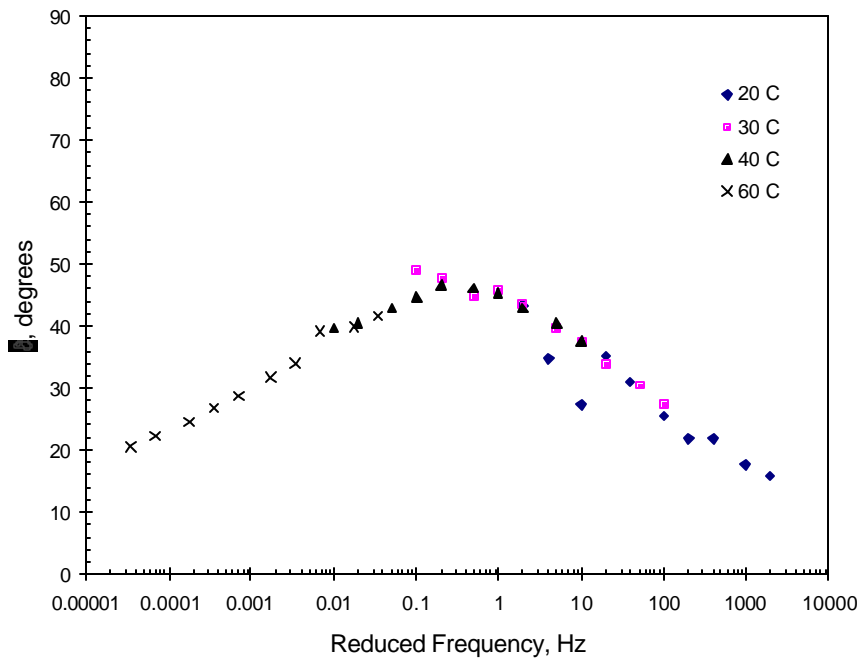


Figure 7-14 Shear phase angle (δ) master curve for AC mix, 40 °C

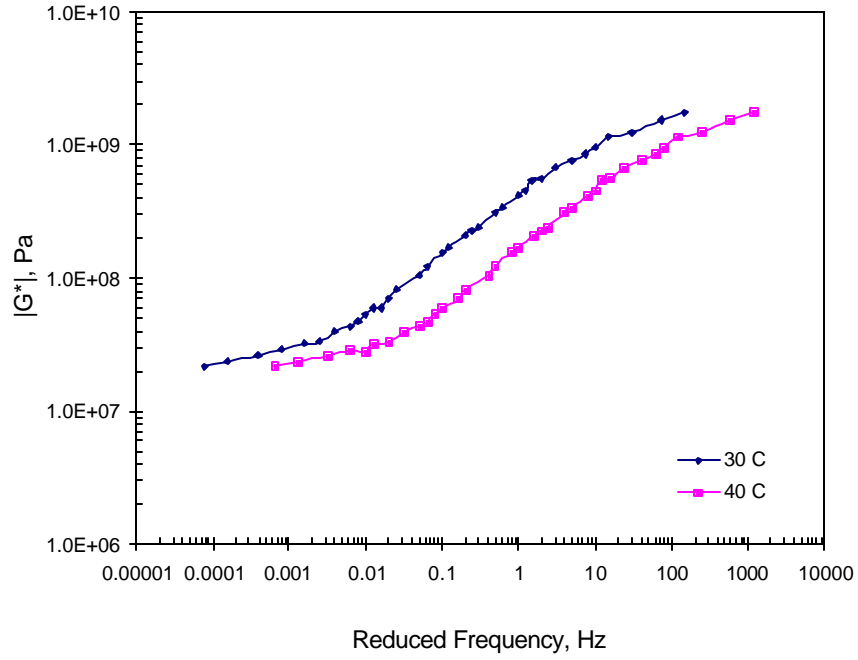


Figure 7-15|G*| master curve for AC mix, 30 and 40 ° C

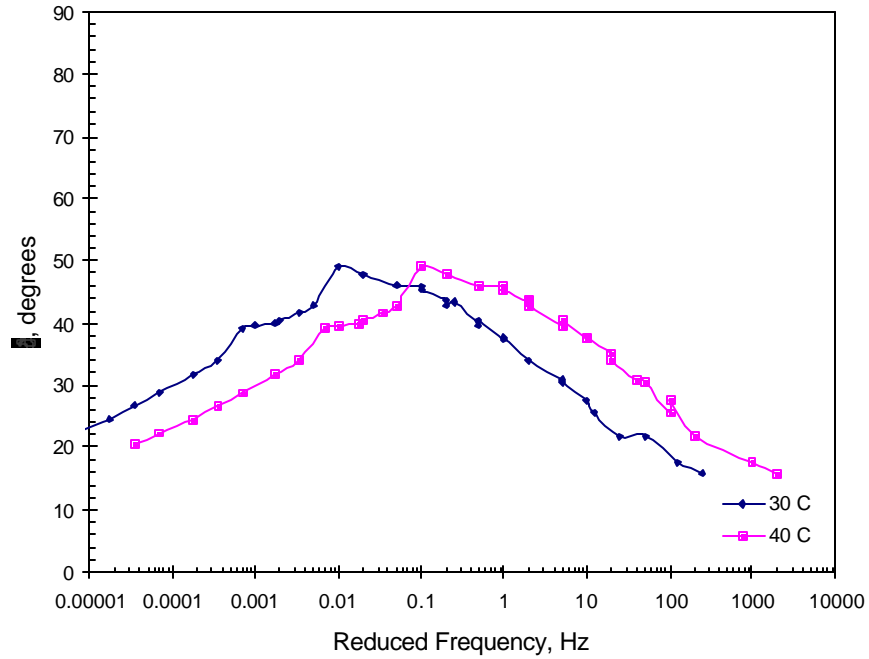


Figure 7-16 Shear phase angle (d) master curve for AC mix, 30 and 40 ° C

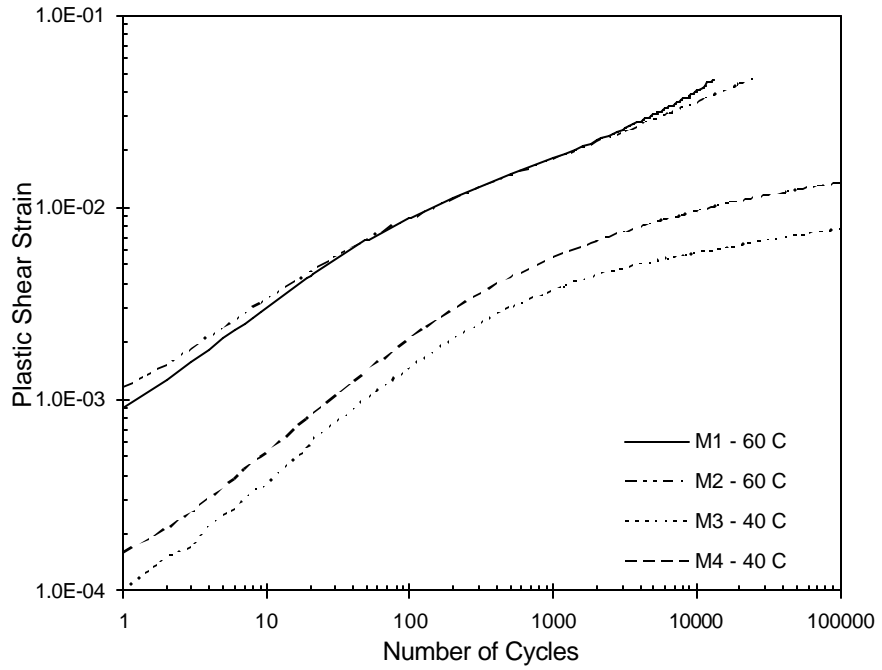


Figure 7-17 Plastic shear strain vs. RSCH cycles, 40 and 60 °C for AC mixes

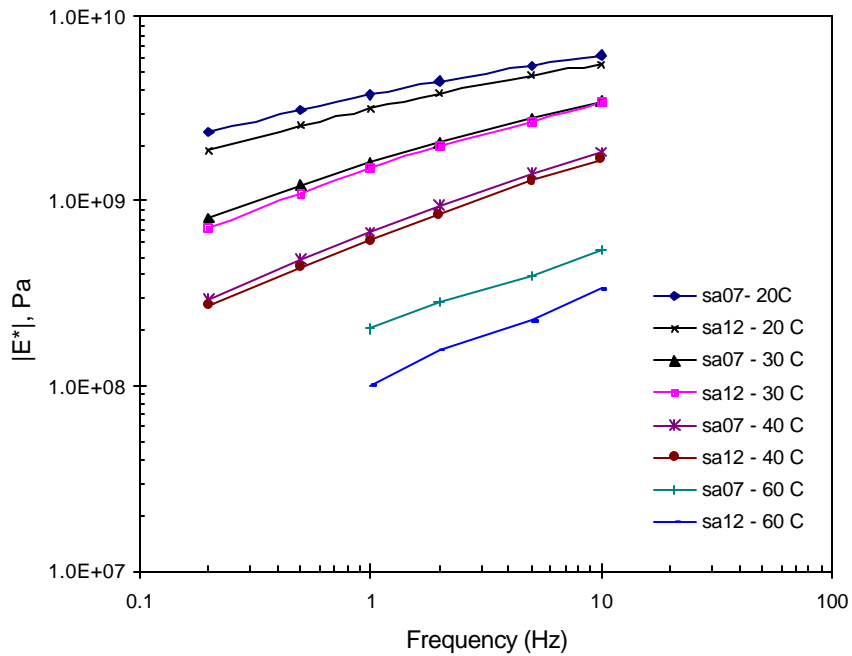


Figure 7-18 Dynamic axial modulus ($|E^*|$) vs. frequency for AC mix

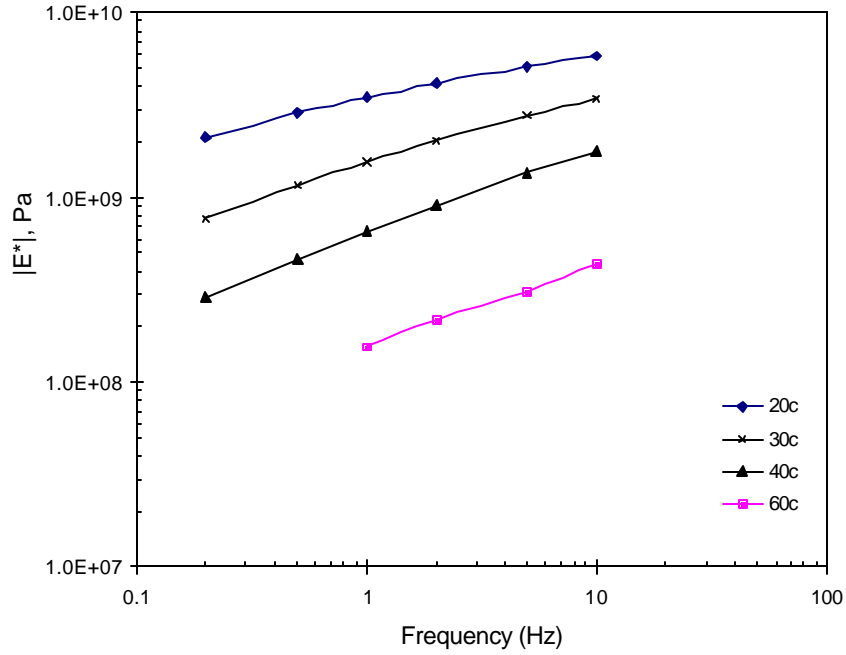


Figure 7-19 Average dynamic axial modulus ($|E^*|$) vs. frequency for AC mix

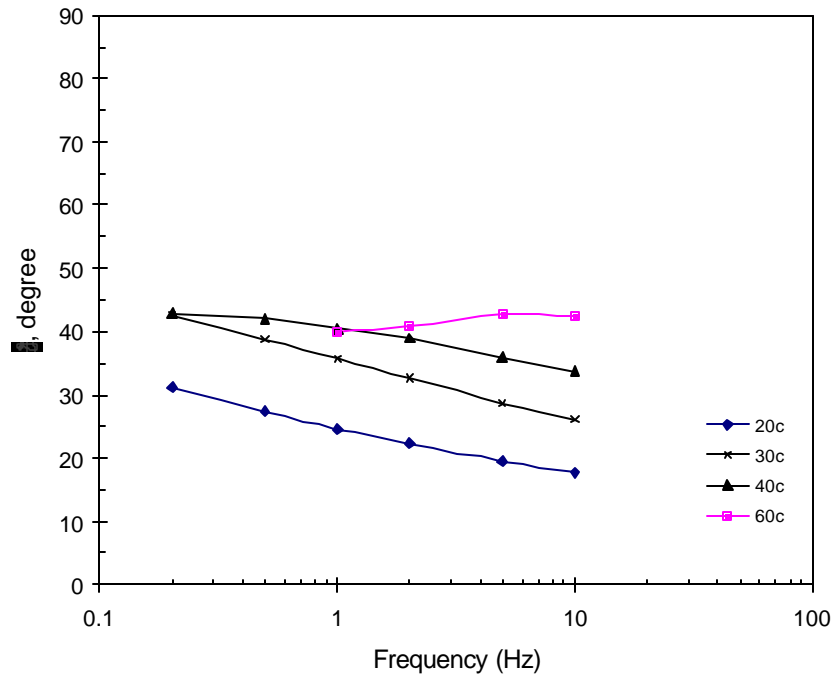


Figure 7-20 Average axial phase angle (δ) vs. frequency for AC mix

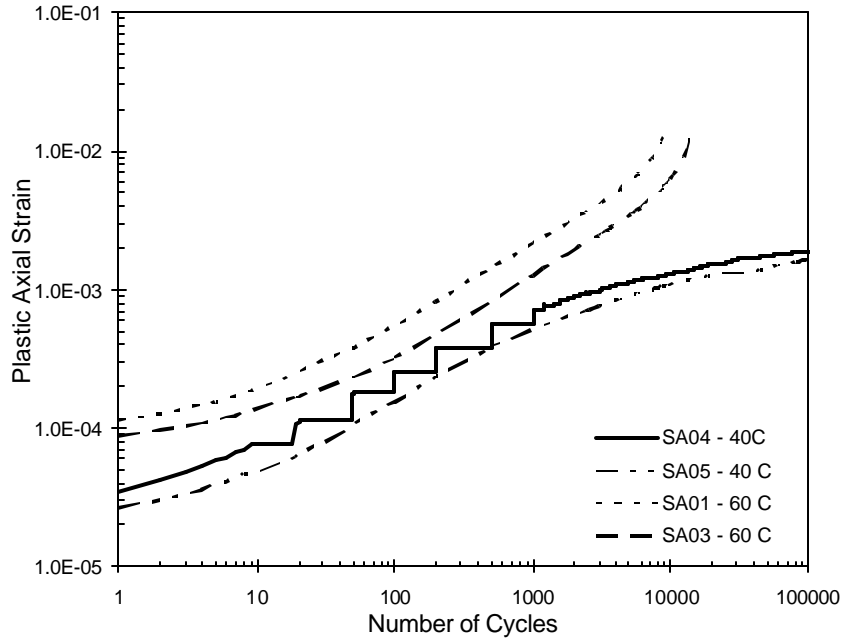


Figure 7-21 Plastic axial strain vs. cycles, 40 and 60 °C for AC mixes

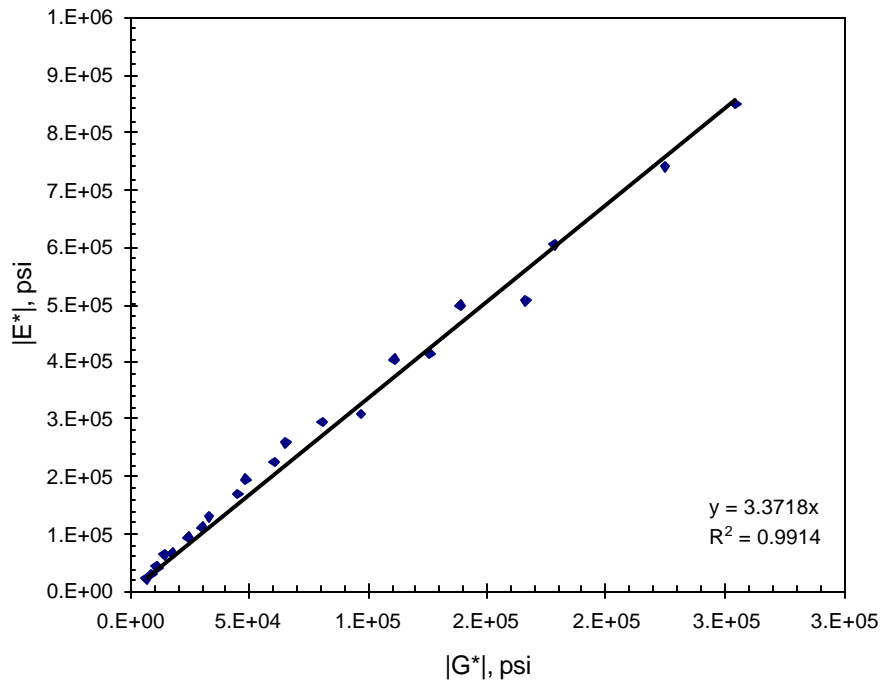


Figure 7-22 Relationship between $|G^*|$ and $|E^*|$ for AC mixes

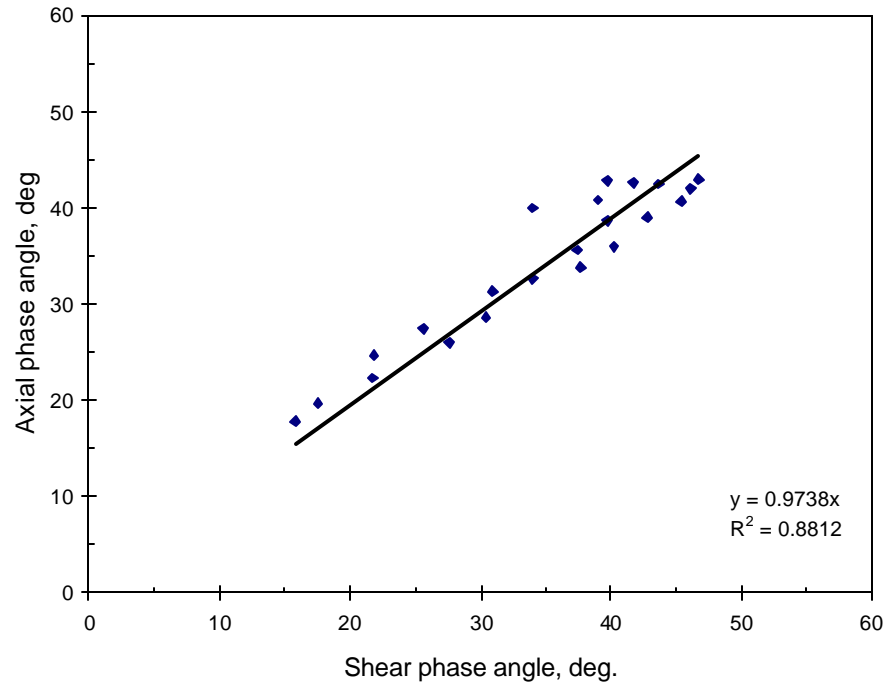


Figure 7-23 Relationship between shear and axial phase angle for AC mixes

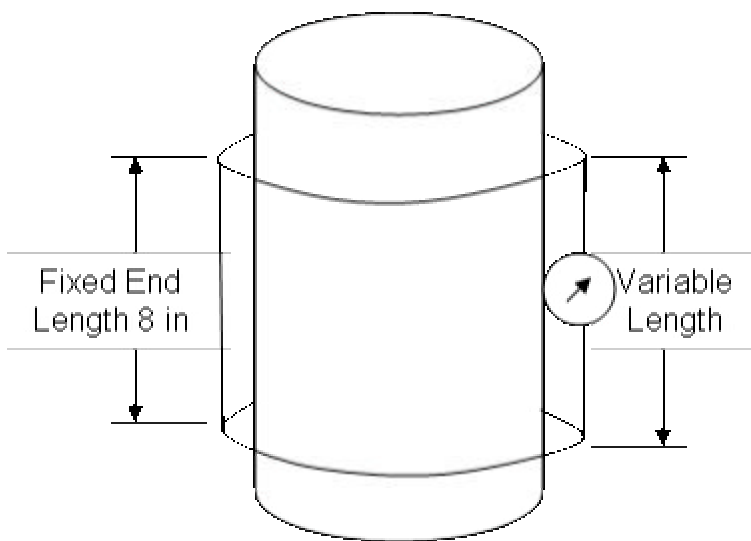


Figure 7-24 Set up for elastic modulus of concrete using a 6x12 cylinder

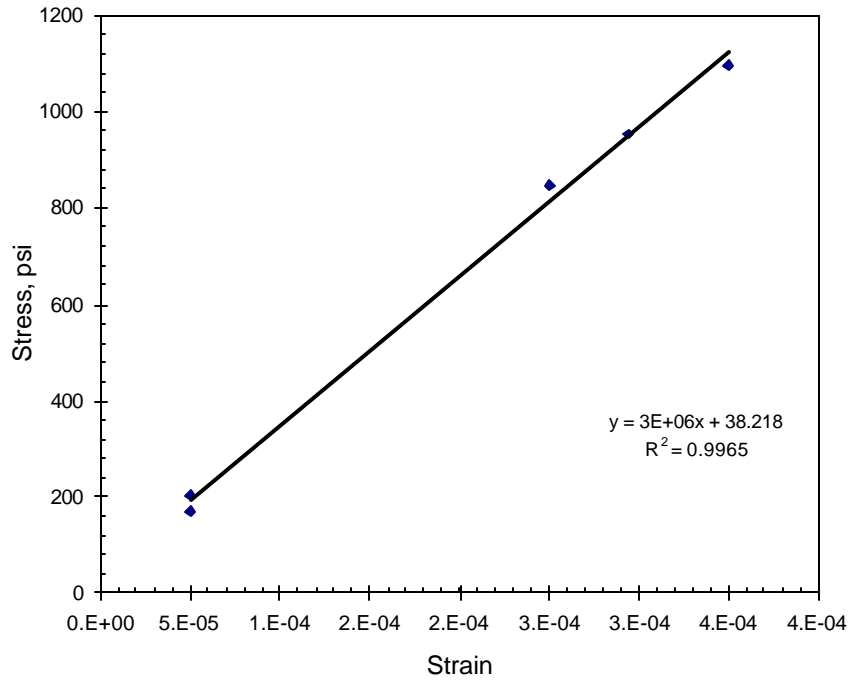


Figure 7-25 Axial stress vs. strain at 7 days for PCC

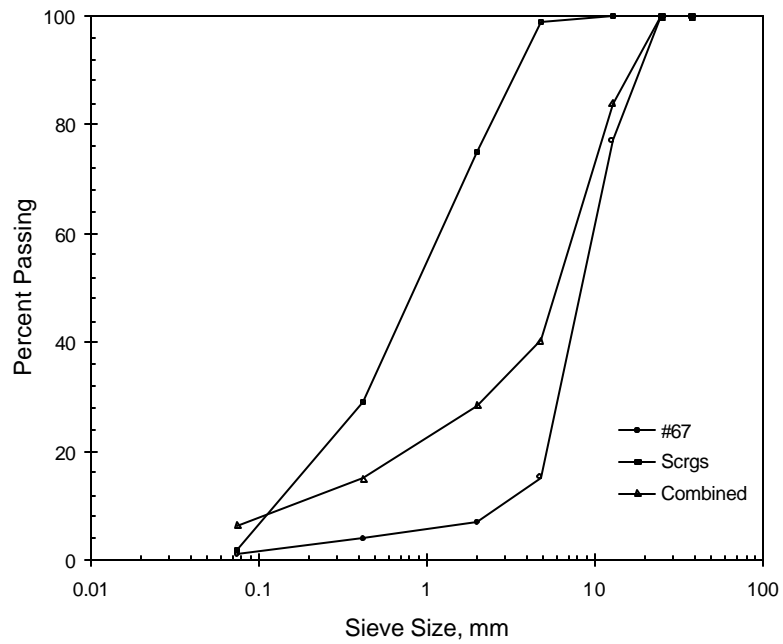


Figure 7-26 Gradation of materials used for CTB

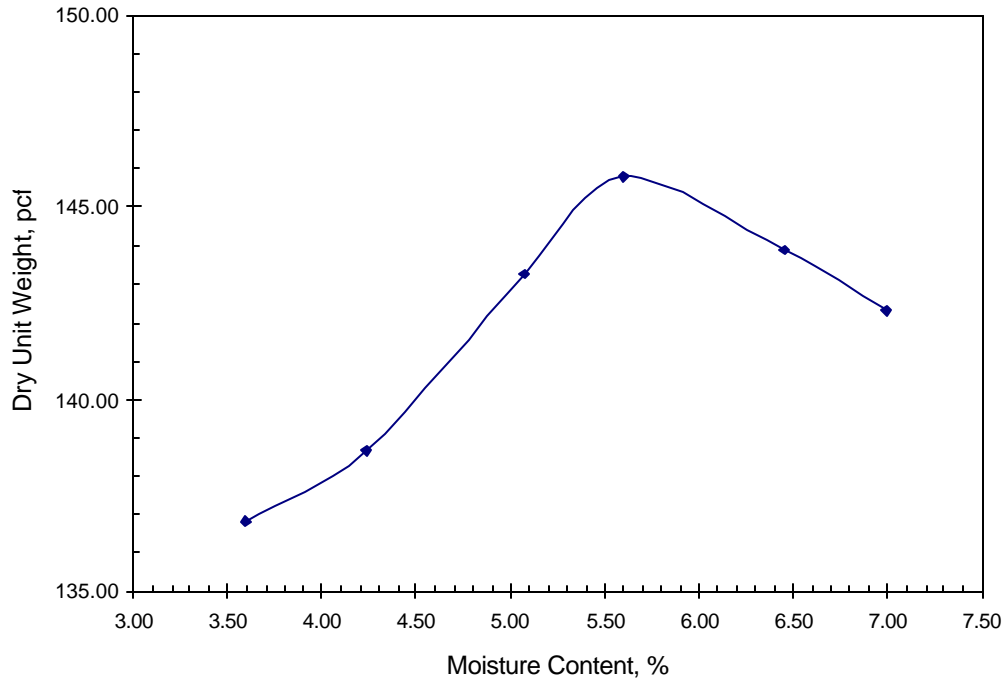


Figure 7-27 Moisture density curve for CTB

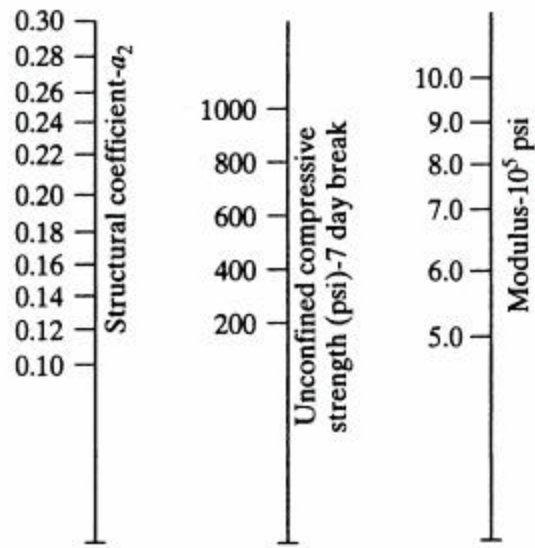


Figure 7-28 Resilient modulus of cement treated bases (CTB), [1, 24]